

University of Louisville

ThinkIR: The University of Louisville's Institutional Repository

Electronic Theses and Dissertations

12-2015

Atmospheric nitrogen assimilation in *Ustilago maydis*.

Michael Cooper
University of Louisville

Follow this and additional works at: <https://ir.library.louisville.edu/etd>

Part of the [Genetics Commons](#)

Recommended Citation

Cooper, Michael, "Atmospheric nitrogen assimilation in *Ustilago maydis*." (2015). *Electronic Theses and Dissertations*. Paper 2322.
<https://doi.org/10.18297/etd/2322>

This Doctoral Dissertation is brought to you for free and open access by ThinkIR: The University of Louisville's Institutional Repository. It has been accepted for inclusion in Electronic Theses and Dissertations by an authorized administrator of ThinkIR: The University of Louisville's Institutional Repository. This title appears here courtesy of the author, who has retained all other copyrights. For more information, please contact thinkir@louisville.edu.

ATMOSPHERIC NITROGEN ASSIMILATION IN
USTILAGO MAYDIS

By

Michael Cooper

A.S., Olympic College, Bremerton, WA 2001

B.S., Murray State University, Murray KY 2008

M.S., Murray State University, Murray KY 2013

A Dissertation

Submitted to the Faculty of the

College of Arts and Sciences of the University of Louisville

in Partial Fulfilment of the Requirements

for the Degree of

Doctor of Philosophy

in Biology

Department of Biology

University of Louisville

Louisville, KY

December 2015

ATMOSPHERIC NITROGEN ASSIMILATION IN
USTILAGO MAYDIS

By

Michael Cooper

A.S., Olympic College, Bremerton, WA 2001

B.S., Murray State University, Murray, KY 2008

M.S., Murray State University, Murray, KY 2012

A Dissertation Approved on

November 18, 2015

By the following Dissertation Committee:

Michael H. Perlin, Dissertation Director

James Graham

David J. Schultz

Joseph M. Steffen

Micah Worley

DEDICATION

The path on which I trod and that led me to this place started, ultimately, with the autism diagnosis my first son, Alexander, received when he was three years-old. The shape of this path has been influenced by others along the way, obviously, as I'm not defending a dissertation related to Autism Spectrum Disorder (ASD). I had already returned to Murray State University seeking to complete an undergraduate degree, at which I had failed at spectacularly in 1989, but that diagnosis spurred my pursuit of at least learning the molecular genetic and epigenetic language in which research on ASD is written.

A special thank-you to my wife, Jennifer, for all her support in completion of this endeavor.

ACKNOWLEDGEMENTS

I would like to thank my mentor, Michael Perlin, for his tireless efforts in helping the completion of this work. Not everyone would be as willing to help a student pursue such a hypothesis as this. I deeply appreciate it. Thanks also to Martin Klotz who initially drew me into the Biology Department at the University of Louisville. Thanks to James Graham, David Schultz, Joseph Stephan and Micah Worley for not only agreeing to serve on my committee but for all the helpful suggestions along the way. From Murray State University I appreciate the help I received from Harry Fannin and Tim Johnston in the form of advice and, in Tim Johnston's case, access to the bacterial strains and various nitrogenase primers I'd used in pursuit of my Master's Degree. Last but not least, thanks to José Ruiz-Herrera for his FB2 and 1/2 *Ustilago maydis* strains.

ABSTRACT

ATMOSPHERIC NITROGEN ASSIMILATION IN *USTILAGO MAYDIS*

Michael R. Cooper

November 18, 2015

Nitrogen is an essential nutrient for all living creatures. Ammonium is one of the most efficiently used and thus preferred, sources of nitrogen. As with other dimorphic fungi, yeast-like cells of *Ustilago maydis*, a fungal pathogen of maize, switches to filamentous growth when starved for nitrogen/ammonium. *U. maydis* carries two genes, *ump1* and *ump2*, encoding ammonium transporters that facilitate both uptake of ammonium and the filamentous response to its absence. While no obvious phenotype is observed when *ump1* is deleted, cells without *ump2* are unable to filament in response to low ammonium, although they can still grow. Surprisingly, *ump1ump2* double mutants can also grow on low ammonium. More amazing still, both wild-type and mutant cells continue to grow, even after strenuous efforts were made to remove all nitrogen sources from their growth media.

To further investigate these unusual observations, we examined the growth character of cells in various low and no-ammonium conditions with variable glucose concentrations, examined isotopic enrichment employing $^{15}\text{N}_2$ gas as a tracer and D-[U- ^{13}C]Glucose, conducted PCR screenings and evaluated the possibility of an endosymbiont. The $\Delta ump1\Delta ump2$ mutant appeared to produce longer cells than the wild-type and achieved higher titers under 50 mM glucose with no ammonium. That mutant

also incorporated more ^{15}N than the wild-type in liquid culture under low and non-ammonium conditions. Cells passed through serial treatments of high levels of antibacterial compounds persisted in growth and ^{15}N accumulation. PCR results indicated there was neither prokaryotic 16S rDNA nor the gene for dinitrogenase reductase, typical of prokaryotic diazotrophs.

Overall our studies indicate the novel discovery of an unknown nitrogen fixation system in *U. maydis*. While the molecular mechanism remains unresolved a metabolic capacity to convert dinitrogen into nitrogen that is bioavailable natively in a eukaryotic system holds the potential to change our understanding of the biogeochemical cycling of nitrogen. Moreover, these findings also present a potential way to reduce the anthropogenic contribution of organic nitrogen that is a large contributor to the accretion of eutrophication, “dead zones”, in our coastal waters and large lake system.

TABLE OF CONTENTS

DEDICATION.....	iii
ACKNOWLEDGEMENTS.....	iv
ABSTRACT.....	v
LIST OF TABLES.....	ix
LIST OF FIGURES.....	x
LIST OF APPENDICES.....	xii
CHAPTER I	
GENERAL INTRODUCTION.....	1
Plantae and Fungi Origins.....	1
Fungal Plant Pathogens.....	4
Ustilago maydis.....	6
Ammonium Transporters.....	12
The Nitrogen Cycle.....	15
Research Interest and Hypothesis.....	22
CHAPTER II	
CHARACTERIZATION OF GROWTH.....	24
Summary.....	24
Introduction.....	25
Material and Methods.....	27
Results.....	28
Discussion.....	43
CHAPTER III	
CHARACTERIZATION OF ATMOSPHERIC NITROGEN ASSIMILATION.....	47
Summary.....	47
Introduction.....	48
Material and Methods.....	50
Results.....	53
Discussion.....	57
CHAPTER IV	
POTENTIAL PROKARYOTIC SYMBIOSIS.....	61
Summary.....	61
Introduction.....	61

Material and Methods	63
Results.....	69
Discussion.....	76
CHAPTER V	80
GENERAL CONCLUSION.....	80
REFERENCES	87
APPENDICES	99
CURRICULUM VITAE.....	129

LIST OF TABLES

Table 1. Summary of Cell Lengths by Strain, Ammonium and Glucose Concentrations.	39
Table 2. SIRMS Comparing tracer vs. no-tracer of strains in SLAD broth with no-ammonium.	53
Table 3. Incorporation of 15N and 13C in liquid media.	56
Table 4. Incorporation of 15N and 13C on solid media.	57
Table 5. Primers to interrogate <i>Ustilago</i> for a diazotroph.	65
Table 6. SIRMS values from protein samples derived from chamber-grown no-ammonium SLAD agar plates.	70
Table 7. Summary of BLAST search results on obtained sequence data.	75
Table 8. Studies involving subcultured isolates cultivated using N-free media.	83
Table 9. Unused Primers for qPCR.	99
Table 10. Top 11 Loci Selected for Use in Golden Gate Reactions.	107
Table 11. Primers for Golden Gate Cloning.	120
Table 12. Transformant Screening Primers.	123

LIST OF FIGURES

Figure 1. Simplified overview of the evolution of Plantae and Fungi with estimated timings of major events.	4
Figure 2. Huitlacoche at market. (photo by Maureen Gilmer, 2013)	7
Figure 3. <i>Ustilago maydis</i> lifecycle, demonstrating infection trajectory.....	9
Figure 4. <i>U. maydis</i> colonies grown on synthetic low ammonium dextrose (SLAD) under low nitrogen conditions. A) wild-type strain 1/2. B) $\Delta ump1$ mutant C) $\Delta ump2$ mutant D) $\Delta ump2$ complemented with wild-type copy of <i>ump2</i> . (Smith, 2003).....	12
Figure 5. The transport of ammonium through an AmtB monomer of <i>Escherichia coli</i> . Ammonium binds, and then is deprotonated. Ammonia transits through the hydrophobic channel and is reprotonated upon exit. (Khademi and Stroud, 2006).....	15
Figure 6. Proportional elemental composition by mass of a <i>Saccharomyces cerevisiae</i> cell.	16
Figure 7. The essential biotic nitrogen cycle, adapted from (Klotz and Stein, 2008).....	18
Figure 8. Cellular morphology of <i>U. maydis</i> strains FB1 and $\Delta ump1, \Delta ump2$ in SLAD.....	29
Figure 9. FB1 wild-type growth curves in SLAD with 2% glucose under various ammonium concentrations. (n=3).....	30
Figure 10 $\Delta ump1, \Delta ump2$ growth curves in SLAD with 2% glucose under various ammonium concentrations. (n=3).....	31
Figure 11. Comparative growth curves between strains in SLAD with either 100 or 50 μ M ammonium.	33
Figure 12. Comparative growth curves between strains in SLAD with either 25 or 10 μ M ammonium.	34
Figure 13. Comparative growth curves between strains in SLAD with no ammonium.	35
Figure 14. Direct counts, by hemacytometer, of strains grown in SLAD broth with 100 μ M or no-ammonium by glucose concentrations.....	37
Figure 15. Direct counts, by hemacytometer, of strains grown in SLAD broth by glucose concentrations with 100 μ M or no-ammonium.....	38
Figure 16. Comparison of cell length distributions between strains in SLAD with 100 mM glucose under low (100 μ M) and no-ammonium concentrations. The p values indicate the result of a single-factor ANOVA between strains based on length (n=200).....	40
Figure 17. Comparison of cell length distributions between strains in SLAD with 50 mM glucose under low (100 μ M) and no-ammonium concentrations. The p values indicate the result of a single-factor ANOVA between strains based on length (n=100).....	41
Figure 18. Comparison of cell length distributions between strains in SLAD with 5 mM glucose under low (100 μ M) and no-ammonium concentrations. The p values indicate the result of a single-factor ANOVA between strains based on length (n=100).....	42
Figure 19. Comparison of cell length distributions within each strain in SLAD broth under glucose concentrations by ammonium. The p values indicate the result of a single-factor ANOVA based on length by glucose concentrations (n=100 except for 100 μ M ammonium, 100 mM glucose in each strain where n=200).	43
Figure 20. Comparison of $\delta^{15}\text{N}$ values across liquid media conditions.....	55
Figure 21. Absorbance (A_{600}) of cured versus uncured <i>U. maydis</i> strains in no-ammonium SLAD broth. ..	69
Figure 22. Gel electrophoresis results following PCR using CRR-14, CRR-15, <i>U. maydis</i> FB1 and FB2 strains as templates with nifHF/nifHR and i37F/i37R primer combinations.	72
Figure 23. Gel electrophoresis results following PCR using CRR-15, <i>U. maydis</i> FB1 and FB2 strains as templates with a38F/a39R, nifHF/nifHR and 68F/1392R primer combinations. The annealing temperature was 56°C.	73

Figure 24. Gel electrophoresis results following PCR using CRR-14, CRR-15, *U. maydis* FB1 and FB2 strains as templates with nifHF/nifHR, p3F/p4R and p5F/p6R. Annealing temperature was 60°C.....74

Figure 25. Dilution series using universal, prokaryotic 16S rDNA primers. There appeared to be some competitive interference from FB1 chromosomal DNA, but the expected-sized fragment was consistently detected.76

Figure 26. Corn biomass by nitrogen availability and infection status.....127

LIST OF APPENDICES

Primers	99
Sequence Data	100
Golden Gate Cloning	106
Growth of <i>Zea mays</i> under nitrogen starvation	124

CHAPTER I

GENERAL INTRODUCTION

Plantae and Fungi Origins

We live in the microbial world. Every interaction with the natural world involves microbial interactions from the endosymbiont that makes aerobic respiration possible to the thermophiles whose enzymes we've learned to turn into molecular tools. Even the evolution of sexual reproduction could have been an answer to adaptation for viral and microbial pathogen defense as illustrated by the Red Queen Hypothesis reflecting that our most essential sexual identity remains an adaptive strategy to evade pathogens. Our ability to assimilate carbon and micronutrients efficiently relies on a complicated intestinal flora community. The nitrogen that is required for all amino acids is fixed from atmospheric dinitrogen by diazotrophs and recycled by denitrifiers where not directly made available as nitrate, nitrite or ammonium. These fundamental biogeochemical cycles are ancient and that essential metabolic activity became established before the cell.

Some 3.8 billion years ago (BYA) the first free-living cells are thought to have emerged from acellular aggregates which arose from prebiotic self-replicating systems contained within inorganic metal-sulfide compartments embedded within the walls of hydrothermal chambers. While still under investigation, these iron-sulfide-walled chambers contained a chemiosmotic gradient within which rudimentary chemolithotrophy and primitive self-catalyzing RNA could have begun the first metabolic cycles (Martin and Russell, 2003). The Iron-Sulfur-World hypothesis, initially

proposed by Wächtershäuser (Wächtershäuser, 1988) enjoys more recent support through work indicating that supercritical steam that would be present in hydrothermal vents does not interact with the pyrite (FeS_2) walls as does water at STP (standard temperature and pressure) such that the binding sites of iron are much more exposed and available, including at reactive point defect sites, for proto-organic interactions (Stirling et al., 2015). Those interactions along with sulfur-dependent fixation of carbon eventually resulted in the RNA World (Gesteland and Atkins, 1983), where RNA is thought to have evolved prior to DNA, first suggested in 1968 (Boyer, 1968; Crick, 1968; Orgel, 1968), though another type of self-catalytic information storage vehicle likely preceded RNA, perhaps a peptide nucleic acid (Egholm et al., 1992).

From these chambers those first cells, eubacteria, are thought to have arisen and from those eubacteria the neomura clade to which archaeobacteria and eukaryotes belong (Cavalier-Smith, 2002b). This transition, about 1 BYA, included the crucial incorporation, characterized by Cavalier-Smith as enslavement, of a photosynthetic purple non-sulfur α -proteobacterium which became mitochondria (Cavalier-Smith, 2006). Chloroplasts are thought to have joined the emerging Plantae lineage some 580 (million years ago) MYA from a cyanobacterial symbiont (Cavalier-Smith, 2002a).

The first eukaryotes to appear were likely substrate-associated heterotrophic ameboflagellates which diverged into two eukaryotic supergroups, the unikonts and bikonts (Cavalier-Smith, 2009). This division is characterized by whether or not the early proto-eukaryotes possessed a single or no emergent flagellum, the unikonts, or had two flagella, the bikonts. From the unikonts arose the podiates, those that evolved pseudopodia for benthic feeding, giving rise to Animalia and Fungi while corticates,

evolved from the bikont lineage that developed cortical alveoli, represent the ancestors of Plantae (Cavalier-Smith, 2013; Cavalier-Smith et al., 2014). The divergence between unikonts and bikonts is thought to have occurred some one billion years ago, at the dawn of Neoproterozoic (Knoll, 1992; Simon et al., 1993). Most recently the divergence of the Ascomycota and Basidiomycota is reported to have occurred around 642 MYA (Beimforde et al., 2014). Monocots and eudicot divergence is estimated at 206 MYA (Taylor and Berbee, 2006). From molecular analyses combined with the fossil evidence of arbuscular mycorrhizae associated with plant rhizomes there is strong evidence that green plants and fungi evolved together to cover the land. Vesicular-arbuscular mycorrhizae (VAM) has been dated to about 400 MYA coinciding, roughly with the appearance of the first land plants which has been placed at about 415 MYA (Simon et al., 1993); indicating that fungal-plant associations predated the emergence of vascular plants. This timeline is summarized in Figure 1.

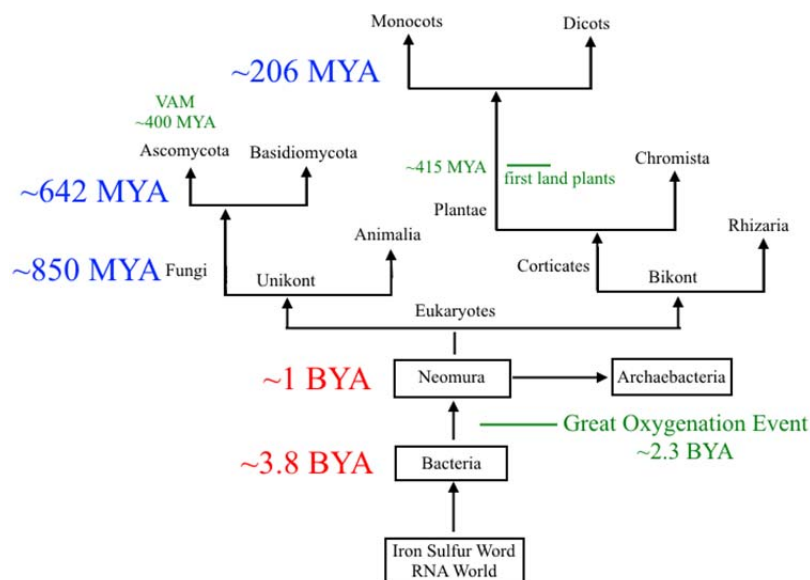


Figure 1. Simplified overview of the evolution of Plantae and Fungi with estimated timings of major events.

Fungal Plant Pathogens

There are an estimated 5.1 million species of fungi with an estimated 270,000 species associated with plants (Blackwell, 2011; Gauthier and Keller, 2013). Those species associated with plants represent over half of all identified fungal species of which there are currently 513,096 records that appear in the Index Fungorum [<http://apps.kew.org/herbtrack/search>]. The vast majority of these interactions are thought to be symbiotic in nature as all plants in the natural environment involved have been found to interact with fungi, be it endophyte, mycorrhizae or both (Rodriguez and Redman, 2008; Rodriguez et al., 2009), there are thousands that engage in pathogenic interactions. Of those plant-associated species approximately 10,000 have been identified as causing disease, most of those belonging to the divisions Ascomycota and Basidiomycota (Agrios, 2005). At least 46 of those plant-pathogenic Ascomycota are also able to cause disease in humans; a dramatic recent example was the 2012 outbreak of meningitis caused by *Exserohilum rostratum*-contaminated methylprednisolone acetate produced by the New England Compounding Center (Gauthier and Keller, 2013).

The mutualistic nature of the majority of fungal-plant interactions is perhaps best reflected in the current understanding of arbuscular mycorrhizal fungi (AMF) interactions with plants of agricultural interest. This appreciation of AMF is relatively recent and potentially will reap substantial benefits when employed with other sustainable farming practices. It is understood that AMF can enhance stress tolerance in plants as well as increase nutrient uptake from soil when combined with sustainable, low-tillage farming practices (Adesemoye et al., 2008; Lehman et al., 2012). Early symbiosis with emerging

vascular plant groups is thought to have had contributed greatly to success of plants. Symbiotes can contribute to nutrient acquisition via association with mycorrhizae, as mentioned, and host defense through the symbiotic endophytes found, so far, in all plants, mostly in the above-ground plant tissues (Faeth and Fagan, 2002). Agricultural application of AMF-enriched soil inoculum has also been demonstrated to increase crop yield, increase phosphorous mobilization as well as reduce nitrogen leaching losses (Bender and van der Heijden, 2015). As the climate continues to change it will likely become more important to understand and utilize these interactions in order to maintain and increase agricultural production in the face of a continually-expanding population.

In agriculture, fungal diseases represent the greatest economic losses as compared with other microbial-induced plant disease, estimated at more than \$200 billion per year (Horbach et al., 2011). Basidiomycota, the division in which mushrooms and the human pathogen *Cryptococcus* reside, includes those pathogens that cause rusts and smuts. Members of sub-division Pucciniomycotina, order Pucciniales (formerly Uredinales (Hibbett et al., 2007)) cause rust diseases, including *Microbotryum* sp., while members of sub-division Ustilagomycotina, order Ustilaginales cause smut diseases. While all smuts are autoecious, completing their lifecycle in a single host this isn't the case for all rusts, with many being autoecious, and some are heteroecious, having two or more hosts. Rusts are characterized by the appearance of pustules on leaves and, in some cases, other aerial parts of affected plants which are widely distributed, including trees, ornamental and crop plants. Within those pustules teliospores develop which produce basidia, completing the rust's lifecycle when those pustules burst. Smuts, on the other hand, primarily affect grasses, mostly attacking the ovaries and fruit, including those of

commercial import such as maize, sugarcane, wheat and barley and some species induce gall formation in which teliospores develop and in this form over-winter, then germinate and eventually burst, releasing haploid basidiospores that are wind-dispersed to begin the next generation.

Ustilago maydis

The Basidiomycota *Ustilago maydis* is one of the smuts that are of commercial concern. Unlike the other fungal infections of *Zea mays*, infection by *U. maydis* results in an edible delicacy that is very popular in Mexico, huitlacoche, also known as cuitlacoche, the “Mexican truffle” or “corn truffle;” the galls are harvested approximately three weeks post-infection, when the galls are still puffy and white prior to turning black. Figure 2 shows what these harvested galls look like at a market. While not entirely clear one possible origin for the term “huitlacoche” could be from Nahuatl, the Aztec language, with a root meaning “raven’s excrement.” Huitlacoche, with a taste that combines the flavor of mushrooms with corn, is also implicated as a possible “neutraceutical” with health benefits when incorporated into one’s daily diet (Valdez-Morales et al., 2010). Infected ears of corn sell for about fifty times that of uninfected corn in Mexico. It has even been employed as a labor-inducing agent by the Zuni Indians (Gilmore, 1919).



Figure 2. Huitlacoche at market. (photo by Maureen Gilmer, 2013)

In the United States it has been colloquially known as “Devil’s corn” and is considered part of agricultural loss. In 2012 total corn production in the United States and Ontario was 11.1 billion bushels. Loss to disease was more than 1.3 billion bushels with *Fusarium* stalk rot figuring the most predominantly in that that total at 124 million bushels lost. Corn smut was responsible for an estimated 83.9 million bushels (Mueller, 2013). One effort to combat that loss is the development of a transgenic maize, expressing the Totivirus antifungal protein KP4, which is highly resistant to corn smut (Allen et al., 2011). This transgenic maize leverages the proteins produced by *U. maydis* infected by the ds-RNA Totiviruses which acts to kill non-infected *U. maydis* (Allen et al., 2013). On the other hand, efforts to increase commercialization of huitlacoche in the United States continue as production is estimated to cost approximately \$6/kg whereas currently it sales to restaurants in the US for as much as \$30 to \$40/kg (Tracy et al., 2007).

Aside from interests associated with agriculture *U. maydis* has been the subject of years of genetics research. The most well-known research that was conducted using *U. maydis* and *Saccharomyces cerevisiae* remains the now-classical work demonstrating homologous recombination, specifically the demonstration of the intermediate form, the Holliday junction (Holliday, 1964). Since then *U. maydis* has been found to be a more appropriate model system for some mammalian cellular processes that are lacking in *S. cerevisiae* such as long-distance transport, mitosis and motor-based microtubule organization, regulation of cell polarity and even the possession of a functional homolog to mammalian *BRCA2* (Steinberg and Perez-Martin, 2008). From a practical perspective *U. maydis* is easily maintained in its haploid, yeast-like form, is amenable to genetic manipulation via homologous recombination, and is relatively easy to freeze for storage and to culture. The nuclear and mitochondrial genomes have been sequenced (Kämper et al., 2006), while work continues on annotation.

Common to all pathogenic Basidiomycota, parasitism is obligate in order for the organism to complete its lifecycle. *U. maydis*, like other biotrophic fungi, have a complicated lifecycle that requires a living host in order to complete sexual reproduction. It can reproduce by budding in its yeast-like state, as basidiospores/sporida which are readily propagated on plates or in broth, outside of a host, as illustrated in Figure 3, adapted from (Pataky, 2006). Compatible mating partners undergo conjugation, forming a dikaryon which infects the corn plant by appressorium formation, sending infectious hyphae into the plant where it acts endophytically, migrating to young leaves/reproductive tissues. When mated cells are introduced by damage to the corn plant, galls can and will form in any of the aerial tissues. Once tissue penetration has

occurred, gall formation is induced where, as the gall matures, plant cells are replaced with fungal cells. Teliospores form with the galls which, in natural infections, undergo meiosis after overwintering to form the basidium which give rise to the haploid basidiospores, also known as sporidia.

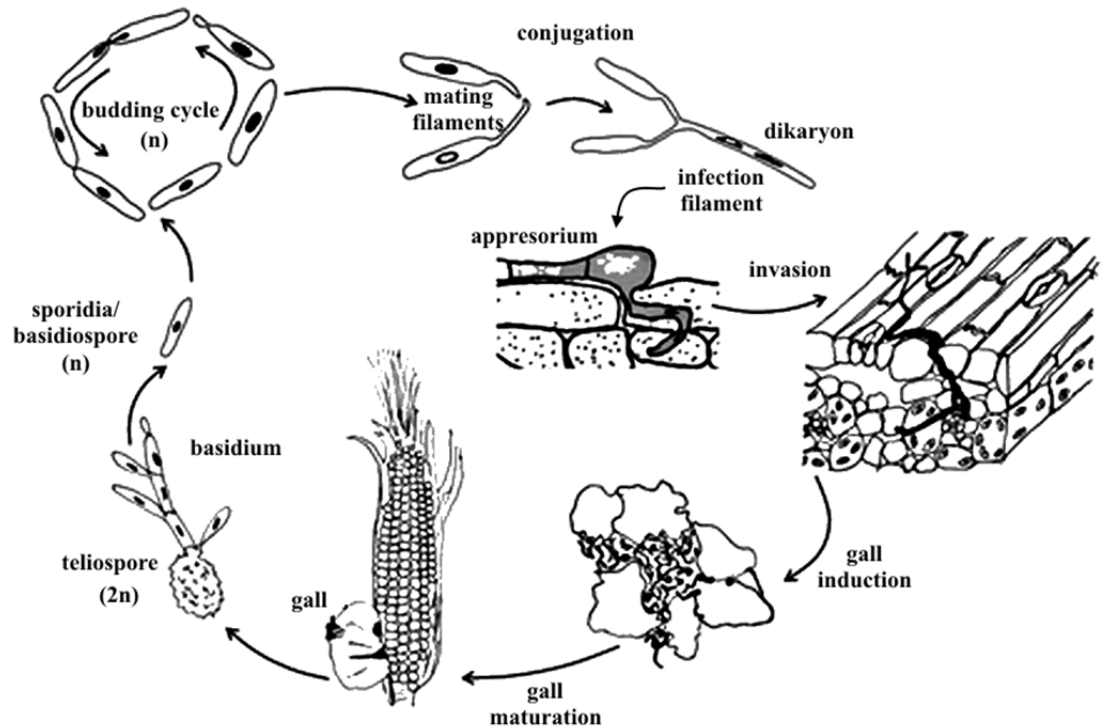


Figure 3. *Ustilago maydis* lifecycle, demonstrating infection trajectory.

Mating is a critical requirement for pathogenesis (Bolker et al., 1995). Whereas *S. cerevisiae* employs a bipolar mating system dependent on a single mating-type (MAT) locus *U. maydis* utilizes a tetrapolar mating system having two MAT loci. The *a* locus, of which there are two idiomorphs, *a1* and *a2*, where *a1* encodes three genes and *a2* has four functional genes and one pseudogene. The *a1* locus is 4.5 kilobases (kb) and the *a2* locus is about 8 kb. The *a1* and *a2* loci each encode both a pheromone that is secreted and receptor for the opposite locus' pheromone, *mfa1/2* and *pra1/2*, respectively. This approach to self, non-self recognition is analogous to what is seen in *S. cerevisiae* (Bolker

et al., 1995). Additionally the *a1* locus encodes the likely mitochondrial membrane target Rba1 whereas the *a2* locus encodes Lga2 and Rga2 along with the pseudogene *rba2* (Klosterman et al., 2007). Lga2 interferes with mitochondrial integrity such that it plays a role in uniparental mitochondrial inheritance (Mahlert et al., 2009). Rga2 appears to provide a protective effect to the parental cell possessing the *a2* locus such that preservation of the *a2* mitochondria is favored (Fedler et al., 2009). The *b* locus also engages in self/non-self-recognition but has, reliably, about 20 alleles, requiring a *bE* and *bW* from different parents in order to form a functional heterodimer. Each *bE* product must have a *bW* product from a different allele in order to form that heterodimer (Klosterman et al., 2007). The *b* locus interactions occur after conjugation tubes fuse and the nuclei are in close proximity in the newly-formed dikaryon. The N terminal interactions between complementary *bE*-*bW* pairs, able to bind DNA using homeobox domains at heterodimers, is well-described; however, the nature of nuclear localization has yet to be precisely described.

This dimorphic switch that enables the transition from yeast-like sporidia to filamentous conjugation partner and subsequent growth is initiated by both detection of pheromone from the opposite mating type and induced by nutrient deprivation. While conjugation is possible in nutrient replete media the proportion of conjugation events relative to the totality of the available mating partners is very low (Bowman, 1946). Induction by pheromone is by the well-described mitogen-activated protein kinase (MAPK) pathway resulting in transcription of *Prf1*, a transcription factor, which upregulates *bE/bW* expression, as well as many other mating-related genes, in a post-translational modification by c-AMP-dependent protein kinase *Adr1* and MAPK *Kpp2*

phosphorylation-dependent manner (Zarnack et al., 2008). The use of activated charcoal media for mating assays ensures sequestration of free ammonia, which may reduce conjugation, though it was initially suggested that the charcoal absorbs some secreted effector that suppresses filamentation (Day and Anagnost.SI, 1971). Successful mating on charcoal media is characterized by formation of white “fuzzy” aerial hyphae. As this switch is critical to pathogenicity there has been much work on various mechanisms that are involved, though nitrogen starvation appears to be the strongest condition.

Nitrogen deprivation induces filamentation in the absence of pheromone in wild-type haploid *U. maydis* strains. The high-affinity ammonium transporter, Ump2, is part of the filamentation response such that haploid mutants lacking *ump2* are unable to filament under low ammonium conditions (Figure 4). The low-affinity ammonium transporter, Ump1, is not required for starvation-induced filamentation while the double deletion of *ump1* and *ump2* results in abnormal filamentation under all conditions (Smith et al., 2003). Smith et al. (2003) also noted that the persistent growth of $\Delta ump1 \Delta ump2$, in low ammonium media suggested another unidentified mechanism for utilization of ammonium.

This transition to filamentous growth results in apical hyphal growth in which Golgi-derived secretory vesicles deliver cellular membrane constituents, exoenzymes, cell-wall synthesis enzymes to the Spitzenkörper, or vesicle supply center (VSC), from which secretion and extension of the hyphal tip originate (Steinberg, 2014). While this has specifically been studied in infectious hyphae the overall mechanisms involved in general hyphal growth can be expected to apply to starvation-induced filamentation. When grown on minimal agar media these vesicles are not readily viewable. In a minimal

liquid media, however, rather than discrete apical hyphal growth there is an apparent accumulation of large lipid-containing bodies throughout the cell (Klose and Kronstad, 2006). Those same lipid bodies, identified by Nile red staining, correspond to the endocytic vacuoles identified by Lucifer Yellow assays (Steinberg et al., 1998).

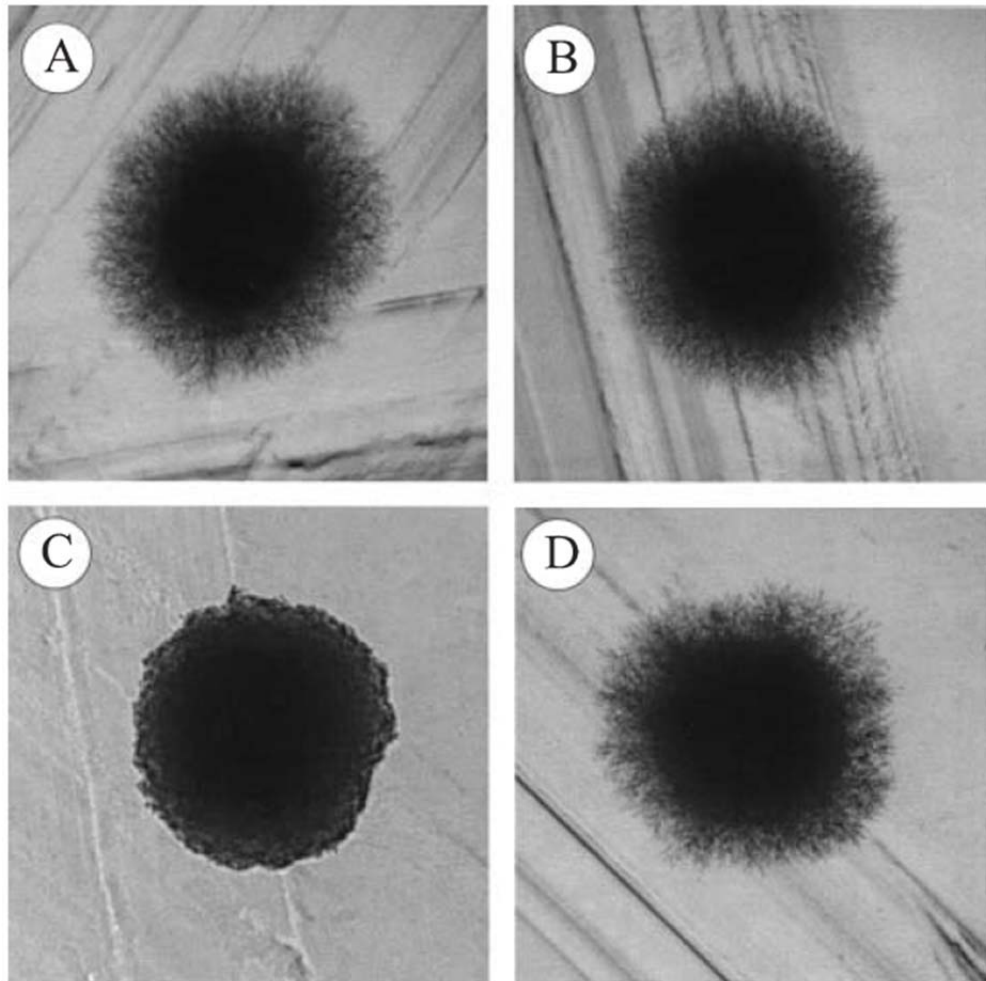


Figure 4. *U. maydis* colonies grown on synthetic low ammonium dextrose (SLAD) under low nitrogen conditions. A) wild-type strain 1/2. B) $\Delta ump1$ mutant C) $\Delta ump2$ mutant D) $\Delta ump2$ complemented with wild-type copy of *ump2*. (Smith, 2003)

Ammonium Transporters

High-affinity ammonium transporters, also called transceptors due to their signaling activity (Kriel et al., 2011), have been found to be necessary for the function of

the dimorphic switch not only in *Ustilago* but also in *Saccharomyces cerevisiae*, *Candida albicans* and *Cryptococcus neoformans* (Biswas and Morschhauser, 2005; Boeckstaens et al., 2007; Lorenz and Heitman, 1998; Rutherford et al., 2008; Smith et al., 2003). In those species disruption of the genes encoding the high-affinity ammonium transporter inhibited the ability to filament under nitrogen starvation, though this did not otherwise impair virulence under experimental conditions; presumably the lack of starvation-induced invasive filamentation would reduce pathogenicity under environmental conditions (Biswas and Morschhauser, 2005; Boeckstaens et al., 2007; Lorenz and Heitman, 1998; Rutherford et al., 2008).

This family of ammonium permeases share functional homology across all domains of life including the Rhesus blood group proteins. These are trimeric integral membrane complexes through which ammonium (NH_4^+) molecules are electrogenically transported unambiguously as determined in two *Archaeoglobus fulgidus* ammonium transporters utilizing solid-supported membrane (SSM)-based electrophysiology (Wacker et al., 2014). This same work determined a pH dependence on activity such that pH below 5.0 resulted in a drop-off of ammonium transport activity as well as high specificity for ammonium.

The current hypothesis for the mechanism of transport, reviewed in (Andrade and Einsle, 2007) and pictured in Figure 5, based on the resolved crystal structure of *A. fulgidus*, involves the binding of ammonium in an extracellular binding pocket in each monomer to the conserved residues Trp 137, forming a cation- π interaction with the Trp indole moiety, and hydrogen bonding with Ser 208. Phe 96 and Phe 204 block direct passage from that binding site thereby implying that conformational rearrangement is

required to open the channel. The channel is hydrophobic aside from two highly conserved histidines, so it is thought that ammonium must be deprotonated before being passaged and must be reprotonated following transport to be biologically useful. A secondary active, symporter function such that NH_3 / H^+ are transported across the membrane to the intracellular compartment seems to be the most likely model at this point (Andrade and Einsle, 2007).

In various filamentous pathogens, the filamentation response tends to be reduced or inhibited as a function of lowering pH (Wacker et al., 2014). This trend could reflect the impact of pH on the ability of active transporters to function in a more hydronium-rich environment. In contrast to that trend, haploid yeast-like budding *U. maydis* cells can be induced from the yeast-like budding form to the filamentous form under low pH conditions (Ruiz-Herrera and Leon, 1995).

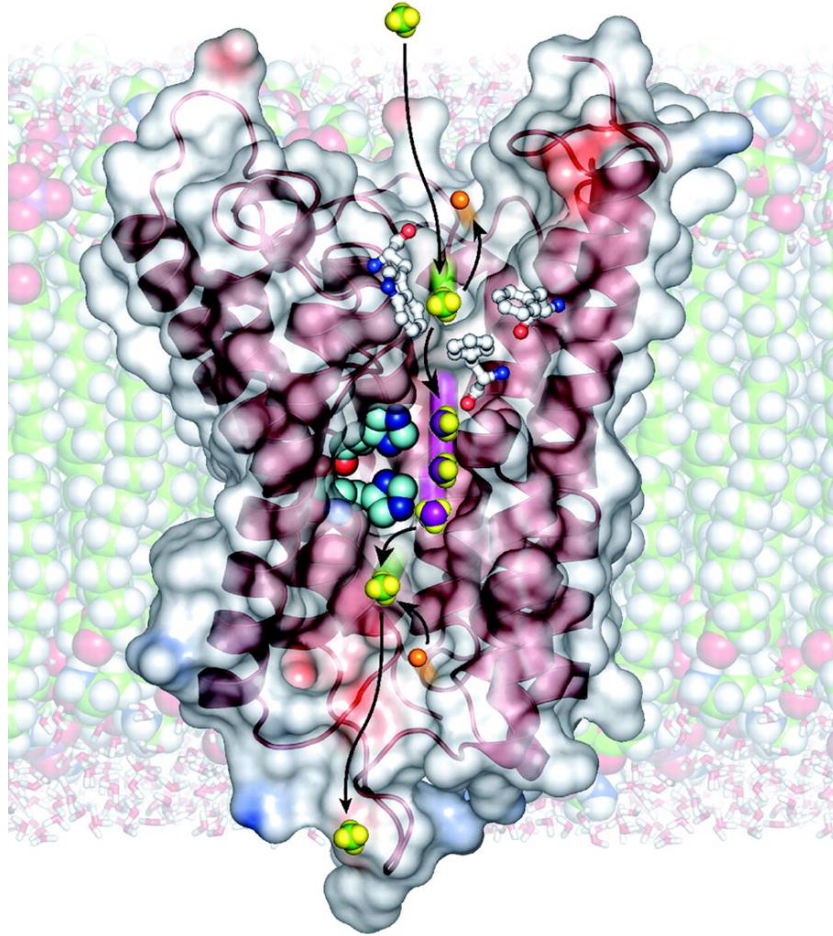


Figure 5. The transport of ammonium through an AmtB monomer of *Escherichia coli*. Ammonium binds, and then is deprotonated. Ammonia transits through the hydrophobic channel and is re protonated upon exit. (Khademi and Stroud, 2006)

The Nitrogen Cycle

Nitrogen is an essential element for all biological systems. Integral to all proteins and nucleic acids, nitrogen is one of the four most abundant elements comprising all living things (Figure 6) and is the most abundant element in the atmosphere. The presence of dinitrogen (N_2) in the atmosphere is thought to have been a natural consequence of the earliest accretion of matter that formed the Earth (Kasting, 1993)

originating with frozen NH_3 that was then oxidized in the mantle and subsequently outgassed as N_2 (Canfield et al., 2010).

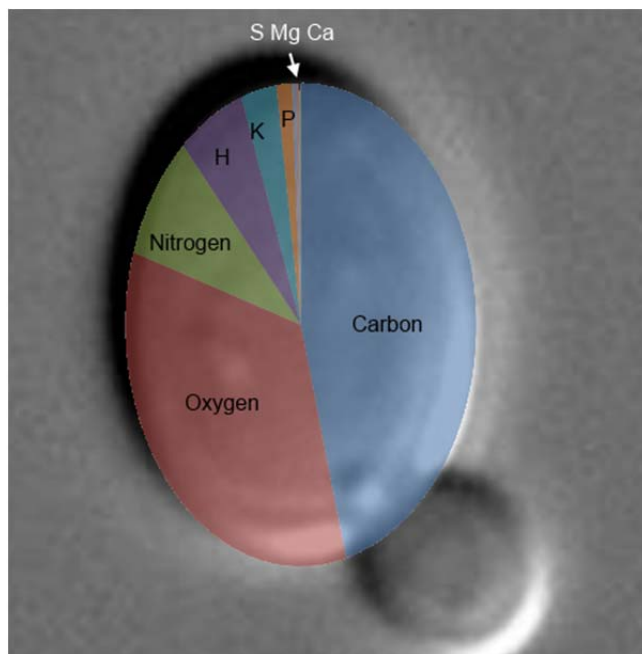


Figure 6. Proportional elemental composition by mass of a *Saccharomyces cerevisiae* cell.

The abiotic nitrogen reactions include atmospheric nitrogen fixation (N_2 to NH_4^+) through lightning and human activity, as well as occurring abiotically at hydrothermal vents. While there is not an estimate for annual global fixed nitrogen contribution by this process it is significant when considering biogenesis (Wächtershäuser, 2007). Dinitrogen (N_2) is also converted to NO , NO_2 (NO_x) and N_2O primarily through combustion reactions for power generation and transportation. The oxidation of NO_x to NO_3^- , in the form of nitric or nitrous acid, occurs in the upper atmosphere. Experimental evidence has demonstrated that a single-step conversion of NO to NH_4^+ is possible under conditions thought to be prevalent in Hadean hydrothermal vent strata (Martin and Russell, 2003), particularly dependent on interactions with FeS (Summers et al., 2012). Similarly

reduction of NO_2^- and NO_3^- to $\text{NH}_3/\text{NH}_4^+$ has been observed at 120°C by interaction with nanometer-sized FeS particles (Gordon et al., 2013). Iron oxides (with mixed Fe(II) and Fe(III) species) have been found to facilitate the aqueous reduction of NO_3^- to NH_4^+ , particularly at slightly acidic pH values (Etique et al., 2014) while NO_2^- has been found to react with magnetite (Fe_3O_4) and goethite ($\alpha\text{-FeOOH}$) yielding NO_x gasses (Dhakal et al., 2013).

Lightning strikes are estimated to contribute 8.6×10^6 metric tons of NO , NO_2 and N_2O to the atmosphere annually (Ott et al., 2010), which is estimated to be only approximately 10% of the NO_x and N_2O contributed by anthropogenic activity (Vitousek et al., 1997) which was estimated at 1.22×10^7 metric tons/year for N_2O alone in 2005 (Olivier et al., 2005). Total anthropogenic activity is estimated to contribute 2.1×10^8 metric tons of reactive nitrogen per year (Fowler et al., 2013). Industrial production of ammonia, by the Haber-Bosch process, which was approximately 1.76×10^7 metric tons in 2014, accounts for approximately 30% of the total, worldwide fixation of nitrogen alone (Smith et al., 2004). According to the Ammonia Industry (ammoniaindustry.com) this production is expected to about 2.5×10^7 metric tons by 2018. The vast majority of that production capacity is for use in agricultural applications. Unfortunately that increased use has dramatically increased the occurrence of dead zones by virtue of eutrophication which is accompanied by increased frequencies of harmful algal bloom occurrences (Howarth, 2008).

The metabolic pathways involved in the biotic nitrogen cycle, Figure 7, are represented in diverse organisms under diverse conditions. Nitrification and denitrification are primarily associated with ammonia-oxidizing bacteria (AOB) and

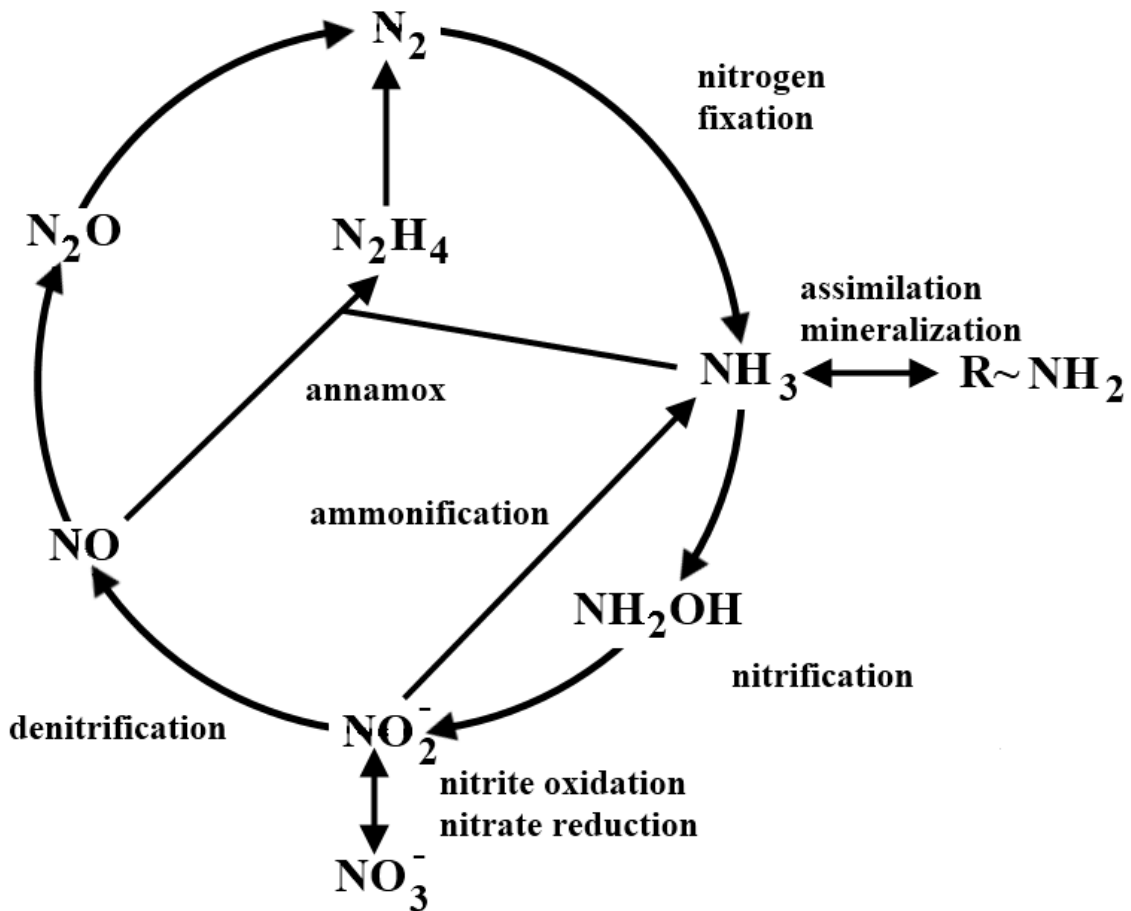


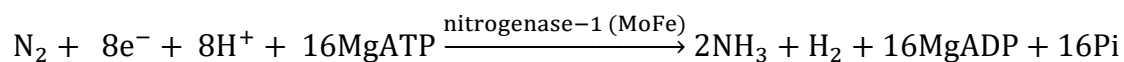
Figure 7. The essential biotic nitrogen cycle, adapted from (Klotz and Stein, 2008). nitrite-oxidizing bacteria (NOB) which oxidize ammonia to nitrite and nitrite to nitrate, respectively (Klotz and Stein, 2008). Nitrification is accomplished by beta- and gamma-proteobacteria as well as marine Crenarchaeota using related ammonia monooxygenase (AMO) inventories (Wuchter et al., 2006) which employs hydroxylamine as an intermediate and, therefore, requires hydroxylamine oxidoreductase (HAO) in order to extract electrons for both the regeneration of AMO as well as contribution to the quinone pool (Sayavedra-Soto et al., 1994). Nitrification is dependent on the availability of oxygen with some organisms able to nitrify under anoxic conditions when supplied with

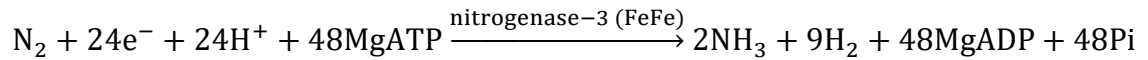
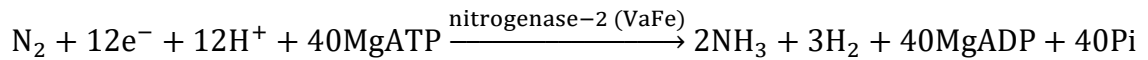
NO₂ (Schmidt et al., 2001). The classical denitrification pathway describes the use of nitrate as the terminal electron acceptor in the oxidation of organic matter under suboxic to anoxic conditions (Brandes et al., 2007). This produces dinitrogen gas. Incomplete denitrification results in nitrous oxide and is the product of detoxification. Biological nitrogen fixation (BNF) only occurs primarily through the use of the nitrogenase enzymes utilized by diazotrophs (nitrogen-fixing organisms) in archaea and bacteria and is the primary contributor of fixed nitrogen in the nitrogen cycle, including consideration of anthropogenic contributions, though, just more than half the total (2.4 x 10⁸ of 4.13 x 10⁸ metric tons/year) as of 2012 (Fowler et al., 2013).

Nitrogen Fixation

The first experimental demonstration of bacterial nitrogen fixation was reported in 1908 by the Dutch scientist, Martinus Beijerinck, (Beijerinck, 1908), based on bacterial cultures initially isolated in 1888, which turned-out to be *Rhizobium leguminosarum*. The bacteria and archaea that are able to fix nitrogen are known collectively as diazotrophs. This capacity is very widely dispersed among very disparate prokaryotic groups and the primordial nitrogenase-like enzyme system is thought to have had appeared more than 2.2 billion years ago (Boyd et al., 2011).

From that initial work, three closely-related nitrogenase complexes were identified. These are isozymes that differ by the metal ion cofactor that is required for their nitrogenase to function. Of these, Mo-Fe, Va-Fe and Fe-Fe, the Mo-Fe system has been characterized most thoroughly (Newton, 2007). These have been identified as nitrogenase-1 through nitrogenase-3, respectively and catalyze the following reactions:





The genes encoding the components of these nitrogenases are identified as *nif*, *vnf* and *anf*, corresponding to Mo-Fe, Va-Fe and Fe-Fe dependent nitrogenases.

All three nitrogenase complexes share the same essential arrangement.

Nitrogenase is a complex of dinitrogenase and dinitrogenase reductase. Dinitrogenase reductase, the Fe protein, is the electron donor to dinitrogenase which is the catalytic core of the enzyme complex. In the *nif* structural operon, for the MoFe complex, the Fe protein is encoded by *nifH* where two NifH proteins form a dimer comprising the assembled Fe protein. The catalytic core, dinitrogenase, is comprised of two heterodimers encoded by *nifD* and *nifK*. The products of those two genes form a heterodimer with two heterodimers assembling to form the dinitrogenase tetramer (Schindelin et al., 1997). Two Fe proteins interact with the tetramer to form the nitrogenase complex such that those Fe proteins do not interact with each other. The activity of the Fe proteins is dependent on its Fe₄S₄ cluster while the activity of dinitrogenase is dependent on the P cluster which receives the electrons imparted by the Fe₄S₄ cluster. The site of substrate reduction in the dinitrogenase is referred to as the FeMo-co (Seefeldt et al., 2009).

A fourth type of nitrogen fixing system, a superoxide dismutase-dependent MoFeS nitrogenase, was isolated from the thermophilic *Streptomyces thermoautotrophicus* and appears to have evolved independently of the other three systems (Ribbe et al., 1997). Unfortunately only a small number of gene and amino acid sequences have been reported with three primary components. ST1 is thought to functionally correspond to dinitrogenase and is a molybdenum-containing heterotrimer.

ST2, a homodimeric superoxidase oxidoreductase contains manganese and is thought to have the same function as dinitrogenase reductase. There is a third necessary component, a carbon monoxide dehydrogenase labeled ST3 (Swain and Abhijita, 2013).

The essential MoFe enzyme complex appears to have evolved within anaerobic archaea which was later laterally transferred to aerobic bacteria (Boyd et al., 2015). All three isozymes are very sensitive to oxygen such that oxygen binds irreversibly in the nitrogen binding site rendering that complex non-functional. Yet nitrogen fixation by obligate aerobes is ubiquitous among diazotrophs. Cyanobacteria, for example, in the genera *Anabaena* and *Nostoc* have differentiated heterocysts where nitrogen fixation is carried-out under oxygen-limited conditions. Cyanobacteria that do not form heterocysts control oxygen availability by limiting nitrogen fixation to periods of darkness. Diazotrophic facultative anaerobes in general have a regulatory mechanism which inhibits transcription of *nif* genes in the presence of oxygen. Among *Proteobacteria* NifA is the enhancer binding protein required to induce the conformational change in σ^{54} that allows it to transcribe the *nif* operon. NifA, in turn, is regulated in response to both fixed nitrogen and oxygen. When oxygen is present NifA is not transcribed (Martinez-Argudo et al., 2004).

Many characterized diazotrophs are engaged in symbiotic relationships with fungi and plants. The most well-known and characterized of these associations involve legumes and their root nodules in which *Rhizobia* species fix nitrogen, which benefits the plant, and receives carbon in exchange. A *Burkholderia* endosymbiont of the arbuscular mycorrhizal fungus *Gigaspora margarita* has been revealed to have the *nif* operon (Minerdi et al., 2001). *G. margarita* has also been found to harbor endobacteria

exhibiting nitrogenase activity where those endobacteria were identified as *Bacillus thuringiensis* (Cruz and Ishii, 2011).

No evidence supporting the existence of a nitrogen-fixing eukaryote has been found to date. The high diversity amongst diazotrophs combined with the high degree of and variety in symbiotic relationships between diazotrophs and various eukaryotes supports the idea that those relationships represent the most evolutionarily advantageous strategy facilitating survival in the face of limited reactive nitrogen resources. The closest to something that could be called eukaryotic nitrogen fixation in the literature is the vertically-transmitted endosymbiont found in the fresh-water diatom *Rhopalodia gibba* which appears derived from the free-living cyanobacterium *Cyanothece*, and which exists in the diatom as a “spheroid body” (Prechtel et al., 2004).

Research Interest and Hypothesis

The research presented in this dissertation is based on the initial observation that *U. maydis* mutants lacking ammonium transporters by virtue of having *ump1* and *ump2* deleted were able to grow at all in a minimal media having only ammonium as the source of nitrogen. Possible explanations for that ability include other unidentified transporters for assimilation of ammonium, contamination of such growth media by some other reactive nitrogen source, inclusion of an endosymbiont capable of fixing nitrogen or, more audaciously, a novel type of nitrogen fixation system that is able to facilitate the conversion of dinitrogen to a reactive nitrogen species able to be utilized by *U. maydis*.

Evidence supporting either an endosymbiont or a novel type of nitrogen fixation could have wide-ranging application to agricultural technology such that reduction of the use of synthetic nitrogen might be possible. This is particularly important since

biotechnological attempts to utilize the prokaryotic nitrogen fixation systems have continued to fail. A nitrogen fixation system that evolved in a eukaryote would be much more likely to be compatible with crop plants. Having a wider variety of crop plants able to fix their own nitrogen would reduce the need for synthetic nitrogen applications which, in turn, would reduce the input of excess reactive nitrogen into waterways, possibly ameliorating coastal and estuarine dead zones caused by eutrophication.

CHAPTER II

CHARACTERIZATION OF GROWTH

Summary

Ustilago maydis is capable of growth under minimal and no-ammonium conditions. Its growth rate and terminal titer were found to be dependent on the concentration of ammonium provided in the media. Growth rates of the two strains varied with ammonium concentration, except that no difference was observed between no-ammonium and 10 μ M ammonium. By absorbance (A_{600}) FB1 wild-type appeared to have an advantage over the mutant under high glucose with 10 μ M ammonium but this was not supported by direct count. The $\Delta ump 1, \Delta ump 2$ double mutant grew to higher concentrations than the wild-type when provided high (100 mM) or medium (50 mM) glucose in media without ammonium. The lengths of cells varied between the two strains with the $\Delta ump 1, \Delta ump 2$ double mutant found to be longer, on average, under all conditions except low ammonium, low glucose where the average lengths of the double mutant and wild-type were the same. The $\Delta ump 1, \Delta ump 2$ double mutant had a more variable length than the wild-type under all conditions. Overall the $\Delta ump 1, \Delta ump 2$ double mutant had an advantage in both the number of cells produced and cell lengths were greater than those of the FB1 wild-type under lower glucose, no-ammonium conditions.

Introduction

Completion of the reproductive lifecycle, in *Ustilago maydis* requires the transition from a budding, yeast-like sporidial form to a filamentous dikaryon. The dimorphic switch governing that transition is induced by both the presence of pheromone from cells of the opposite mating type as well as nutrient deprivation. The transition of haploid cells to the filamentous form has been readily observed in media in the absence of pheromone, particularly when that medium is nutrient deficient (Bowman, 1946).

A key component of this dimorphic switch of haploid cells to the filamentous form has been found to be dependent on the ability of *U. maydis* to respond to available ammonium. Homologs of the yeast methylammonium permeases (MEPs) have been characterized in *U. maydis*. The *ump1* gene (UMAG_04523) was found to encode a low-affinity ammonium transporter while the *ump2* gene (UMAG_05889) was determined to encode the high-affinity ammonium transporter (Smith et al., 2003). The Ump2 protein was specifically identified as the high-affinity ammonium transporter following measurements of the uptake of [¹⁴C]-methylammonium (methylamine). The uptake of methylamine in cells deleted for *ump2* was dramatically reduced whereas mutants lacking both ammonium transporters demonstrated a methylamine accumulation that was effectively zero. Further, cells deleted for *ump2* failed to filament on low ammonium medium, in contrast to the wild-type. Mutants deleted for both the *ump1* and *ump2* ($\Deltaump1, \Deltaump2$) tend to flocculate and sink in rich media and produce unusual, “tangled” filamentous colonies on low ammonium (Smith et al., 2003). Remarkably the double-mutant remained able to grow on low ammonium.

The role of these ammonium transporters in the dimorphic transition was further elucidated by confirmation that the signaling protein Rho1 directly interacts with both Ump1 and Ump2 (Paul et al., 2014). Rho1, a small GTPase, has been shown to localize at the growing tip and septum of *U. maydis* cells during cytokinesis as well as modulating *b*-induced filament formation (Pham et al., 2009).

That surprising observation, that the *U. maydis* $\Delta ump1, \Delta ump2$ double-mutant continued to not only be viable but also were able to grow in starvation nitrogen media (Holliday Salt Solution (Holliday, 1974) supplemented with 100 μM NH_4^+ in the form of ammonium sulfate), was initially described in 2003 (Smith et al., 2003). This prompted a series of experiments to investigate growth and morphology in various media, including low (100 μM , 50 μM , 25 μM and 10 μM NH_4^+) and no-ammonium, conditions to characterize this phenomenon.

Additionally, considering the metabolic cost of nitrogen fixation and further considering that the $\Delta ump1, \Delta ump2$ double deletion mutant was demonstrated to be unable to transport ammonium (Smith et al., 2003), growth of that mutant was examined under various glucose concentrations, 100mM, 50mM, 5mM and 0.5mM. This carbon source restriction was predicted to reduce cell density particularly in the $\Delta ump1, \Delta ump2$ mutant where ammonium was available in the media as compared to the FB1 wild-type. If there was a mechanism like diazotrophy (nitrogen fixation) involved in the growth of that mutant then it would be reasonable to conclude that such a process would impose a metabolic cost that may be observable.

Material and Methods

Strains and growth conditions. *U. maydis* strain FB1 wild-type (Banuett and Herskowitz, 1989) and FB1 $\Delta ump1, \Delta ump2$ (Smith et al., 2003) cells were grown in YPD (1% yeast, 2% peptone, 2% dextrose) at 27 °C, overnight, shaking at 200 RPM. All overnight cultures that were used as inocula for growth experiments were collected as pellets then washed twice with sterile water. Such inocula were then used at very low density, 10 μ l of the twice-washed overnight into 5 mL broth for a 1/500 dilution for approximately 16,000-24,000 cells/mL. Synthetic Low Ammonium Dextrose (SLAD) broth (0.17% Yeast Nitrogen Base Broth, 2% glucose except where indicated). Ammonium sulfate and dextrose was used at the concentrations indicated; (100, 50, 25, 10) μ M ammonium sulfate and (100, 50, 5) mM glucose.

Agrobacterium tumefaciens strain CRR-14, a diazotrophic obligate aerobe, was utilized as a positive biological control while *Dickeya chrysanthemi* (*Erwinia chrysanthemi*) strain CRR-15, a diazotrophic facultative anaerobe, was employed as a negative biological control as it has no capacity to protect its nitrogenase from oxygen and so is unable to fix nitrogen in an aerobic condition. CRR-14 and CRR-15 were obtained from Tim Johnston's lab at Murray State University as I characterized those strains while a student there, utilizing 16S rRNA DNA sequence data; CRR-14 having the accession number HM016242 and CRR-15 with HM016083 (Cooper, 2013). CRR-15, *Dickeya chrysanthemi* and CRR-14, *Agrobacterium tumefaciens*, were incubated under similar conditions as the *Ustilago* strains and employed as biological controls to ensure there is no nitrogen source contamination in the media.

Absorbance (A_{600}) and cell measurements. All A_{600} measurements were obtained on a NanoDrop™ 2000 UV-Vis Spectrophotometer [Thermo Fisher Scientific, Waltham, MA] and direct cell counts and measurements performed with a Spenser Bright-Line hemacytometer [American Optical Corporation, Buffalo, NY]. Absorbance measurements used three biological replicates. Measurements of length were made by using images of cells, captured through the ocular of a light microscope, an Olympus model CHB [Olympus America, Center Valley, PA], at 400x total magnification with a 13-megapixel digital camera, the Samsung Galaxy S4 [Samsung Electronics, Ridgefield Park, NJ], in a hemacytometer with each small grid line measuring 40 microns. The lengths of cells were recorded in pixels then converted to microns relative to the known grid line length using the freely-available program Paint.NET™ [dotPDN LLC, Kirkland, WA] after determination that JImage could not be used to successfully auto analyze the images. 100 measurements were taken of each strain in each condition and the resulting data were analyzed in R [The R Foundation for Statistical Computing] version 3.0.0 (released 4/3/2013) using single-factor ANOVA and data were plotted using the built-in boxplot function.

Results

Distinct growth observations of FB1 wild-type and $\Deltaump1, \Deltaump2$. As previously observed, FB1 wild-type grew in the “budding” phenotype, no filamentation or development of aerial hyphae, on nutrient replete solid media or in broth. Low to no-ammonium media induced filamentation in the wild-type on solid media but not in liquid media. Also as previously observed, the $\Deltaump1, \Deltaump2$ mutant did not produce normal filaments on solid media, nutrient replete or SLAD with minimal to no-ammonium. In

broth the haploid cells did not tend to develop filaments, though the $\Deltaump1,\Deltaump2$ mutant did tend to cluster and fall to the bottom of a resting broth as observed previously (Smith et al., 2003). Cells of both strains contained a series of vacuoles under nitrogen limitation. Figure 8 depicts the irregular morphology in both strains. The mutant $\Deltaump1,\Deltaump2$ did appear to have more cells of irregular length and arrangement than FB1 wild-type, though this is not obvious from this figure.

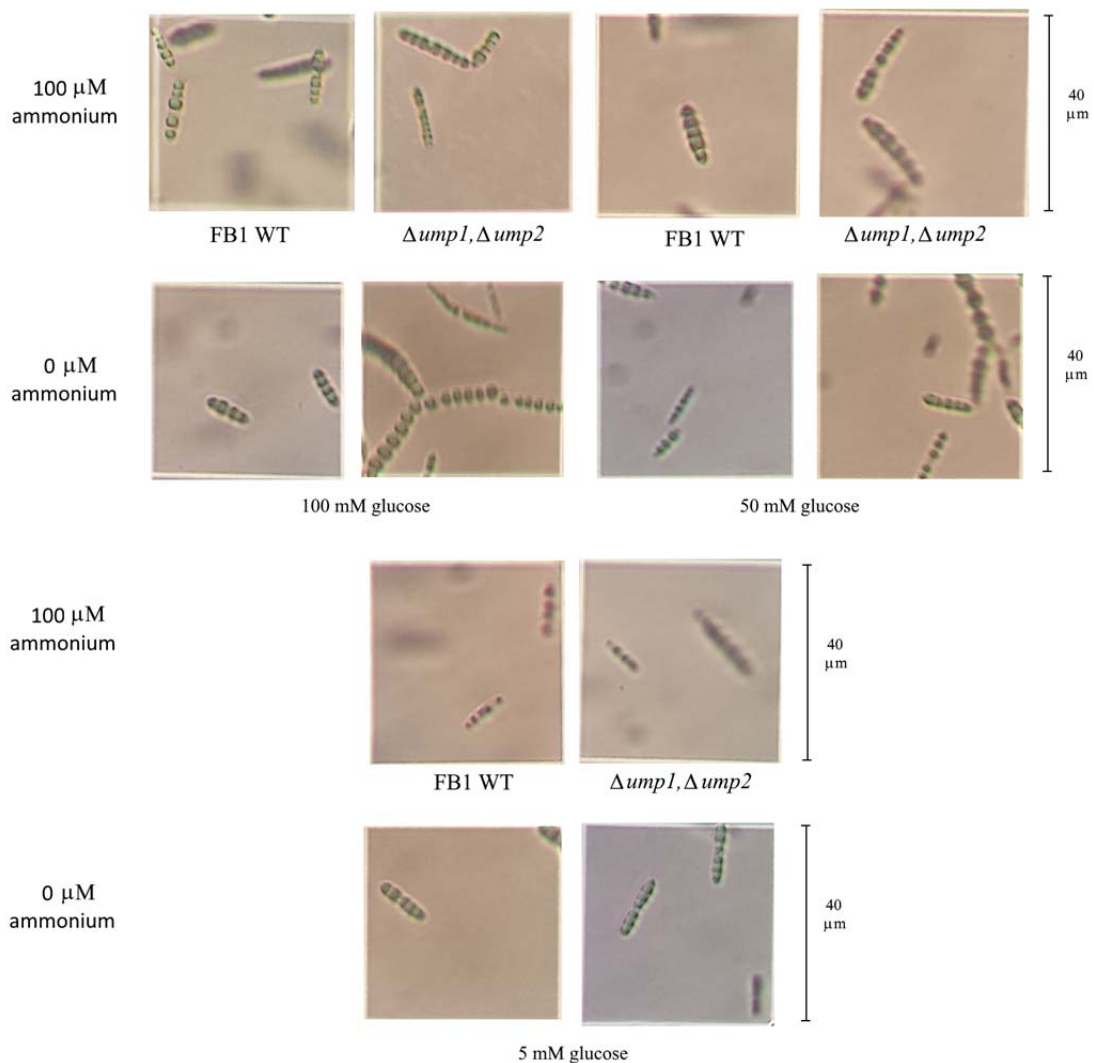


Figure 8. Cellular morphology of *U. maydis* strains FB1 and $\Deltaump1,\Deltaump2$ in SLAD under various low-ammonium and glucose concentrations.

Growth characteristics as assayed by absorbance (A_{600}). Under a gradient of ammonium the FB1 wild-type achieved, as depicted in Figure 9, approximately the same stationary-phase A_{600} under 100, 50 and 25 μM ammonium. There was no significant difference in stationary-phase A_{600} between 0 and 10 μM ammonium.

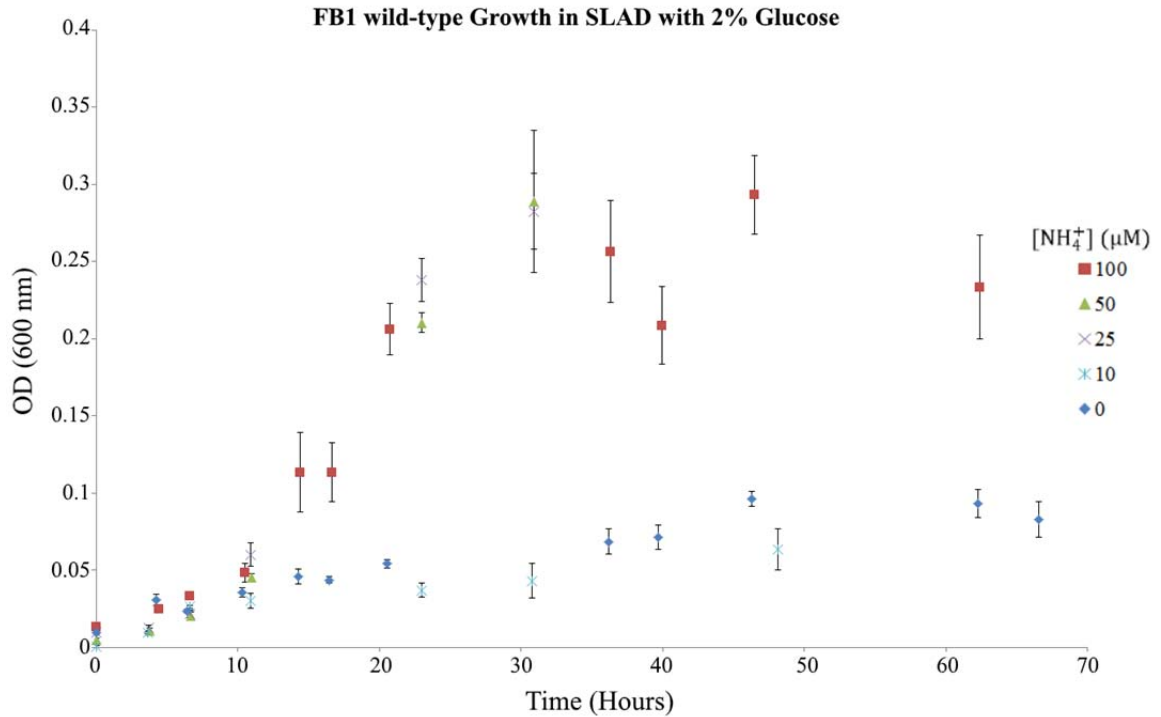


Figure 9. FB1 wild-type growth curves in SLAD with 2% glucose under various ammonium concentrations. (n=3)

At the upper ammonium concentration, wild-type FB1 produced a final average A_{600} of 0.27, while at the no and lowest ammonium concentrations, cells achieved a final stationary phase average A_{600} of 0.079. This corresponded to approximately 5.4×10^6 and 1.58×10^6 cells/mL, respectively. With an initial inoculum having an average A_{600} reading of 0.0074, corresponding to an estimated 1.48×10^5 cells/mL, this indicates about a 36-fold and 10-fold increase in cell density. These were only conservative approximations; however, as spectroscopic accuracy below 0.05 is not particularly robust.

The $\Delta ump1, \Delta ump2$ mutant behaved, in Figure 10, similarly to the FB1 wild-type in that concentration gradient, no significant difference was observed amongst 100, 50 and 25 μM ammonium ($p=0.35$) nor between 0 and 10 μM ammonium ($p=0.16$).

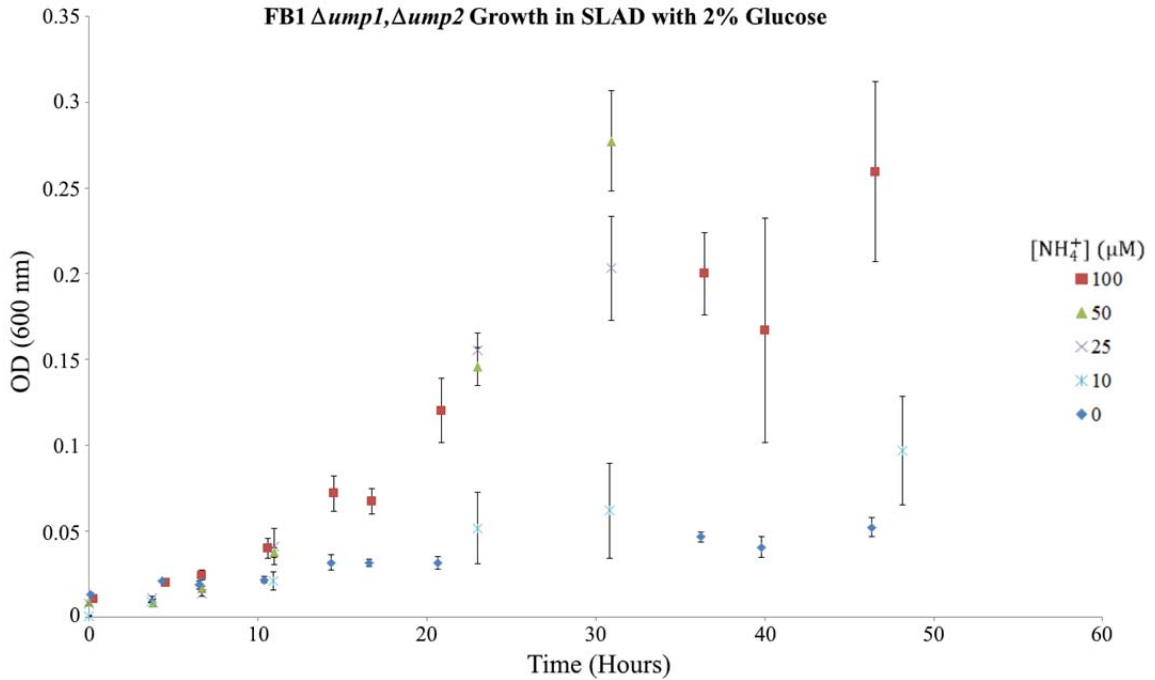


Figure. 10 $\Delta ump1, \Delta ump2$ growth curves in SLAD with 2% glucose under various ammonium concentrations. (n=3)

The final stationary phase average A_{600} reading for the upper ammonium treatments was 0.24 for an estimated 4.8×10^6 cells/mL and the no and lowest dosage average A_{600} of 0.076 for an estimated 1.52×10^6 cells/mL.

Comparing the growth curves between strains under the various ammonium conditions (Figures 11-13) demonstrated that while FB1 wild-type appeared to achieve a higher stationary phase A_{600} than $\Delta ump1, \Delta ump2$ mutant under 25 μM ammonium, but this difference was not statistically significant, whereas the stationary phase A_{600} of FB1

wild-type was significantly higher than that of the $\Deltaump1,\Deltaump2$ mutant when no ammonium was provided ($p=0.02$). The stationary phase A_{600} of the $\Deltaump1,\Deltaump2$ mutant trended higher under 10 μ M ammonium, though this difference was not statistically significant.

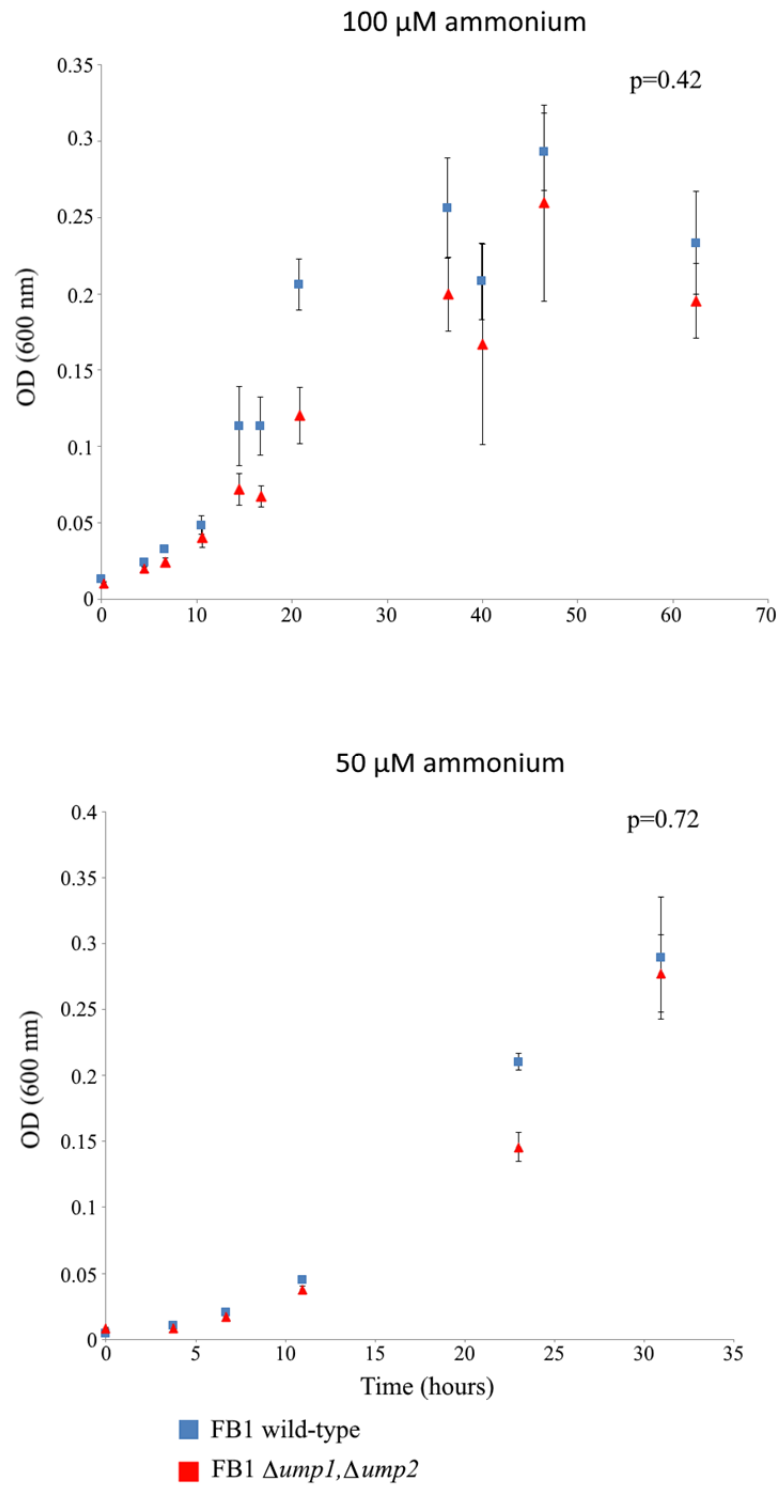


Figure 11. Comparative growth curves between strains in SLAD with either 100 or 50 μ M ammonium.

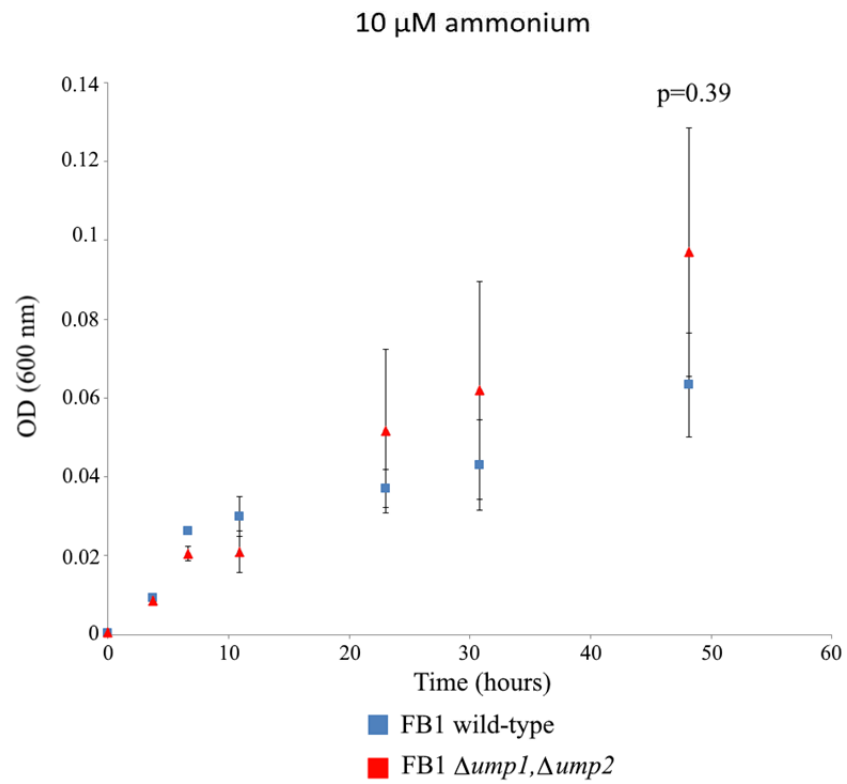
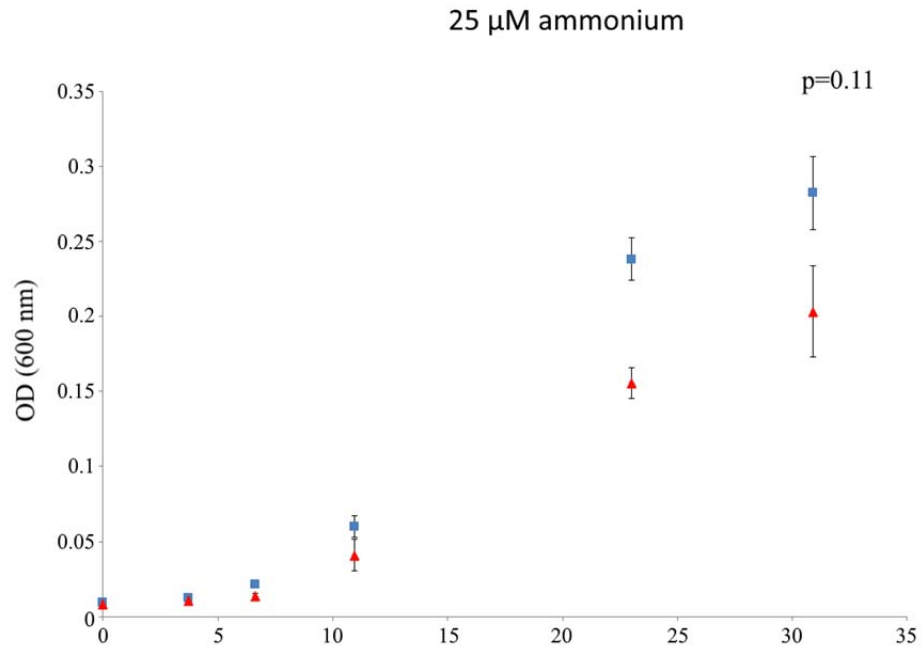


Figure 12. Comparative growth curves between strains in SLAD with either 25 or 10 μM ammonium.

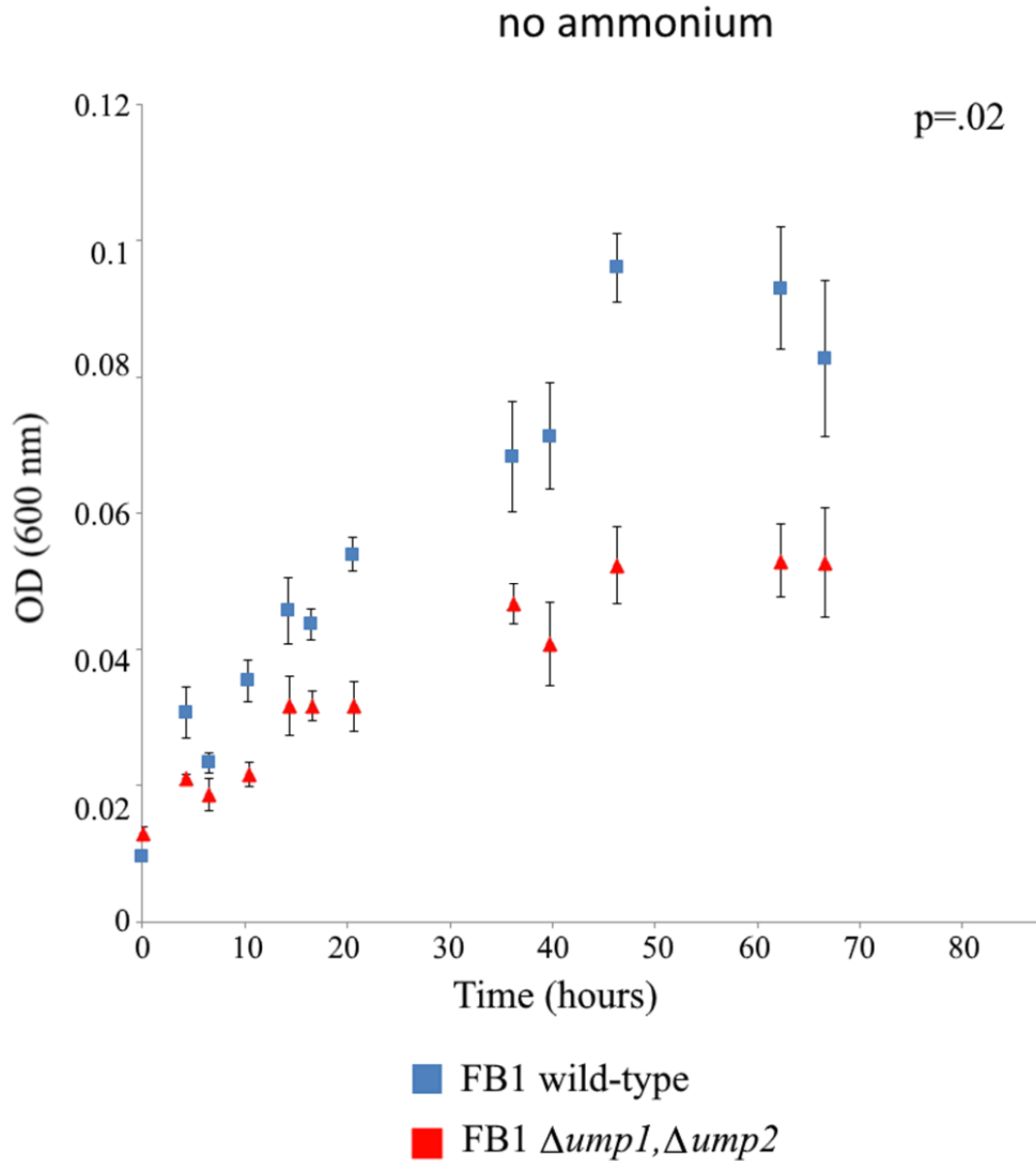


Figure 13. Comparative growth curves between strains in SLAD with no ammonium.

Direct counts of cells. Based on the observation of irregular cell sizes, depicted in Figure 6, direct cell counts were used as an alternative to A_{600} measurements. Figure 14 provides comparisons of cell counts for FB1 wild-type and the $\Deltaump1, \Deltaump2$ double mutant grown in medium either with no or low (100 μ M) ammonium, with glucose concentrations also being varied for each ammonium concentration; high (100 mM), medium (50 mM) and low (5 mM). A glucose concentration of 0.5 mM was attempted

under low and no-ammonium conditions. No growth was observed after 72 hours. These experiments revealed that, under no-ammonium conditions, there was a higher density of cells in the cultures of $\Deltaump1,\Deltaump2$ cells with concomitant high and medium glucose levels as compared to the FB1 wild-type under the same conditions (Figures 14 and 15). Overall, there was a higher density of cells under low ammonium as compared to no-ammonium media, and this was not different between strains for each glucose condition. Interestingly, while there was no significant difference over the gradient of glucose under the no-ammonium condition for $\Deltaump1,\Deltaump2$, there was not a statistically significant trend towards increased cell counts in low ammonium as glucose concentrations in the media increased. When considering the counts of cells by strain and ammonium across the glucose gradient there was no significant difference between low and no-ammonium conditions by strain under 5 mM glucose though there was a trend towards higher cell density under low ammonium. Under 50 mM or 100 mM glucose there was no significant difference between strains under the low ammonium condition. There was a significant difference between the strains in no-ammonium with $\Deltaump1,\Deltaump2$ achieving a higher overall density than wild-type at 50 mM ($p=0.03$) and 100 mM glucose ($p=0$).

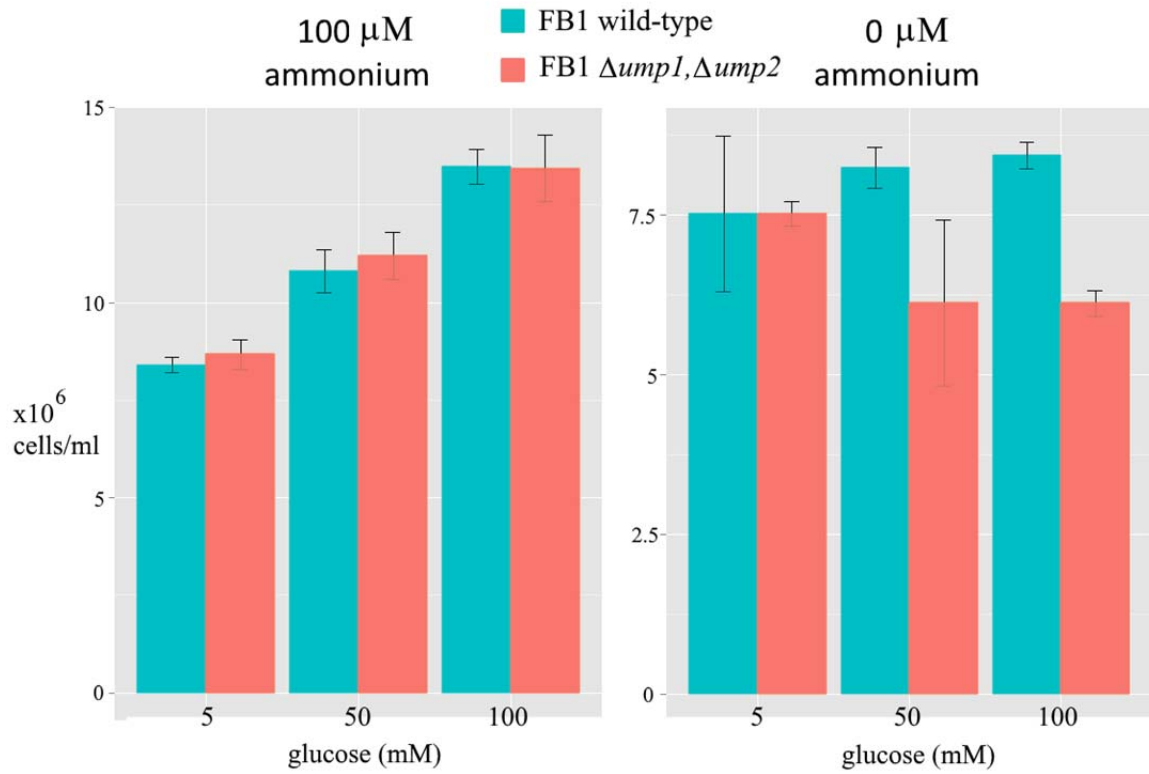


Figure 14. Direct counts, by hemacytometer, of strains grown in SLAD broth with 100 μM or no-ammonium by glucose concentrations.

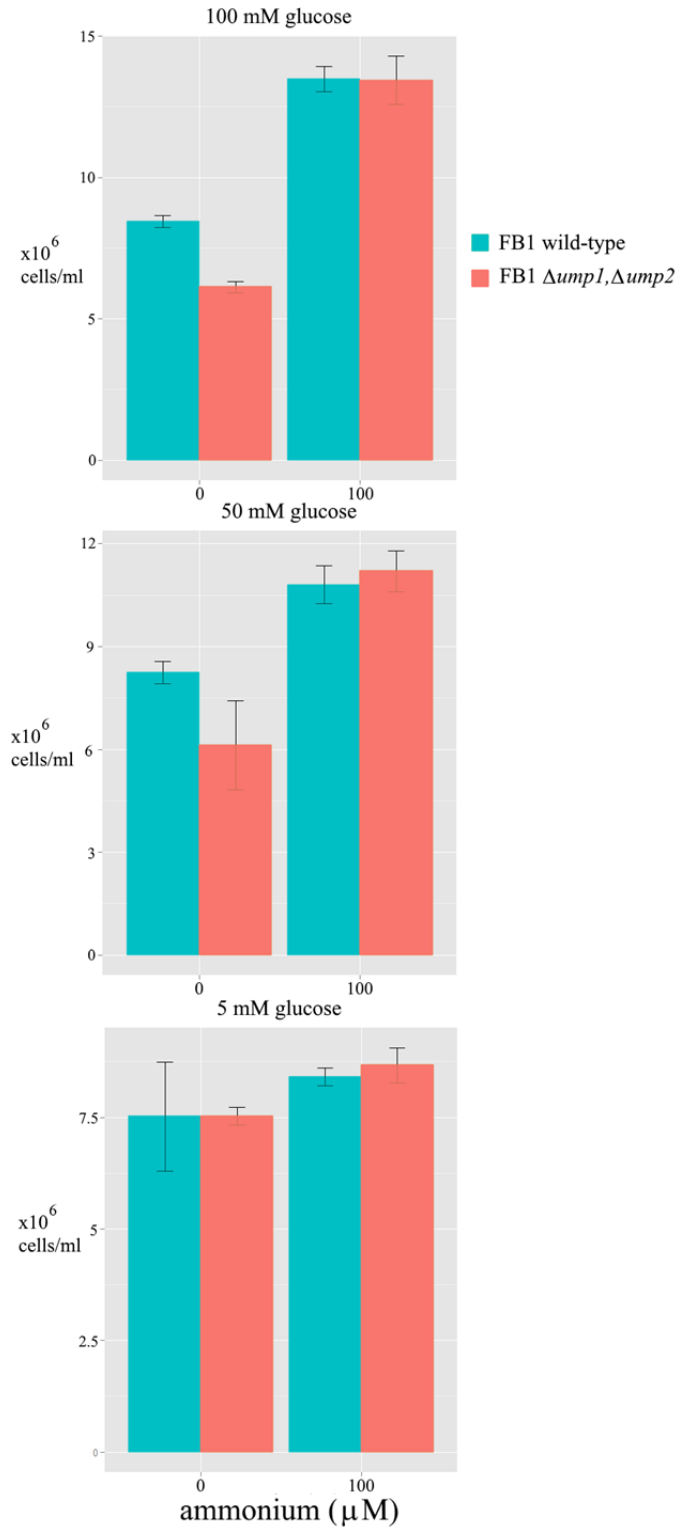


Figure 15. Direct counts, by hemacytometer, of strains grown in SLAD broth by glucose concentrations with 100 μM or no-ammonium.

Cell lengths under various conditions. Table 1 summarizes the means and standard deviations of measurements obtained by strain as well as by ammonium and glucose concentrations. The double-mutant tended to be longer than the wild-type under each glucose condition in the presence or absence of ammonium (Figures 16-18) with the exception of low (5 mM) glucose as indicated in Figure 18. Glucose concentration did not have a statistically significant effect on cell length in either the low or no-ammonium condition within each strain (Figure 19).

Table 1. Summary of Cell Lengths by Strain, Ammonium and Glucose Concentrations.

Strain	ammonium (μM)	glucose (mM)	average length (μm)	standard deviation (μm)	number of measures
FB1 wild-type	100	100	11.45	2.89	200
$\Deltaump1, \Deltaump2$	100	100	12.81	4.3	200
FB1 wild-type	100	50	11.92	2.59	100
$\Deltaump1, \Deltaump2$	100	50	12.91	3.75	100
FB1 wild-type	100	5	12.18	3.03	100
$\Deltaump1, \Deltaump2$	100	5	12.16	2.66	100
FB1 wild-type	0	100	10.21	1.94	100
$\Deltaump1, \Deltaump2$	0	100	13.65	4.44	100
FB1 wild-type	0	50	10.63	2.14	100
$\Deltaump1, \Deltaump2$	0	50	14.6	6.04	100
FB1 wild-type	0	5	10.46	2.31	100
$\Deltaump1, \Deltaump2$	0	5	13.98	5.74	100

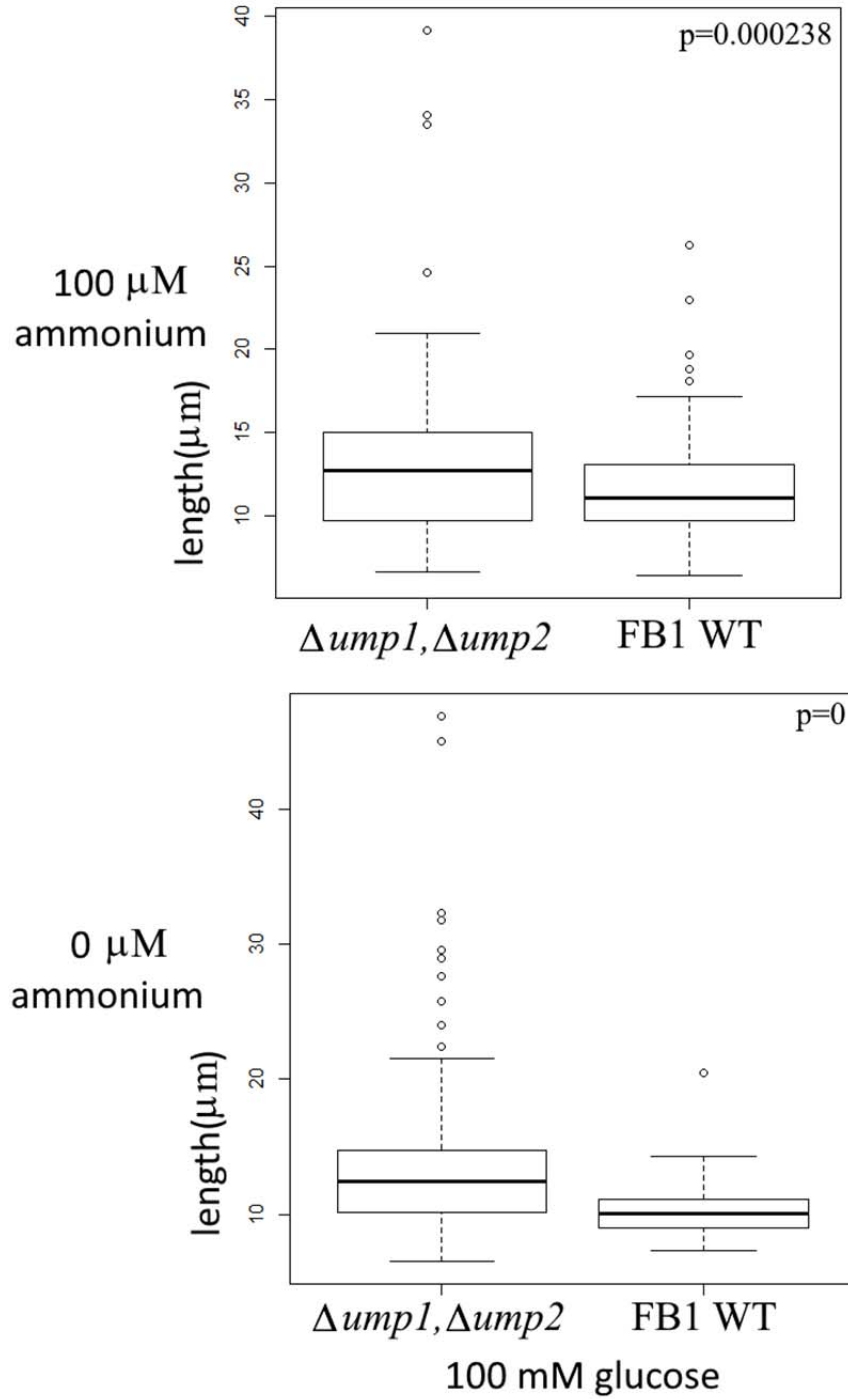


Figure 16. Comparison of cell length distributions between strains in SLAD with 100 mM glucose under low (100 μM) and no-ammonium concentrations. The p values indicate the result of a single-factor ANOVA between strains based on length (n=200).

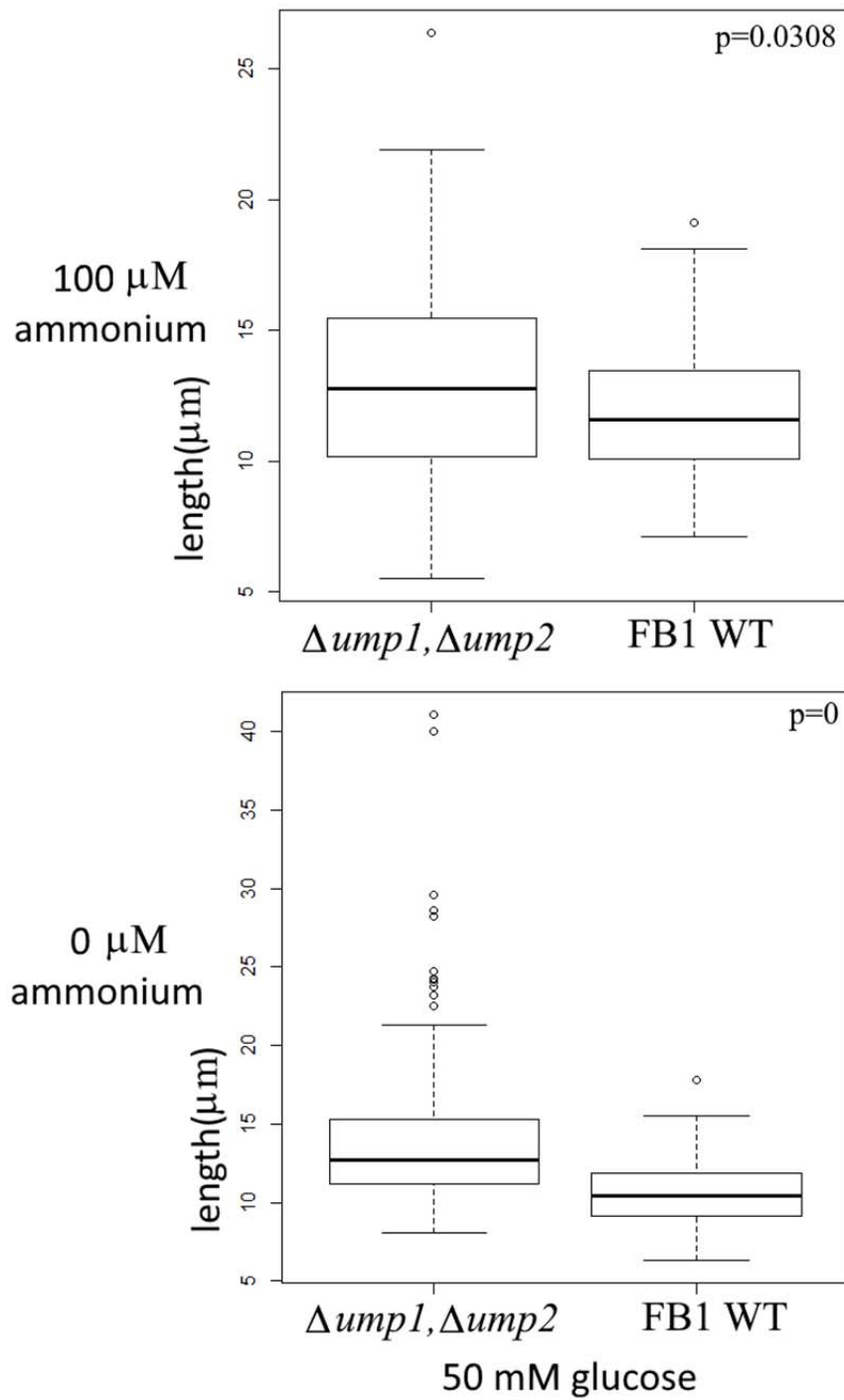


Figure 17. Comparison of cell length distributions between strains in SLAD with 50 mM glucose under low (100 μM) and no-ammonium concentrations. The p values indicate the result of a single-factor ANOVA between strains based on length (n=100).

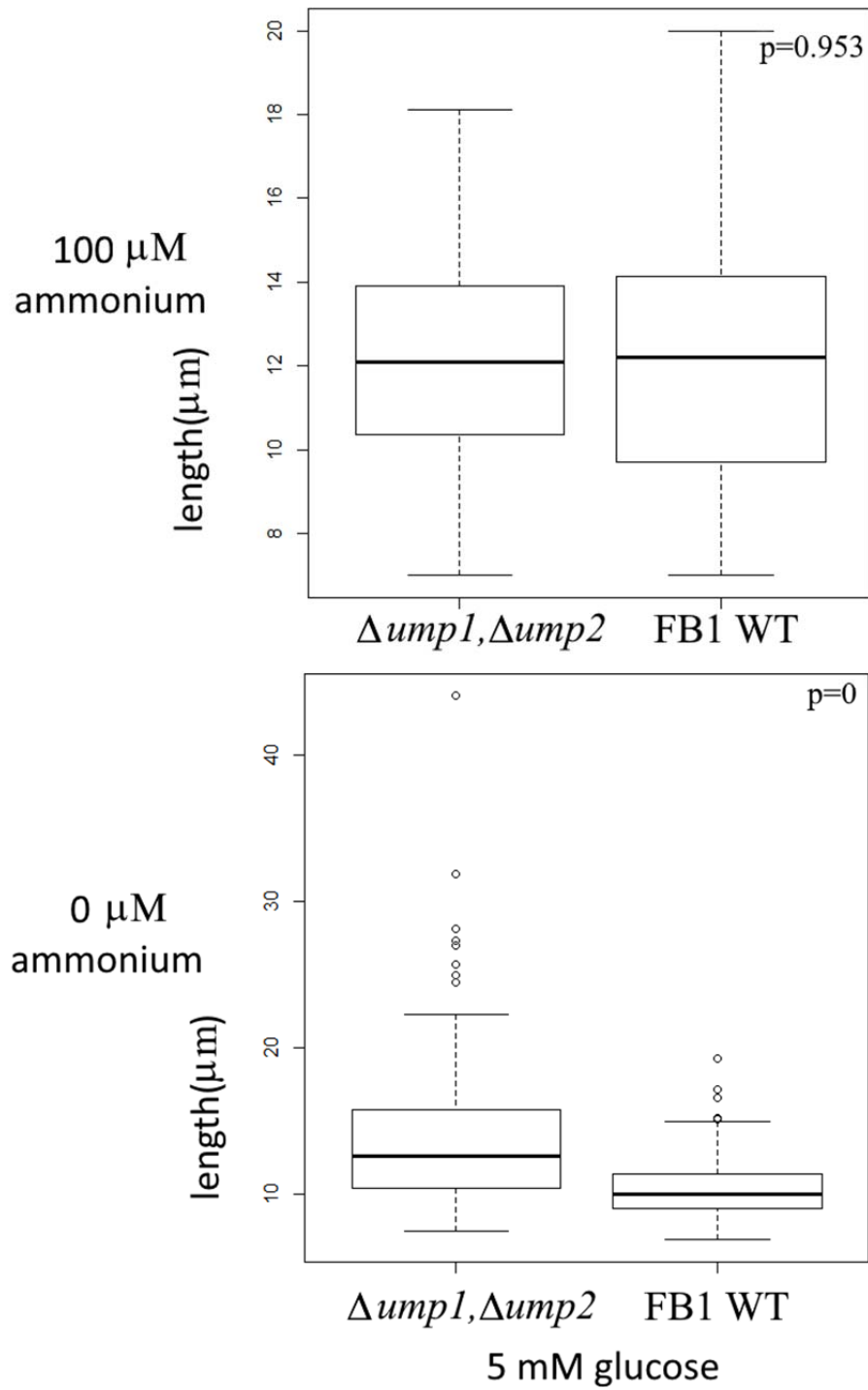


Figure 18. Comparison of cell length distributions between strains in SLAD with 5 mM glucose under low (100 μM) and no-ammonium concentrations. The p values indicate the result of a single-factor ANOVA between strains based on length (n=100).

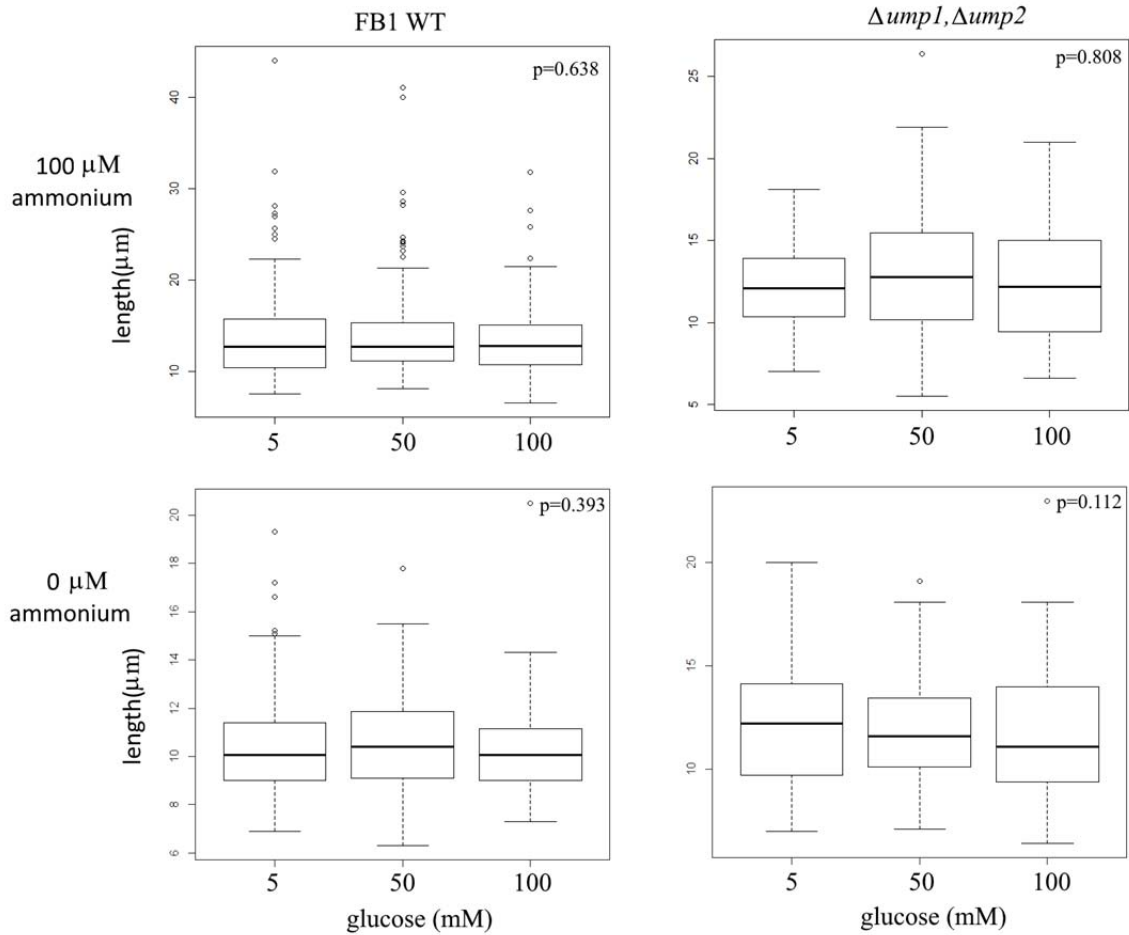


Figure 19. Comparison of cell length distributions within each strain in SLAD broth under glucose concentrations by ammonium. The p values indicate the result of a single-factor ANOVA based on length by glucose concentrations (n=100 except for 100 μM ammonium, 100 mM glucose in each strain where n=200).

Discussion

In this Chapter we found that while *U. maydis* was capable of growth under non-ammonium conditions, that growth never approached the same density as under less restrictive nitrogen conditions. Whether this was due to a lack of some

micronutrient/trace element or specific cellular response to starvation remains undetermined.

The difference in cell lengths made interpretation of A_{600} data potentially problematic with respect to cell numbers but was still useful for assaying rough biomass. That difference could contribute to the conflicting results between A_{600} and direct counts between strains under no-ammonium with high glucose conditions. Our results for A_{600} indicated a higher overall biomass in FB1 wild-type than $\Delta ump1, \Delta ump2$, whereas direct counts did not show a difference. Those results taken together with the net increase in average cell length indicated that the $\Delta ump1, \Delta ump2$ mutant has a slight advantage relative to the FB1 wild-type under lower glucose conditions.

The $\Delta ump1, \Delta ump2$ double deletion mutant has been found to be unable to transport ammonium in any significant amounts (Smith et al., 2003) yet that mutant was able to grow to densities approximately the same as the FB1 wild-type, as measured by absorbance, which was higher than that achieved under no-ammonium when provided 2% glucose. Without ammonium, by direct counts, the growth density of $\Delta ump1, \Delta ump2$ was unaffected by the changes in glucose concentration. However, while in low ammonium, glucose concentration played a role in the densities achieved by the mutant. Since ammonium was limiting there was either another sensor other than the Ump1 or Ump2 able to detect ammonium levels and relay that signal such that there was a corresponding response in the cell cycle or there is an alternative mechanism for the transport of ammonium that is not able to similarly transport methylamine.

Thus, the hypothesis for some type of canonical nitrogen fixation was not supported, at least by our experimental approach. As the $\Delta ump1, \Delta ump2$ mutant was

unable to transport ammonium it was reasonable to anticipate that the mutant could be disadvantaged in, at least, stationary phase growth density as compared to the FB1 wild-type. On the contrary, those $\Delta ump1, \Delta ump2$ cells averaged to be statistically significantly larger than the wild-type cells. That indicated that, at the very least, the possibility for an increased net biomass in the $\Delta ump1, \Delta ump2$ cells relative to the wild-type cells.

More highly variable cell lengths in the mutant were to be expected considering that in the absence of Ump1p and Ump2p the colonies produce a disorganized filamentous response. It should be noted that with one exception (Lovely et al., 2011), neither wild-type nor any other *U. maydis* haploid mutant filament in liquid media, unless as a response to low pH (Ruiz-Herrera et al., 1995). Among all the cells measured for the data collected above there were a few rare examples in a field of what appeared to be hyphal elongation particularly in the no-ammonium, low glucose condition, but they did not appear to be representative of the observed population. There were many examples of overly-long and apparently “Y” or sea star-shaped arrangements reminiscent of a multiple-budding phenotype, particularly across the no-ammonium condition, similar to that observed for $\Delta umpde1$ and $\Delta ubc1$ mutant strains (Agarwal et al., 2013).

Overall it was clear that haploid cells unable to transport ammonium were able to grow in these starvation-like conditions. Under the most nutrient-deprived conditions the FB1 wild-type and the $\Delta ump1, \Delta ump2$ mutant performed similarly. While it remained possible that the $\Delta ump1, \Delta ump2$ mutant was able to transport ammonium in a way undetected by the methylamine assay (Smith et al., 2003) another possibility is that there was some conversion of other ever-present but generally biologically-unavailable nitrogen such as dinitrogen in the atmosphere. A third alternative, that there was some

other source of nitrogen present in the form of contamination in the form of free, airborne ammonium has been suggested as a possible explanation for the growth in nitrogen-free media, of organisms not known to be diazotrophs (Hill and Postgate, 1969). We found that very unlikely through our use of biological controls, particularly CRR-15, which is fully capable of nitrogen fixation but only in an anaerobic environment (Cooper, 2013).

CHAPTER III
CHARACTERIZATION OF ATMOSPHERIC NITROGEN
ASSIMILATION

Summary

Stable Isotope Ratio Mass Spectrometry (SIRMS) has been for decades a ubiquitous tool to investigate the relationship between nitrogen fixing organisms (diazotrophs) and the communities associated with them. The natural abundance of ^{15}N relative to ^{14}N has been used to determine an organism's relative trophic level, particularly in heterotrophs, as well as how closely plants have been associated with free-living or symbiotic diazotrophs. The use of labeled stable isotopes has allowed for more fine discriminations in metabolic utilization of substrates. In this work SIRMS was used to demonstrate that $^{15}\text{N}_2$ was incorporated into cells, including discrete inclusion into protein biomass in both the *Ustilago maydis* FB1 wild-type and the $\Delta ump1, \Delta ump2$ mutant. The extent of such incorporation depended on both genotype of the strain and ammonium concentration in liquid media; similar results were obtained in one experiment on solid media, but there the differential effect of strain genotype on the magnitude of $^{15}\text{N}_2$ incorporation disappeared. In contrast, the filamentation character of colonies differed between genotypes tested. ^{13}C supplied as D-[U- ^{13}C]Glucose was also found to be incorporated into both whole cell biomass and proteins with a differential

appropriation between nutrient replete and no-ammonium conditions that did not vary by strain.

These results demonstrated both that dinitrogen gas was being transformed by some means into a form usable by the cells and showed that differential incorporation of ^{13}C reflected differential appropriation of glucose dependent on the nutrient conditions of the media.

Introduction

Stable Isotope Ratio Mass Spectrometry (SIRMS) represents a reliable method to assay the isotopic ratios between these commonly measured elements: ^{12}C and ^{13}C , ^{14}N and ^{15}N as well as between ^{16}O and ^{18}O . The ratio of ^{14}N to ^{15}N is commonly used in ecological surveys of soil or plant biomass to indicate the primary source of fixed nitrogen made available in that system since ^{15}N tends to accumulate both higher up the food chain and when recycled by saprophytes where dead organic matter is converted to a form usable by both those organisms and shared, as in the relationship between arbuscular mycorrhizal fungi (AMF) and plants.

$\delta^{15}\text{N}$ values are calculated by the formula $\delta^{15}\text{N} = \left(\frac{R_{\text{sample}} - R_{\text{standard}}}{R_{\text{standard}}} \right) * 1000 \text{ ‰}$ (per mille), where $R = \left(\frac{\text{At}\%^{15}\text{N}}{\text{At}\%^{14}\text{N}} \right)$ for which the standard is the ratio of $^{15}\text{N}/^{14}\text{N}$ of atmospheric dinitrogen. Here the standard is an atmospheric percentage (At%) of 0.3663033, where $\text{At}\%^{15}\text{N}$ is calculated by $\left(\frac{^{15}\text{N}}{^{14}\text{N} + ^{15}\text{N}} \right) * 100 \text{ At}\%$. This formula is used to indicate the fraction of ^{15}N accumulation in a sample relative to air. Terrestrial plants have $\delta^{15}\text{N}$ values ranging between 0 and 10‰, with those in tight associations with

diazotrophs, such as legumes, being closest to 0‰. Herbivores have a $\delta^{15}\text{N}$ value about 3‰ greater than the plants upon which they feed while carnivores about 3‰ greater than that (Edwards and Vandenabeele, 2012).

A common method employed to assay nitrogen fixation remains the acetylene reduction assay (ARA) (Capone, 1993). The ability of nitrogenase to reduce acetylene to ethylene has been leveraged since 1966 to quantify not only the presence of nitrogenase activity but also nitrogen fixation rates (Dilworth, 1966). Dinitrogen tracer assays, by SIRMS, have been found to be more accurate than ARA, though ARA is still commonly employed (Montoya et al., 1996).

For these reasons stable isotope ratio analysis using $^{15}\text{N}_2$ tracer was utilized to investigate the observations of growth of *Ustilago maydis* in media lacking ammonium or other provided nitrogen sources. *U. maydis* strains FB1 wild-type and FB1 $\Delta\text{ump1},\Delta\text{ump2}$ were tested to determine whether or not the observed growth was facilitated by nitrogen acquired from atmospheric dinitrogen.

The diazotrophs CRR-15, *Dickeya chrysanthemi* (*Erwinia chrysanthemi*, *Dickeya dadantii*) and CRR-14, *Agrobacterium tumefaciens* were employed as controls. CRR-14 has been determined to be able to fix nitrogen under aerobic conditions whereas CRR-15 is only able to fix nitrogen under anaerobic conditions, though the precise maximal partial pressure of oxygen under which fixation can occur has not been determined (Cooper, 2013). The whole genome of *Agrobacterium* sp. H13-3 (Wibberg et al., 2011) has been found to very closely match the completed, though as of yet unpublished, whole genome sequence of CRR-14.

^{13}C in the form of D-[U- ^{13}C]Glucose was also introduced to confirm that any observed change in nitrogen isotope ratios were from newly-grown biomass. Here we present evidence that both wild-type and the mutant *U. maydis* cells incorporate nitrogen available in the atmosphere.

Material and Methods

Strains and growth conditions. *U. maydis* strains FB1 wild-type (Banuett and Herskowitz, 1989) and FB1 $\Delta ump 1, \Delta ump 2$ (Smith et al., 2003) were grown in YPS (1% yeast, 2% peptone, 2% sucrose) broth at 27 °C, overnight, shaking at 200 RPM. All inocula for stable isotope experiments were taken from the aforementioned overnight cultures in YPS; these cultures were pelleted by centrifugation and then washed twice in sterile dH₂O that had been autoclaved twice. Synthetic Low Ammonium Dextrose (SLAD, 0.17% Yeast Nitrogen Base Broth, 2% glucose) was utilized in all minimal media applications either with or without 2% agar for solid media or broth, respectively. YPD (1% yeast, 2% peptone, 2% dextrose) broth, or plates with 1.5% agar was used for all nutrient replete media applications. Ammonium sulfate was used at the concentrations indicated. CRR-15, *Dickeya chrysanthemi* (alternatively *Erwinia chrysanthemi* or *Dickeya dadantii* (Samson et al., 2005)) (Cooper, 2013) and CRR-14, *Agrobacterium tumefaciens*, were each incubated under similar conditions as the *Ustilago* strains and employed as biological controls to ensure there was no nitrogen source contamination in the media. It was expected that CRR-14 would grow without ammonium provided in the medium, whereas CRR-15 would not fix nitrogen or be able to grow under aerobic conditions lacking ammonium (Cooper, 2013).

¹⁵N₂ tracer application and sample preparation. Stable isotope ratio experiments were conducted in both liquid and on solid media. Liquid media, SLAD or YPD, was used for minimal or nutrient replete conditions, respectively, with the SLAD supplemented with ammonium sulfate at the indicated concentrations in minimal media. These were inoculated and incubated in 120 mL septum bottles, which were cleaned before each usage with alcoholic potassium hydroxide (2M KOH in 95% ethanol). We used 80 mL of media which was sterilized and deaerated by a standard liquid autoclave cycle, leaving 40 mL of head space. The septum bottles were inoculated with 10 µl of twice-washed overnight cultures yielding approximately 16,000-24,000 cells/mL. Following culture inoculation the bottles were sealed with aluminum crimp caps and then injected with 0.15 µl of dinitrogen gas tracer [¹⁵N₂, Cambridge Isotope Laboratories, Tewksbury, MA, cat. #NLM-363-PK], raising the δ¹⁵N to approximately 13.2‰. Incubation was at 27 °C, shaking at 200 RPM for up to 14 days per trial. Agar plates were incubated in a modified GasPak™ EZ Large Incubation Chamber [BD Biosciences, Franklin Lakes, NJ, cat. #10-260672]. The chamber was modified by the addition of a gas injection port with an isolation valve with the chamber penetration coated on each side by three coats of a silicone sealant. The seal integrity was verified by simple fermentation by *Saccharomyces cerevisiae* in two liters of YPS. Plates were inoculated with 100 µl of cells from overnight cultures, washed twice in sterile dH₂O for approximately 160,000-240,000 cells, then distributed across the surface of the agar with a plate spreader. After securing the lid of the chamber 2 mL of tracer was injected raising the δ¹⁵N to approximately 10.3‰. ¹³C was added to solid media in the form of D-[U-¹³C]Glucose [Sigma-Aldrich, St. Louis, MO, cat. #389374] to a proportion 0.05% of the 2% glucose.

Following incubation the liquid media cultures were filtered by vacuum, then dried in microcentrifuge tubes. For growth on solid medium, plates were scraped then dried in microcentrifuge tubes. Those samples utilized in protein analyses were processed as described in the next section prior to drying. All samples were then crushed and weighed into large tin (Sn) sample capsules [Costech Analytical Technologies, Valencia, CA, cat. #041073] which were then crushed and shipped for analysis.

Protein extraction and precipitation. Protein extraction was based on a post-alkaline extraction protocol (Kushnirov, 2000). Cells were harvested from plates or recovered from liquid media by centrifugation and thoroughly suspended in sterile water. The mixture was pelleted in a microcentrifuge, resuspended in 100 μ l dH₂O. 100 μ l of 0.2M NaOH was added and the mixture was allowed to incubate for 5 minutes at room temperature. After incubation the mixture was pelleted, and the supernatant discarded. The pellet was resuspended in 50 μ l SDS sample buffer (0.06M Tris-HCl at pH 6.8, 5% glycerol, 2% SDS and 2% β -mercaptoethanol). This mixture was then boiled for 3 minutes and subsequently centrifuged, and, the supernatant was saved for precipitation. Acetone precipitation, adapted from Thermo Scientific protocol TR0049.1, was accomplished by adding 200 μ l of -20°C acetone (i.e., four times the sample volume). The sample was vortexed then incubated at -20°C for one hour. Centrifugation for 10 minutes at top speed in a microcentrifuge followed, and then the supernatant was decanted. The pellet was dried, and then processed as the whole-cell biomass for addition to tin sample capsules.

Stable Isotope Ratio Analysis (SIRMS). Two facilities were used for SIRMS. The Stable Isotope Research Unit at the Department of Crop and Soil Science in the

College of Agricultural Sciences at Oregon State University (OSU) utilized a PDZ-Europa 20/20 Isotope Ratio Mass Spectrometer using a Sercon GSL with Gilson gas autosampler. The point of contact was David Myrold; as of last contact their spectrometers were off-line. The other facility, the Mass Spectrometry Facility in the Department of Chemistry and Biochemistry at Southern Illinois University (SIU) in Carbondale, IL used continuous flow EA-IRMS on a Thermo Delta V Plus IRMS with a Costech ECS 4010. The analyses were conducted by Mihai Lefticariu. The standard employed for $\delta^{15}\text{N}$ is air. The standard for $\delta^{13}\text{C}$ is based on Pee Dee Belemnite (PDB) derived from fossils found in the Pee Dee Formation in South Carolina. This material has an unusually high ^{13}C content such that most samples have a negative $\delta^{13}\text{C}$ value. Organic material tends to have a $\delta^{13}\text{C}$ value of about -25‰ .

Results

Pilot experimental comparison of tracer to no-tracer. The initial experiment compared samples that had tracer added to those that did not using whole-cell biomass in SLAD broth without ammonium added. This analysis was conducted at OSU. The FB1 wild-type with tracer had not grown sufficiently to be included in this analysis. The experiments with *U. maydis* $\Delta ump1, \Delta ump2$ and CRR-14 both indicate significant incorporation of tracer, which, conservatively, is any value over 4‰ of that from samples analyzed without tracer (Montoya et al., 1996).

Table 2. SIRMS Comparing tracer vs. no-tracer of strains in SLAD broth with no-ammonium.

Sample*	Tracer	Weight (mg)	At% ^{15}N	$\delta^{15}\text{N}$ (‰)
FB1 wild-type	none	1.2	0.356936	-1.00734
<i>$\Delta ump1, \Delta ump2$</i>	none	1.8	0.366403	0.273637

CRR-14	none	1.5	0.366428	0.342326
CRR-14	+	1.1	0.386411	55.10754
<i>Δump1,Δump2</i>	+	1.2	0.390874	67.33956

*FB1 wild-type failed to provide sufficient cell density in SLAD when tracer was added to be included in this analysis.

Incorporation of $^{15}\text{N}_2$ tracer under different media conditions across strains in

liquid media. As seen in Figure 20, the FB1 wild-type, *Δump1,Δump2* and CRR-14 were all found to incorporate ^{15}N under minimal and no-ammonium conditions. CRR-15, as a facultative anaerobe lacking the ability to fix nitrogen in an aerobic environment, did not grow under the no-ammonium conditions. It did, however, demonstrate very high $\delta^{15}\text{N}$ values under low ammonium. Considering the high cell density found in those bottles it stands reasonable to speculate that sufficient ammonium was available to support aerobic growth; after depletion of available oxygen this strain was then able to fix nitrogen in the sealed septum bottles. Additionally the *Δump1,Δump2* mutant incorporated far more ^{15}N than did the FB1 wild-type. This analysis was also conducted at OSU; the remaining analyses were conducted at SIU.

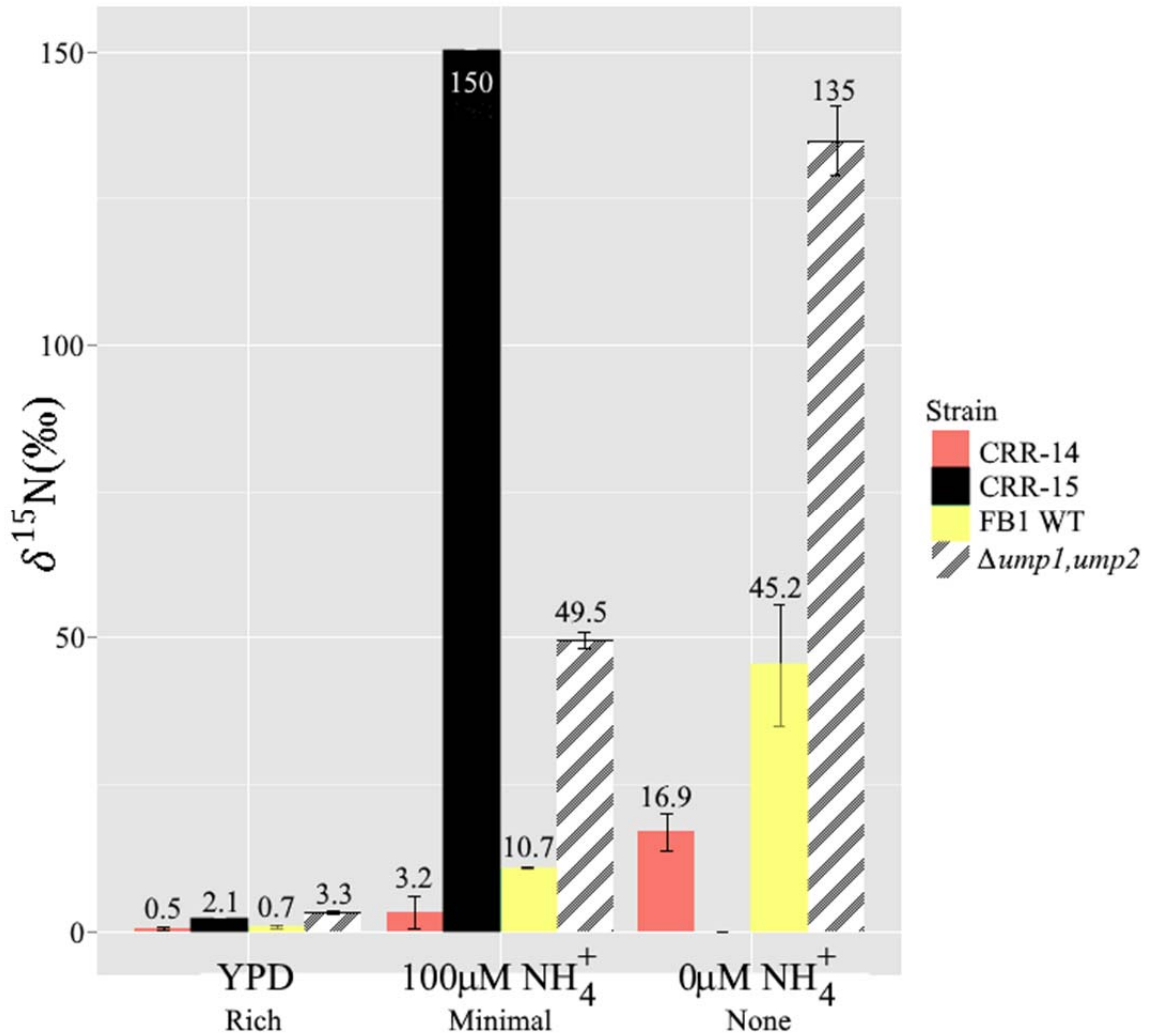


Figure 20. Comparison of $\delta^{15}\text{N}$ values across liquid media conditions.

Incorporation of ^{15}N and ^{13}C in liquid media. Each strain demonstrated, in Table 3, incorporation of both ^{15}N and ^{13}C , with the $\Delta ump1, \Delta ump2$ mutant incorporating significantly more ^{15}N than FB1 wild-type particularly under the lower ammonium condition. The ^{13}C incorporation showed utilization of the $^{13}\text{C}_6$ -glucose anabolically such that significant incorporation into newly produced macromolecules was observed. At 100 μM NH_4^+ the wild-type FB1 has a higher $\delta^{15}\text{N}$ (‰) than the $\Delta ump1, \Delta ump2$ mutant; in contrast, at 10 μM NH_4^+ the $\Delta ump1, \Delta ump2$ mutant showed nearly twice the

incorporation of $^{15}\text{N}_2$ as wild-type. Under nutrient replete media there was no significant indication of $^{15}\text{N}_2$ incorporation in the FB1 wild-type. The $\delta^{13}\text{C}(\text{‰})$ value for FB1 wild-type corresponded closely to the average value for organic material as this sample excluded the $^{13}\text{C}_6$ -glucose tracer. The inclusion of $^{13}\text{C}_6$ -glucose under all minimal media conditions were clearly significant relative to the FB1 wild-type without $^{13}\text{C}_6$ -glucose.

Table 3. Incorporation of ^{15}N and ^{13}C in liquid media.

Strain	Media	Tracer (^{15}N , ^{13}C)	$\delta^{15}\text{N}$ (‰)	$\delta^{13}\text{C}$ (‰)
FB1 wild-type	nutrient replete	+, -	1.26	-22.02
	+100 μM NH_4^+	+, +	38.81	150.48
	+10 μM NH_4^+	+, +	46.44	185.80
$\Delta\text{ump1}, \Delta\text{ump2}$	+100 μM NH_4^+	+, +	26.78	197.94
	+10 μM NH_4^+	+, +	85.59	167.46

Incorporation of ^{15}N and ^{13}C in cells grown on solid media. The growth plates incubated in the modified anaerobic chamber all included $^{13}\text{C}_6$ -glucose. Both $\delta^{15}\text{N}$ values and $\delta^{13}\text{C}$ values were determined for strains grown on nutrient replete (YPD, 1.5% agar) conditions and no-ammonium (SLAD, 2% agar) (Table 4) Under these conditions there was a significant difference between nutrient replete and no-ammonium with $\delta^{15}\text{N}$ about 6 times higher accumulation into whole cell biomass than under nutrient replete media for both wild-type and mutant *U. maydis* strains. There was no significant difference either between strains or in $\delta^{15}\text{N}$ values between whole cell biomass or protein extractions, although the $\Delta\text{ump1}, \Delta\text{ump2}$ mutant did have a higher $\delta^{15}\text{N}(\text{‰})$ than wild-type for incorporation into protein when grown without ammonium. $\delta^{13}\text{C}(\text{‰})$ values in protein samples did appear to be greater in nutrient replete conditions. This difference was not dependent on strain genotype and no corresponding difference was

seen comparing nutrient replete and no-ammonium media by $\delta^{13}\text{C}(\text{‰})$ values for whole-cell biomass.

Table 4. Incorporation of ^{15}N and ^{13}C on solid media.

Strain	Sample Type	Media	$\delta^{15}\text{N}$ (‰)	$\delta^{13}\text{C}$ (‰)
FB1 wild-type	whole biomass	nutrient replete	4.12	157.64
	whole biomass	no-ammonium	27.51	166.68
	protein	nutrient replete	4.94	71.48
	protein	no-ammonium	25.27	39.89
$\Delta ump1, \Delta ump2$	whole biomass	nutrient replete	4.57	161.75
	whole biomass	no-ammonium	24.81	166.05
	protein	nutrient replete	4.61	74.68
	protein	no-ammonium	37.8	47.79

Discussion

Overall these results indicate that *U. maydis* incorporates N_2 into cellular biomass including proteins. In the experiments employing liquid media the $\Delta ump1, \Delta ump2$ mutant incorporated significantly more $^{15}\text{N}_2$ than FB1 wild-type, although both incorporated more as a function of decreasing available ammonium. This difference all but disappeared when tested from cultures grown on solid media. In liquid media, under minimal conditions, neither strain was able to significantly filament, remaining in the “budding” yeast-like form. The only condition under which significant filamentation had been observed in liquid media was in response to low pH (Ruiz-Herrera and Leon, 1995). The primary morphological difference between cells grown in YPD broth versus SLAD or HSS broth is the appearance of large vacuoles under minimal media. On agar both strains do switch from budding to filamentous under minimal media conditions, but the filamentous character of the mutant is abnormal and reflects a likely dysregulation of the signaling that allows wild-type to filament in response to low ammonium (Smith et al., 2003). Perhaps the large vacuoles are accumulating material for filamentation, leaving

the cells restrained in that transitional moment, unable to actually extend filaments but continuing to accumulate cell wall synthesizing materials. Since the $\Deltaump1, \Deltaump2$ mutant has already been observed having an abnormal filamentous phenotype relative to the wild-type more cellular resources may be devoted to attempted filamentation, meaning more cellular constituents are being accumulated. As observed in Figure 8, in Chapter 2, the *Ustilago* cells appear distended, more so in the $\Deltaump1, \Deltaump2$ mutant, though this observation on the size of the vacuoles and degree of distention has not been quantified.

As with the growth experiments in Chapter 2, CRR-14 and CRR-15 were employed as biological controls. Interestingly the stable isotope work involving minimal ammonium (100 μ M) was sufficient for the CRR-15 to be able to scavenge the available oxygen and subsequently fix nitrogen as indicated by the incorporation of tracer into cellular biomass as depicted in Figure 14. CRR-14 also incorporated N_2 tracer, though to a lesser degree than the *Ustilago* strains.

The marked difference in total ^{15}N accumulation between the FB1 wild-type and the $\Deltaump1, \Deltaump2$ mutant also indicated that the ammonium transporters play a role in this metabolic activity, at least in the cells in liquid media, apparently unable to switch to filamentous growth, as demonstrated in Figure 8. More stable isotope experiments are needed to determine if the lack of difference in $\delta^{15}N$ values between strains on solid media is consistent under no-ammonium conditions as well as minimal ammonium conditions.

The $\delta^{13}C$ values in Table 4 present an interesting possibility. While there was no apparent difference between samples taken from whole-cell biomass there did appear to

be a differential partitioning of ^{13}C between media conditions in protein samples with roughly half the $\delta^{13}\text{C}$ values in samples grown under no-ammonium conditions as compared to protein samples derived from nutrient replete media. This could reflect a difference in gross metabolic glucose utilization as apportioned into protein synthesis between budding and filamentous cells. Filamentous colonies devote more metabolic resources to cell wall and membrane constituents than do budding cells. Alternatively that difference could be explained by sequestration of carbon under low-ammonium conditions. A useful future experiment to compare these $\delta^{13}\text{C}$ values would be to compare agar-grown strains under no-ammonium conditions to the vacuole-filled “locked budding” phenotype exhibited by strains grown under nitrogen limitation in liquid media.

These results presented a very intriguing possibility. The simplest explanation for these SIRMS results would be the presence of a prokaryotic diazotroph, and this hypothesis was examined in Chapter IV. The alternative explanation describes a novel nitrogen fixation system in a eukaryote. The potential for evidence supporting the existence of a novel, eukaryotic nitrogen fixation system would overturn decades of work predicated on the hypothesis that only prokaryotes represent the biogenic nitrogen input from atmospheric nitrogen into the nitrogen cycle. The existence of such a system would explain why multiple studies have failed to find nitrogenase genes in environmental samples and why acetylene reduction assays in some of the same studies revealed no reduction of acetylene (detailed in Chapter V). This could also account for deficits in nitrogen budgets attributed to uncharacterized diazotrophs.

Even if this fixation system were to be demonstrated to occur in mitochondria, the implications for potential reductions in the agricultural use of anhydrous ammonia could

have wide-ranging impacts. Reduction of nitrate inputs to local waterways could reduce the expansion of zones of eutrophication in lakes and coastal waters. A wider range of crop plants able to be supported with a fungal endophyte or directly modified by transgenic methods could even contribute to enhanced agricultural success in nitrogen-poor soils. This has been the goal in work attempting to adapt the MoFe nitrogenase to be expressed and utilized in plants, with no success to date.

CHAPTER IV

POTENTIAL PROKARYOTIC SYMBIOSIS

Summary

The possibility of a prokaryotic endosymbiont to explain apparent atmospheric nitrogen assimilation by *Ustilago maydis* was explored. *U. maydis* strains were grown with high concentrations of antibacterial compounds and passaged multiple times under these conditions. These treatments were used in an attempt to “cure” the cells of possible endosymbiotic prokaryotes. Successful curing was assessed by both PCR screening for prokaryotic target sequences and assaying growth in no-ammonium media. Passaged cells continued to be able to grow under no-ammonium conditions and demonstrated assimilation of isotope tracers including $^{15}\text{N}_2$, into proteinacious mass. Potential PCR product, if any, of approximately correct sizes for prokaryotic targets were sequenced and found not to represent prokaryotic sequences, either 16S rDNA or the *nifH* characteristic of the vast majority of diazotrophs. These results suggest that if *U. maydis* cells do harbor endosymbionts, such prokaryotes are not required for assimilation of atmospheric nitrogen.

Introduction

In Chapter II, it was demonstrated that *Ustilago maydis* is able to grow under both low and no-ammonium conditions, whether or not it has functional ammonium transporters. In Chapter III, I showed that inorganic dinitrogen has been

transformed into organic nitrogen and incorporated as biomass, including proteins. The only known mechanism for this is nitrogen fixation primarily by FeMo nitrogenase and the more rare superoxidase-dependent MoFeS nitrogenase observed in *Streptomyces thermoautotrophicus* (Ribbe et al., 1997). Therefore the simplest explanation for these observations is the presence of a prokaryotic diazotroph associated with *U. maydis*. In fact, Ruiz-Herrera et al. (Ruiz-Herrera et al., 2015) recently reported the existence of just such an endosymbiont in *U. maydis*.

Considering the possibility of biological contamination of the growth media or strain sources with a free-living diazotroph or a novel endosymbiont, a series of experiments were devised to either confirm or deny the presence of a prokaryotic diazotroph associated with *U. maydis*. Initially PCR screenings for characteristic prokaryotic genes were conducted for DNA sequences such as 16S rDNA and *nifH* which are present in all known diazotrophs and which would therefore be diagnostic of such organisms in our samples. In the event that PCR detected any such products of approximately the expected sizes, such products were purified and their sequences analyzed.

In an effort to ensure no free-living or endosymbiotic diazotroph could survive in our cultures, *Ustilago* strains were subjected to a series of passages through very high concentrations of a variety of antibacterial compounds. The resulting cured strains were then evaluated for growth in no-ammonium medium and accumulation of ^{15}N as measured by Stable Isotope Ratio Mass Spectrometry (SIRMS), and retested by PCR.

Finally to estimate the lowest of detection of 16S rDNA in FB1 wild-type chromosomal DNA, a screening by PCR was conducted in separate reactions with

various concentrations of CRR-15 chromosomal DNA. Since the *U. maydis* genome is 19.68 megabases (Mb) and the *Dickeya chrysanthemi* genome is 4.67 Mb, by raw nucleotide numbers it would require about 4.21 *D. chrysanthemi* cells to be equivalent to a single *U. maydis* cell; this ratio was utilized to develop a dilution range such that at 10^{-6} dilution there would be one hypothetical *D. chrysanthemi* cell to about 247,000 *U. maydis* cells. In this way, we intended to evaluate a lowest detection threshold for the presence of endosymbiont DNA in our samples.

Material and Methods

Growth Conditions, SIRMS. Primary inocula were grown and partitioned as conducted for the experiments in Chapter III. Stable isotope samples were derived from solid media cultures grown in the modified anaerobic chamber also as indicated in Chapter III. The additional *Ustilago maydis* strains FB2 (Banuett and Herskowitz, 1989) and 1/2 (Kronstad and Leong, 1989) used in this study were provided by José Ruiz-Herrera.

Curing *U. maydis*. Serial passages of *U. maydis* strains through very high concentrations of antibacterial compounds were conducted in YPS (1% yeast, 2% peptone, 2% sucrose) broth at 27 °C. Incubation was for over 72 hours, shaking at 250 RPM. The *Ustilago* strains employed included FB1 wild-type, $\Delta ump1, \Delta ump2$, FB2 wild-type (provided by the José Ruiz-Herrera lab). The first two passages utilized ampicillin at concentrations of 1000 $\mu\text{g/mL}$ and 2000 $\mu\text{g/mL}$. The third passage was with trimethoprim at 1500 $\mu\text{g/mL}$. The fourth passage used streptomycin at 1000 $\mu\text{g/mL}$. The fifth passage was with tetracycline at 1500 $\mu\text{g/mL}$, while the final passage used ampicillin at 500 $\mu\text{g/mL}$, trimethoprim at 100 $\mu\text{g/mL}$, streptomycin at 100 $\mu\text{g/mL}$ and tetracycline at 150 $\mu\text{g/mL}$.

DNA Extraction and Precipitation. Overnight cultures of 4 mL were grown in YPS and

verified as *U. maydis* without observable contaminants by microscopic examination. Cultures were pelleted by microcentrifugation at 14,000 rpm for 1 minute and the supernatant discarded. Cells were washed by resuspending in dH₂O, pelleting and then the supernatant was discarded. Cells were resuspended in lysis buffer (0.5M NaCl, 0.01M EDTA at pH 8.0, 0.2M Tris-Cl at pH 7.5, 1% SDS) and 0.3 g of 0.5 mm glass beads was added. Next, 250 µL PCI (25:24:1 v/v phenol:chloroform:isoamyl alcohol) was added. The mixture was vortexed for 5 min and centrifuged at 14,000 rpm for 3 minutes. The upper phase was collected, and added to 800 µL isopropanol which was then centrifuged for 15 minutes and supernatant discarded. The DNA pellet was dried, after which it was resuspended in 10 to 100 µL of either water or TE (pH 8.0), that volume dependent on how obvious the DNA pellet appeared in the microcentrifuge tube during precipitation. Assessment of DNA concentration and purity was obtained using a NanoDrop™ 2000 UV-Vis Spectrophotometer [Thermo Fisher Scientific, Waltham, MA].

PCR Screenings. Genomic DNA was used as template in PCR. The primers used in this effort are found in Table 5. 16S rDNA PCR amplification was performed using bacterial primers 68F (Borneman et al., 1996a) and 1392R (Amann et al., 1995a) for identification of prokaryotic sequences (Brosius et al., 1981). These primers amplify a 1324 base pair (bp) fragment of bacterial 16S rDNA. The initial *nifH* PCR amplification was performed using the degenerate primers *nifHF* and *nifHR* (Zehr and McReynolds, 1989). These primers have been shown to amplify a 360 bp fragment of *nifH*, specifically the DNA coding for the nitrogenase iron-binding domain of dinitrogenase reductase (Zehr and McReynolds, 1989). Based on communication between Michael Perlin and José Ruiz-Herrera *Azospirillum*-specific *nifH* primers were used as well. The primers a38F and

a39R should produce an amplicon from within *nifH* of 205 base pairs (Shime–Hattori et al., 2011). As a control primers for the *U. maydis*, locus UMAG_00037, the primers i37F and i37R were used, which amplify an expected amplicon of 614 bp and this pair has no apparent affinity for prokaryotic sequences as assayed by both BLAST search (Altschul et al., 1990) including specific searches against *Agrobacterium* sp. and *Dickeya chrysanthemi* whole-genome sequences.

Table 5. Primers to interrogate *Ustilago* for a diazotroph.

Name	Sequence (5' to 3')	Target	Source
68F	TWAWACATGCAAGTCGAKCG	prokaryotic 16S rRNA	(Borneman et al., 1996b)
1392R	ACGGGCGGTGTGTRC		(Amann et al., 1995)
nifHF	TGYGAYCCNAARGCNGA	<i>nifH</i>	(Zehr and McReynolds, 1989)
nifHR	ADNGCCATCATYYCNCC		(Zehr and McReynolds, 1989)
a38F	GACCCGCCTGATCCTGCACG	<i>Azospirillum</i>	(Shime–Hattori et al., 2011)
a39R	GTTCTCTTCCAGGAAGTTGATCGA	<i>nifH</i>	(Zehr and McReynolds, 1989)
p3F	AGAGGTTTGATCCTGGCTCAG	<i>Bacillus pumilus</i> 16S rRNA	(Ruiz-Herrera et al., 2015)
p4R	CTACGGRTACCTTGTTACGAC		(Ruiz-Herrera et al., 2015)
p5F	ACCCGCCTGATCCTGAACTCGAAGGCGC	<i>Bacillus pumilus</i> <i>nifH</i>	(Ruiz-Herrera et al., 2015)
p6R	GGCCGCGTACATCGCCATCATCTCGCCGG		(Ruiz-Herrera et al., 2015)
i37F	ATGCCGACAAGGTTACCTGG	<i>U. maydis</i> locus	this study
i37R	TTGGTAGCGGGAGAAACACC	UMAG_00037	this study

IUPAC nucleotide code: D=A or G or T, K=G or T, N=any, R=A or G, W=A or T, Y=C or T

The primers identified here as p3F and p4R as well as the primer set p5F and p6R were used in an attempt to replicate the results reported by José Ruiz-Herrera (Ruiz-Herrera et al., 2015). The p3F/p4R primer pair amplified an expected fragment size of 1485 bp matching the *Bacillus pumilus* 16S ribosomal RNA gene while the p5F/p6R amplified an expected fragment size of 323 bp matching the *Bacillus pumilus* *nifH* gene, both as determined by BLAST (Altschul et al., 1990).

The amplification mixtures included 100 ng of chromosomal DNA, 1 μ l of Apex[®] *Taq* DNA polymerase (1.25 unit/50 μ l) [Genesee Scientific, San Diego, CA], 0.2 μ M of each primer pair (Table 5), 200 μ M of dNTP mix, 1X Ammonium PCR Buffer, 1X *Taq* PCR Buffer, and 1.5 mM MgCl with nuclease-free H₂O [Thermo Fisher Scientific, Waltham, MA] for a final volume of 50 μ l. Reactions were run in a PTC-200 Peltier Thermal Cycler [Bio-Rad, Hercules, CA] using a Hot+ protocol. The reaction conditions were as follows: initial denaturation step at 94 °C for 90 seconds followed by thirty seconds, annealing at 58 °C (unless otherwise noted) for 30 seconds, extension at 72°C for 1.5 min. Thirty-five cycles total with a final extension at 72 °C for five minutes.

PCR products were separated by gel electrophoresis on a 0.8% agarose gel in TAE with ethidium bromide (EtBr). Hi-Lo[™] DNA Marker [Minnesota Molecular, Minneapolis, MN] was used as the size standard. Images were captured using a Gel Logic 112 with a UV Transilluminator (UVP) [Carestream, Rochester, NY]. The Carestream Molecular Imaging Software (v. 5.0.7.22) [Carestream] was used to collect and export gel images.

DNA Sequencing. PCR products were extracted from agarose using the Zymoclean[™] Gel DNA Recovery Kit [Zymo Research, Irvine, CA] and purified for direct sequencing or cloned into pCR[®]2.1 TOPO[®] [Thermo Fisher Scientific, Waltham, MA] with plasmids extracted by alkaline lysis (Maniatis et al., 1982). The resulting DNA was quantified using the NanoDrop[®] 2000 [Thermo Fisher Scientific] then used with the Applied Biosystems[®] BigDye[®] Terminator v3.1 Cycle Sequencing Kit [Thermo Fisher Scientific]. These reactions were assembled in 20 μ L volumes. Each reaction included 2 μ L of Reaction Mix, 4 μ L of Sequence Buffer (5x), 1 μ L of 20 μ M sequencing primer, 2 μ L of

template and 11 μL dH_2O . The primers used were either M13(-21)F (5'-TGTAACGACGGCCAGT-3'), for cloned fragments or 68F/1392R, nifHF/nifHR for PCR products. Despite the degeneracy inherent in those primers it has been found that direct sequencing of PCR amplicons using primers up to 512-fold degeneracy resulted in sequences that were over 99% identical to sequences from cloned fragments (Santos and Ochman, 2004).

Samples were run in the Bio-Rad PTC-200 Thermal Cycler [Bio-Rad, Hercules, CA] with a 30 second denaturation at 96°C followed by a 15 second annealing step at 50°C then a 4 minute elongation step at 60°C . Those steps are repeated 25 additional times. Following that amplification the samples were purified and precipitated using ethanol as follows.

To each sample was added 2 μL of 3M sodium acetate (NaOAc at pH 5.2) and 60 μL of ice cold 100% ethanol. Samples were mixed and quick-spun then incubated at -20°C for thirty minutes. Tubes were then centrifuged at maximum speed in a microcentrifuge for 10 minutes. Following aspiration, 200 μL of ice cold 70% ethanol was added to wash the DNA which was then spun for five minutes, aspirated and dried.

Prepared samples were then analyzed at the Center for Genetics and Molecular Medicine (CGeMM) DNA Facility Core using an ABI automated sequencer that employed capillary gel electrophoresis.

Cloning for Subsequent Sequencing. Cloning of PCR products was accomplished using TOPO pCR2.1 vector into commercially-competent Invitrogen *Escherichia coli* strain TOP10 [Thermo Fisher Scientific, F- *mcrA* Δ (*mrr-hsdRMS-mcrBC*) ϕ 80*lacZ* Δ M15 Δ *lacX74 nupG recA1 araD139 Δ (*ara-leu*)7697 *galE15 galK16 rpsL*(Str^R) *endA1* λ].*

Ligation reactions were transformed into TOP10 cells, plated on 100 µg/mL ampicillin LB plates with Xgal for routine blue-white screening.

Plasmid extraction was performed by alkaline lysis. Isolated (white) colonies were grown overnight in CircleGrow® broth. Cells pelleted and resuspended in Cell Resuspension Solution (50mM Tris-HCl, 10 mM EDTA, 100 µg/mL Rnase A, pH at 7.5), the Lysis Solution (1% SDS, 0.2M NaOH) was added, cells were gently mixed; after 5 minutes Neutralization Solution (1.32M KAc at pH 4.8) was added. Cells were then centrifuged at maximum speed for 15 minutes (typical protocol calls for 3-5 minutes). The supernatant was decanted into isopropanol for precipitation as described under DNA Extraction and Purification, above.

DNA Dilution. The ratio of FB1 wild-type to CRR-15 was calculated based on genome size such that the total DNA from a single FB1 wild-type cell was estimated as equivalent to about 4.21 CRR-15 cells. The concentration of purified FB1 wild-type chromosomal DNA used was 100 ng/µl. The concentrations of CRR-15 chromosomal DNA used included the serial dilution range of 10^{-3} to 10^{-6} , stepwise in 1:10 dilutions. At 10^{-6} the calculated concentration of CRR-15 DNA was 4.03 pg/µl, which would be expected to be the equivalent DNA yield from an estimated 159.5 CRR-15 cells (Based on a genome size of 4.67 Mb with a GC content of 57% for an estimated DNA mass per cell of 0.02527 pg) per microliter. At that same dilution there would be an estimated 247,000 FB1 wild-type cells to a single CRR-15 cell.

The PCRs were performed in a T100™ Thermal Cycler [Bio-Rad, Hercules, CA] with an initial denaturation at 95°C for 1 minute followed by 30 seconds at 95°C, annealing for 30 seconds at 58°C, extension for 1.5 min at 72°C for 35 total cycles and a

5 minute final extension. The amplification mixtures included 1 μ l of *Taq* DNA polymerase (1.25 unit/50 μ l) (Apex), 0.2 μ M of each primer pair (Table 4), 200 μ M of dNTP mix, 1X Ammonium PCR Buffer, 1X *Taq* PCR Buffer, and 1.5 mM MgCl with nuclease-free H₂O (Fisher) for a final volume of 50 μ l. Two μ l of template at the indicated dilutions were added such that the concentration of *U. maydis* DNA was constant at 100 ng/ μ l while the concentrations of CRR-15 DNA in each reaction decreased as described above.

Results

Growth persists of cured *Ustilago* under no-ammonium conditions. By absorbance measurements (A_{600}) the cured *Ustilago* strains, Figure 21, were able to grow in

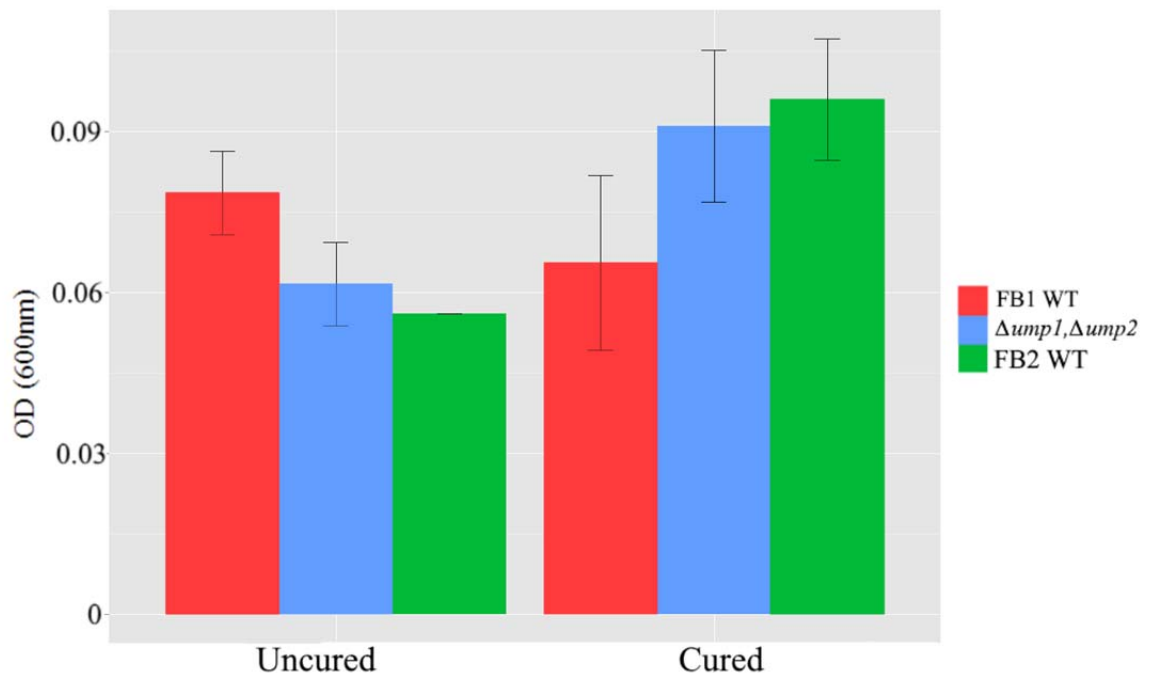


Figure 21. Absorbance (A_{600}) of cured versus uncured *U. maydis* strains in no-ammonium SLAD broth. (n=2)
no-ammonium SLAD (additionally confirmed to be nitrogen-free by the lack of observed growth by CRR-15) at A_{600} values slightly greater than that of the uncured strains.

SIRMS $\delta^{15}\text{N}$, $\delta^{13}\text{C}$ values. Protein samples extracted from biomass collected from no-ammonium SLAD plates that were incubated in the modified anaerobic chamber, as described in Chapter III, were sent to SIU for analysis resulting in the values indicated in Table 6. $\delta^{15}\text{N}$ (‰) values indicated $^{15}\text{N}_2$ was incorporated into cellular biomass in both wild-type and $\Deltaump\ 1,\Deltaump\ 2$ cells. $\delta^{13}\text{C}$ (‰) values further indicate that $^{13}\text{C}_6$ -glucose was also incorporated into proteinacious biomass, though those values were found to be curiously variable between the uncured and cured FB1 wild-type as well as the uncured and cured $\Deltaump\ 1,\Deltaump\ 2$ mutant. The FB2 cured $\delta^{15}\text{N}$ (‰) value was lower than that of the FB2 uncured, but still of sufficient value, 7.41‰, to indicate $^{15}\text{N}_2$ incorporation. The $\Deltaump\ 1,\Deltaump\ 2$ cured mutant also returned a $\delta^{15}\text{N}$ (‰) lower than that of the $\Deltaump\ 1,\Deltaump\ 2$ mutant that had not been passaged.

Table 6. SIRMS values from protein samples derived from chamber-grown no-ammonium SLAD agar plates.

Strain	$\delta^{15}\text{N}$ (‰)	$\delta^{13}\text{C}$ (‰)
FB1 wild-type	25.27	38.89
FB1 cured	21.23	100.43
FB2 wild-type	18.95	89.24
FB2 cured	7.41	92.85
$\Deltaump\ 1,\Deltaump\ 2$	37.8	47.79
$\Deltaump\ 1,\Deltaump\ 2$ cured	13.21	120.33

PCR Screenings. For interrogations with universal, degenerate primers where there was an amplicon of the appropriate size, those fragments were sequenced and the results were summarized in the following section with sequence data in the Appendices.

The initial PCR screening of CRR-14, CRR-15, along with *U. maydis* strains FB1 and FB2 with the *nifH* primers nifHF and nifHR (Figure 17) revealed a fragment of about 360 bp amplified from CRR-15. The CRR-14 fragment between 1000 and 1440 base

pairs approximated results from previous work (Cooper, 2013). No amplicon was observed from either FB1 or FB2.

The use of the i37F/i37R primers on those same templates resulted in fragments of approximately 600 bp from FB1 and FB2 with no corresponding fragments from CRR-14 or CRR-15. This reaction demonstrated that the genomic DNA from FB1 and FB2 was of sufficient quality that any *nifH* that might have had been present could have been amplified.

When primers recommended for the amplification of *Azospirillum nifH* a38F/a39R were used, Figure 22, under a slightly lower annealing temperature, 56°C, multiple fragments were observed using CRR-15 as a template. This included a fragment

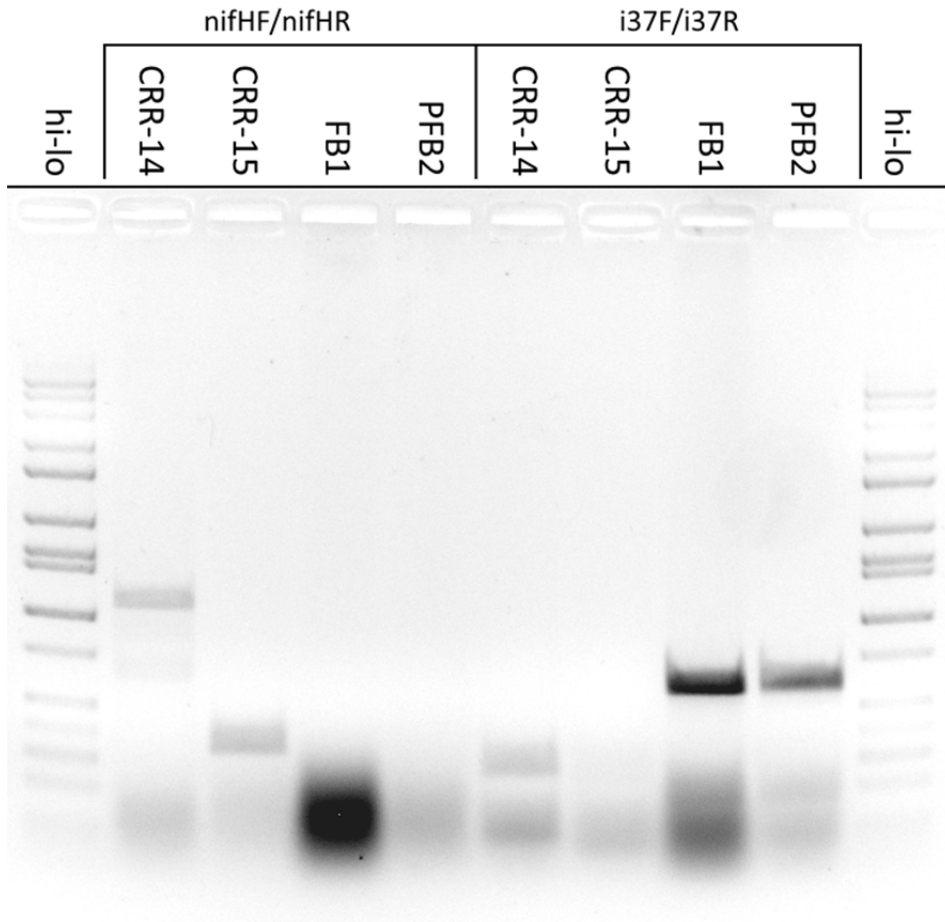


Figure 22. Gel electrophoresis results following PCR using CRR-14, CRR-15, *U. maydis* FB1 and FB2 strains as templates with nifHF/nifHR and i37F/i37R primer combinations.

of approximately 200 bp which matched the anticipated fragment size from *Azospirillum*. The nifHF and nifHR primers under those same conditions revealed fragments from CRR-15 and *U. maydis* strains FB1 and FB2 between 300 and 400 bp. The fragment from CRR-15 was directly sequence while the fragment from FB1 was cloned and then sequenced (Table 7).

The universal prokaryotic 16S rDNA primers 68F and 1392R amplified a fragment from CRR-15 of approximately 1300 bp. No amplicon was observed from the same reaction attempted with *U. maydis* FB1 or FB2 (Figure 23).

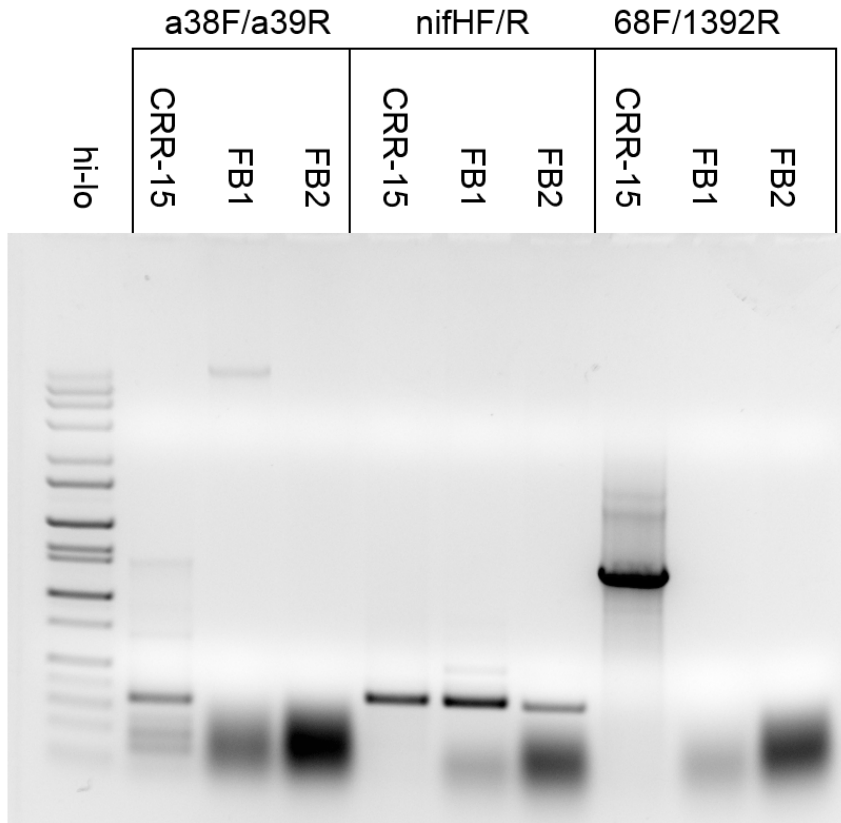


Figure 23. Gel electrophoresis results following PCR using CRR-15, *U. maydis* FB1 and FB2 strains as templates with a38F/a39R, nifHF/nifHR and 68F/1392R primer combinations. The annealing temperature was 56°C.

Additional PCR screenings using primers designed for the *Bacillus pumilus* 16S rRNA gene and *nifH* were performed (Figure 24). The primer set p5F/p6R was expected to amplify a fragment of 323 bp. No amplicon was observed from reactions with FB1 or FB2. Reactions using CRR-14 and CRR-15 templates did produce visible fragments

where both had at least one fragment near that target size. The primer set p3F/p4R was expected to amplify a fragment of 1485 bp. Again, no amplicon was observed using either FB1 or FB2 genomic DNA as a template or curiously, even the genomic DNA of CRR-15, though CRR-14 did have a fragment near that expected size. Meanwhile amplification with the nifHF/nifHR primer set also failed to amplify DNA fragments from FB1 or FB2 as well as from CRR-14. Strain CRR-15 again demonstrated amplification of a band with the expected size, about 360 bp.

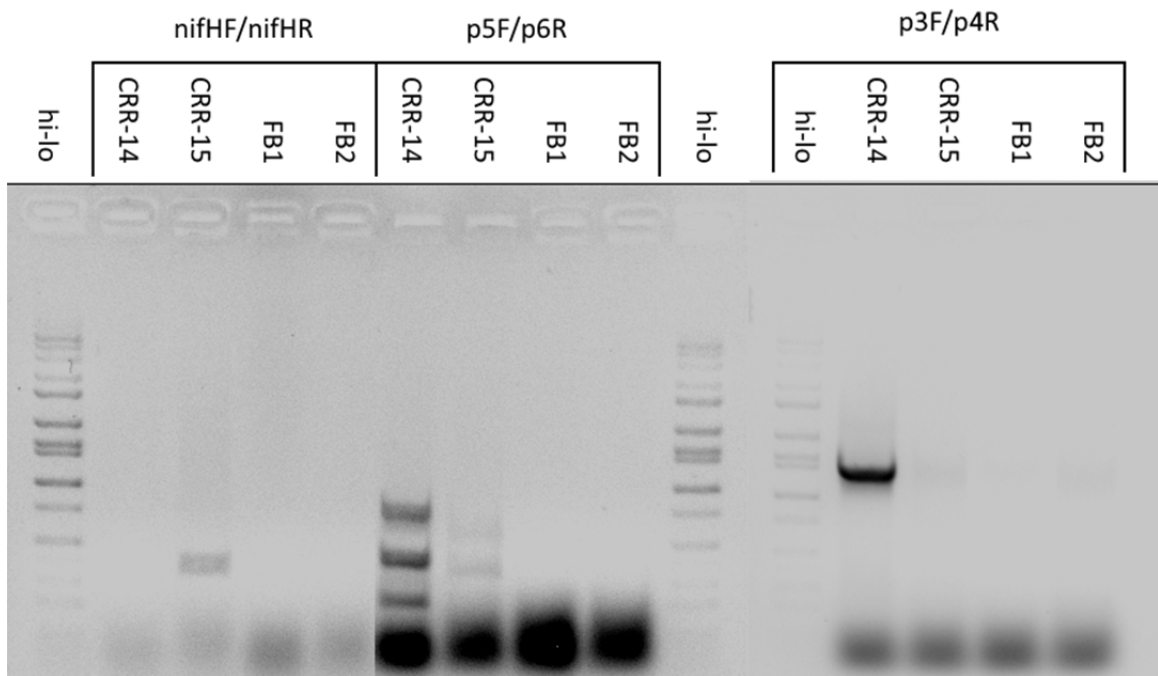


Figure 24. Gel electrophoresis results following PCR using CRR-14, CRR-15, *U. maydis* FB1 and FB2 strains as templates with nifHF/nifHR, p3F/p4R and p5F/p6R. Annealing temperature was 60°C.

Sequence Data. Amplified DNA fragments obtained from PCR were either sequenced directly from PCR product or following cloning. Cloning was employed after a number of sequencing reactions yielded no usable DNA sequence information. Table 7 summarizes the useful sequence data that was obtained.

Initial DNA sequences derived from 16S rDNA amplification reactions in *U. maydis* strains did reveal some 16S ribosomal RNA gene matches. The *Staphylococcus aureus* matches from DNA fragments amplified with 16S primers from the *U. maydis* strains 1/2 and FB2 as well as the sequence match to *Pseudomonas synxantha* were most

Table 7. Summary* of BLAST search results on obtained sequence data.

Source	Fragment	Primer(s)	Size (bp)	Match	Identity
CRR-15	16S-like	68F	1009	<i>Erwinia chrysanthemi</i> strain CRR-15 16S rRNA gene	97%
CRR-15	nifH-like	nifHF	360	<i>Dickeya dadantii</i> 3937, <i>nifH</i>	72%
FB1 WT	16S-like	68F	1025	<i>Pseudomonas synxantha</i> strain A1 16S rRNA gene	95%
FB1 WT	nifH-like	M13(-21)F	382	UMAG_05454	98%
$\Delta ump1, \Delta ump2$	16S-like	M13(-21)F	901	UMAG_02524	99%
$\Delta ump1, \Delta ump2$	nifH-like	M13(-21)F	556	UMAG_10959	99%
$\Delta ump1, \Delta ump2$	nifH-like	M13(-21)F	477	UMAG_05454	99%
1/2	16S-like	M13(-21)F M13R	1484	<i>Staphylococcus aureus</i> subsp. <i>aureus</i> , 16S rRNA	99%
FB2	16S-like	M13(-21)F M13R	1506	<i>Staphylococcus aureus</i> strain XN108, 16S rRNA	93%

*Complete entries for these results are in the Sequence Data included in the Appendices.

likely derived from contaminating DNA as those PCR results failed to be replicated in subsequent amplification attempts. The DNA sequences obtained from CRR-15 amplicons matched their expected targets for both 16S rDNA and *nifH*.

The DNA sequence data from the FB1 wild-type and $\Delta ump1, \Delta ump2$ mutant matched, to high identities, various *Ustilago maydis* loci. None of those loci have been characterized beyond predicted amino acid sequences and putative protein domains, however, none of those loci matched either *nifH* or 16S rDNA.

DNA Dilution. The dilution of CRR-15 chromosomal DNA into *U. maydis* strain FB1 wild-type chromosomal DNA, Figure 25, revealed that 16S rDNA would still be accessible by PCR. Relative band densities appeared to indicate potential competitive interference by *U. maydis* chromosomal DNA.

Dilution PCR Series Using 68F/1392R

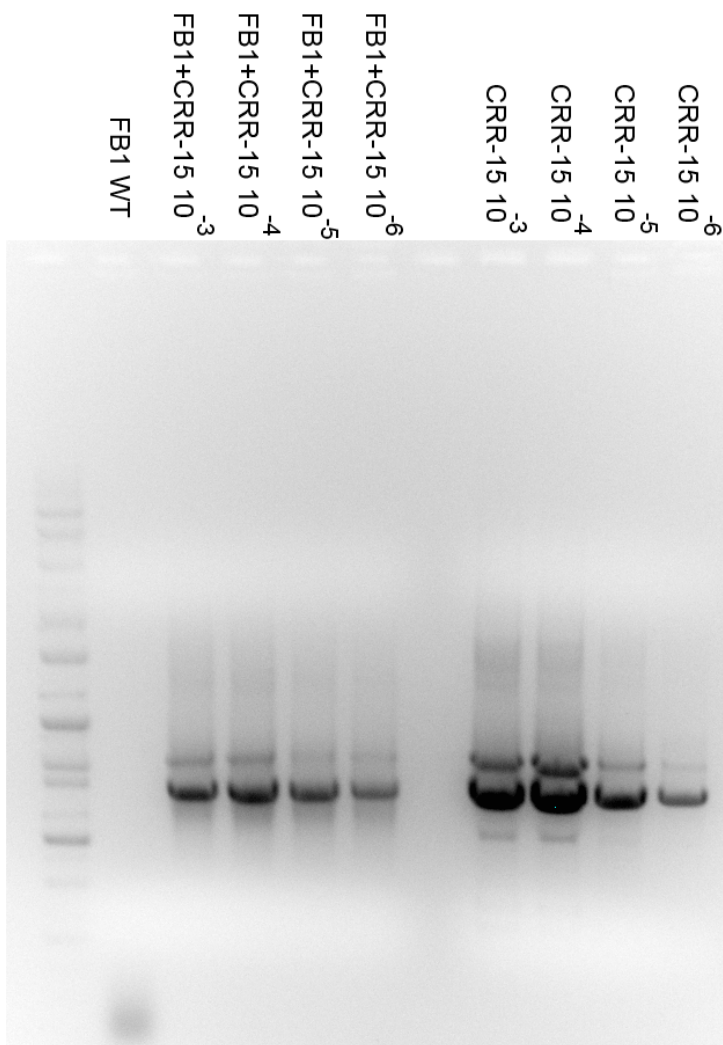


Figure 25. Dilution series using universal, prokaryotic 16S rDNA primers. There appeared to be some competitive interference from FB1 chromosomal DNA, but the expected-sized fragment was consistently detected.

Discussion

The elimination of a prokaryotic endosymbiont from a eukaryotic host has been successfully accomplished in the elimination of *Wolbachia* from the springtail species *Folsomia candida* (Pike and Kingcombe, 2009) through the use of antibiotic treatments. Similar treatments were used to eliminate endosymbionts from the rove beetle species

Paederus sabaesus (Kellner, 2001). The arbuscular mycorrhizal fungus (AMF) *Gigaspora margarita* had been cured of its endobacteria by use of serial single-spore *in vitro* inocula technique (Lumini et al., 2007). Two passages through single antibiotic treatments of *U. maydis* that were claimed to harbor endosymbionts failed to eliminate the ability to grow in no-ammonium media, but was reported to reduce growth in nitrogen-free media in the first and second passage (Ruiz-Herrera et al., 2015). Therefore we attempted serial passages through very high doses of antimicrobial compounds as a way to further ensure loss of any putative endosymbiont prokaryote species. In contrast to those observations, we found not only continued growth in no-ammonium conditions but two of the passaged *U. maydis* strains, the FB1 $\Delta ump 1, \Delta ump 2$ mutant and FB2 (obtained from José Ruiz-Herrera) achieved higher stationary-phase absorbance (A_{600}) values (Figure 18). While that observation could be an artifact of selection by the passaging protocol, where a small volume (10 μ L) of vigorously growing cells was transferred serially over the course of a week, the ability to continue to grow without ammonium could suggest that any potential endosymbiont that had been present induced a growth deficit rather than contributing to growth in a no-ammonium condition. Additional work is being conducted to reassess this result with particular emphasis on a higher number of replicates. The $\delta^{15}\text{N}$ values derived from SIRMS, unfortunately, lacked replication for the cured and uncured FB1 and FB2 wild-types and the $\Delta ump 1, \Delta ump 2$ mutant, making it difficult to draw a conclusion regarding differences that could be attributed to the “curing” process. Those values did demonstrate, though, that $^{15}\text{N}_2$ was still being incorporated into proteinacious biomass regardless of treatment status, as with the passaged cell growth results this will be examined in more detail with replication.

Considering that no PCR results confirmed the presence of the *nifH* gene in any *U. maydis* strains with or without serial antimicrobial compound treatment, PCR could not be used to confirm that the passaged *U. maydis* cells had, indeed been cured of any potential endosymbiont. While multiple PCR results indicated that no 16S rDNA-sized fragments were found, the 16S rDNA sequence data recovered from *U. maydis* was not replicated and most likely represented contamination by normal bacterial flora, though it was clear in the DNA dilution experiment that it was still possible to detect that gene from *Dickeya dadantii* even at very low copy numbers particularly in relation to the number of copies of available *U. maydis* FB1 DNA in those reactions. (Of note, the *Dickeya dadantii* Ech703 complete genome shows seven copies of the 16S ribosomal RNA genes.)

Our initial contact with the Ruiz-Herrera lab followed the presentation of some of the data reported in both Chapter II and III as well as some of the data reported in this chapter to the *Ustilago* satellite meeting at the 27th Fungal Genetics Conference at Asilomar, CA (Cooper and Perlin, 2013). José Ruiz-Herrera contacted Michael Perlin relaying their observations and were convinced that there was an endosymbiont involved. Working with their *U. maydis* 1/2 and FB2 strains we were unable to replicate their results, not finding evidence of either prokaryotic 16S *rRNA* genes or *nifH*, the most commonly assayed structural gene in the *nifHDK* operon.

Absent evidence of an endosymbiont from our experiments, along with the lack of the ubiquitous nitrogenase operon, leaves the possibility of a novel type of nitrogen fixation. Moreover neither the *U. maydis* genome sequence (Kämper et al., 2006), nor subsequent RNA-Seq experiments have identified gene expression indicative of a

canonical nitrogenase as would be found in an endosymbiont. For example, in our lab, RNA-Seq of wild-type and *ump2* mutants in nutrient replete and low-ammonium media did not reveal transcripts for components of the classical *nif* operon, even when considering unmapped reads that matched prokaryotes (Wallen, M, unpublished data).

Additionally, this capacity was also not related to the unique MoFeS nitrogenase system found in *Streptomyces thermophiles* (Ribbe et al., 1997). Considering the sensitivity of the Mo-Fe, Va-Fe and Fe-Fe nitrogenases to oxygen, some mechanism would need to be present to prevent inhibition of a hypothetical nitrogen fixation system in *U. maydis* if it was at all similar to those nitrogenases. Perhaps the numerous vacuoles that form in nitrogen starved cells (Figure 8) could satisfy such a requirement for low oxygen. The future for this line of research may fundamentally alter our understanding of biogeochemical nitrogen cycling, but also could lead to agricultural improvements which could dramatically reduce anthropogenic contributions to deleterious ecological impacts such as eutrophication.

CHAPTER V

GENERAL CONCLUSION

Overall our results point to a previously unidentified metabolic capacity to convert atmospheric dinitrogen to biologically-available nitrogen that was incorporated into *Ustilago maydis* biomass. We demonstrated that this ability is related to genotype, particularly in the FB1 $\Delta ump1, \Delta ump2$ mutant which consistently incorporated more atmospheric dinitrogen as compared to the FB1 wild-type in liquid media.

While it would be easy to conclude that there is an endosymbiont utilizing canonical nitrogen fixation through the MoFe nitrogenase system these data do not support that conclusion. This leaves more than one alternative explanation for the observed incorporation of $^{15}\text{N}_2$ tracer into cellular biomass. These alternatives include a novel prokaryotic nitrogen fixation system that does not rely on nitrogenase and is employed by an endosymbiont with a cryptic 16S rDNA sequence unable to be reliably amplified by PCR, a eukaryotic nitrogen fixation system that, also, bears no close homology to either the superoxidase-dependent nitrogen fixation system in *Streptomyces thermophiles* or the canonical nitrogenases, or that, perhaps, these observations could be explained by an alternative metabolic pathway in the *Ustilago maydis*, perhaps in the mitochondria. Any of those alternatives would prove very interesting.

The extant *S. thermophiles* sequences suggested to be part of its superoxidase-dependent nitrogenase, a combination of amino-acid and DNA sequences, was obtained from a graduate thesis written by a student of Ortwin Meyer, Carla Hofmann-Findeklee, presented at Bayreuth University, in Bayreuth, Germany. While her dissertation is available online, her thesis is not. Those sequences were communicated to me via email by Cory Tobin, a graduate student of Biology at Caltech on February 13, 2014. None of those sequences bore any significant homology to any *U. maydis* DNA sequences. They are, however, included in the Appendices.

Additional support for a novel nitrogen pathway is found in the results involving the *Agrobacterium* strain CRR-14 which has been confirmed to incorporate ^{15}N tracer. That particular strain was sequenced (the two chromosomes, linear and circular, and an accessory plasmid) with no sequences matching any nitrogenase-related gene (Johnston, T, Murray State University, unpublished data). Attempts at assaying acetylene reduction using CRR-14 also failed; the acetylene concentration fell with no detection of an ethylene peak, though other work had found positive acetylene reduction results in another *A. tumefaciens* strain (Kanvinde and Sastry, 1990). The CRR-14 whole genome sequencing project contradicted the results I had obtained in detecting *nifH* but without the ability to amplify any other portion of that *nif* operon. For that work the tentative conclusion was reached that MoFe nitrogenase was present, but either in a novel operon arrangement or persistently unable to be amplified and cloned from the CRR-14 background due to the amplification of other, non-nitrogenase related *Agrobacterium* sequences despite repeated attempts at PCR using a variety of primers as well as

temperature and magnesium chloride concentration gradient optimizations. Inverse PCR was also attempted, and failed to recover relevant sequence data (Cooper, 2013).

Interestingly subsequent work by Kanvinde revealed a 29,000 bp region between the *his19* and *trp20* genes, including “nif” genes (The “nif” designation is what they referred to these genes in their work as the “*Agrobacterium* nitrogenase” despite the lack of hybridization to *nif* DNA probes.) In that work they transferred that region of DNA by recombination to a nitrogen-fixation incompetent *Rhizobium meliloti* (*nifH*, *nifK*) which was then demonstrated to be able to fix nitrogen including enabling the growth of Alfalfa in sterilized vermiculite (Shoushtari et al., 2010). No open reading frames in that *his-trp* region, as obtained from the H13-3 genomic DNA sequences, bore any significant homology to any *U. maydis* sequences.

Extant literature describing evidence for diazotroph activity in all types of conditions generally relies on PCR using primers for *nifH* fragments. Usually that work is based on DNA obtained directly from terrestrial soils or sediments underlying freshwater bodies and directly from seawater samples. Along with PCR attempts experiments utilizing ^{15}N tracer, and stable isotope ratio analysis (SIRMS) in this work (Montoya et al., 1996) isotope dilution using $^{15}\text{NO}_3^-$ or similarly labeled ammonium are also commonly employed, where the lower the $\delta^{15}\text{N}$ values the more the nitrogen in the sample was incorporated from N_2 (Barraclough, 1995; Boddey et al., 1996; Busse, 2000; Chalk, 1985). The isotope dilution method is better-suited to field applications as it does not require sealed incubators into which $^{15}\text{N}_2$ can be delivered. In estimations of the marine nitrogen fixation budget dissolved $^{15}\text{N}_2$ in seawater, rather than addition as a gas has been found to be more accurate (Mohr et al., 2010) and, as the samples are already

liquid, readily accomplished. Future work seeking to identify nitrogen fixation rates in *U. maydis* in liquid media may benefit from that approach. The acetylene reduction assay (ARA) (Capone, 1993) is still commonly employed, sometimes with SIRMS. Those three methods, PCR screening, ARA and SIRMS represent the primary methodological approaches for all current and past work investigating diazotrophy.

Much of that work is done directly with environmental samples, with no attempt to isolate potential diazotrophs in pure culture. Considering the unculturable nature of the estimated majority of microorganisms (Kamagata and Tamaki, 2005) that represents a current limitation in the discrete characterization of specific diazotrophs. That is particularly true considering the prevalence of the lateral gene transfer of *nifH* genes as compared to 16S rDNA sequences (Zehr et al., 2003b). Of studies that have obtained and tested isolates there are some interesting exceptions to the essential *nifH*, ARA and SIRMS results reported in most work indicating the possibility of an, as of yet, uncharacterized type of nitrogen fixation. Table 8 lists some of these studies. In these

Table 8. Studies involving subcultured isolates cultivated using N-free media.

Isolates	PCR	ARA	¹⁵ N ₂ Tracer	Reference
5	na	0	negative	(Hill and Postgate, 1969)
251	70 ¹	31 ¹	na	(Ozawa et al., 2003)
11	1	1	na	(Dalton et al., 2004)
7	0	0	positive ²	(Hoefsloot et al., 2005)
3	3	0	na	(Chou et al., 2008)
17	7	5	na	(Doty et al., 2009)
178	11	11	na	(Montanez et al., 2009)
534	23	23 ³	na	(Jin et al., 2011)
47	0	0	na	(Bentzon-Tilia et al., 2014)
231	34	34 ³	na	(Kumar et al., 2014)
11	2	na	na	(Burbano et al., 2015)
30	na	28	na	(Santos et al., 2015)
60	10	11 ³	na	(Sarathambal et al., 2015)

na: not applicable, that test was either not utilized or not reported in that study.

¹ Some were found to have *nifH* and not reduce acetylene and vice-versa.

² As assayed in the sugarcane from which those isolates were derived.

³ Only the *nifH* + isolates were tested by ARA.

works SIRMS was not widely used. While growth using N-free media is not an indication of nitrogen fixation, it is widely used as an initial screening of potential diazotrophs.

The suggestion that contamination of media by ammonia secretion, even into gas-tight containers (Hill and Postgate, 1969), is the reason bacterial isolates are able to grow in N-free media is difficult to countenance. Possible contamination by other sources of nitrogen seems much more reasonable, but perhaps not for every study providing evidence of growth in N-free media without detection of *nifH* by PCR or ethylene in ARA. There is also a potential confounding effect on the detection and elucidation of *nifH* by PCR and RT-PCR as, under many conditions, it is possible to amplify *nifH* fragments from negative controls and reagent blanks (Zehr et al., 2003a), leading to the very real possibility of false positive results. This could have had been a factor in those results reported in Table 8. Compounding that potential source of error is the discovery of contamination of $^{15}\text{N}_2$, as tested with gas from both Sigma-Aldrich and Cambridge Isotopes (Dabundo et al., 2014). Those results do not impact the interpretation of any data presented here as the maximal value observed for $\delta^{15}\text{N}$ was 5‰ in samples where $^{15}\text{N}_2$ was added. In that series of experiments 2 mL of $^{15}\text{N}_2$ was added to a 20 mL serum vial with 10 mL of 10 $\mu\text{m/L}$ sodium nitrate which is at least 2 order of magnitude higher tracer addition than any experimental additions of $^{15}\text{N}_2$ tracer in our work.

An alternative description of organisms able to grow without significant nitrogen was briefly in the literature until about 1980 (Fedorov and Kalininskaya, 1959; Kvasnikov et al., 1971; Line and Loutit, 1973; Mal'tseva and Ivanitskaia, 1980; Sarić,

1978), following its initial use by Martinus Beijerinck (Beijerinck, 1901) to apparently describe nitrogen-fixing organisms, or at least organisms that appear to be able to grow under very low ammonium. (There is an exception from 2002, though it appears that those authors meant to use the term “oligotrophic” rather than “oligonitrophilic” (Hamelin et al., 2002).)

Our work did not support the conclusions reached in Ruiz-Herrera (Ruiz-Herrera et al., 2015). We did not find evidence supporting the presence of an endosymbiont related to *Bacillus pumilus* having a canonical *nif* MoFe nitrogenase or, indeed, for any endosymbiont. Even testing their *U. maydis* strains FB2 and 1/2 gave disparate findings between our two labs.

In *U. maydis* multiple attempts were made during this work to create mutants deficient in selected putative genes to see if a disruption of those genes would result in an effect on the growth of *U. maydis* in low to no-ammonium conditions. Finding a gene involved in this atmospheric nitrogen assimilation pathway would be convincing evidence supporting this atmospheric dinitrogen assimilation (ANNA) in *U. maydis*. Potential targets were selected primarily based on the potential of those putative genes' involvement in nitrogen metabolism based on predicted amino acid sequences. Considering how necessary the dinitrogenase reductase is to the nitrogenase complex, predicted proteins having iron-sulfur (Fe₂S₄)-containing domains were of particular interest. Methodological considerations included examining the flanks of putative genes for adequate non-coding sequence, about 1,000 bp, as well as restriction enzyme sites within the gene and those flanks were also involved. While a number of transformants of *U. maydis* were obtained, none had lost the targeted gene.

Any conclusion that involves a nitrogen-fixation system that is directly compatible with eukaryotic metabolism has the very exciting potential to be incorporated into agricultural cultivars such that a reduction in synthetic nitrogen fertilization would be possible. While this goal has been approached utilizing canonical nitrogenases it has remained elusive. This could, eventually, at least, contribute to a reduction in eutrophication as well as being incorporated into emerging sustainable farming practices.

In looking for a possible symbiotic interaction a pilot growth experiment was also conducted comparing *Zea mays* (golden bantam) fertilized in a sand substrate using Hoagland's Solution either with or without nitrogen, that was either uninfected or infected with two different titers of *U. maydis* strain SG200 (Bolker et al., 1995). Those results are not reported here formally as the method followed to measure the dry mass of the plants after two weeks of growth appeared too imprecise to offer clear resolution. Summary of this experiment appears in the Appendices. This particular experiment could merit a repetition as, even with the loss of accuracy found in obtaining the masses of dried plants in envelopes, there did appear to be more biomass in the infected, nitrogen-free plants than in the uninfected, nitrogen-free plants. That experimental approach using $^{15}\text{N}_2$ and using SIRMS on plant tissues could provide a much more definite answer.

REFERENCES

- Adesemoye, A.O., Torbert, H.A., and Kloepper, J.W. (2008). Enhanced plant nutrient use efficiency with PGPR and AMF in an integrated nutrient management system. *Canadian Journal of Microbiology* 54, 876-886.
- Agarwal, C., Aulakh, K.B., Edelen, K., Cooper, M., Wallen, R.M., Adams, S., Schultz, D.J., and Perlin, M.H. (2013). *Ustilago maydis* phosphodiesterases play a role in the dimorphic switch and in pathogenicity. *Microbiol-Sgm* 159, 857-868.
- Agrios, A.G. (2005). *Plant Pathology*, 5 edn (Burlington, MA: Elsevier Academic Press).
- Allen, A., Islamovic, E., Kaur, J., Gold, S., Shah, D., and Smith, T.J. (2011). Transgenic maize plants expressing the Totivirus antifungal protein, KP4, are highly resistant to corn smut. *Plant Biotechnology Journal* 9, 857-864.
- Allen, A., Islamovic, E., Kaur, J., Gold, S., Shah, D., and Smith, T.J. (2013). The virally encoded killer proteins from *Ustilago maydis*. *Fungal Biol Rev* 26, 166-173.
- Altschul, S.F., Gish, W., Miller, W., Myers, E.W., and Lipman, D.J. (1990). Basic local alignment search tool. *J Mol Biol* 215, 403-410.
- Amann, R.I., Ludwig, W., and Schleifer, K.-H. (1995). Phylogenetic identification and in situ detection of individual microbial cells without cultivation. *Microbiological reviews* 59, 143-169.
- Andrade, S.L.A., and Einsle, O. (2007). The Amt/Mep/Rh family of ammonium transport proteins. *Mol Membr Biol* 24, 357-365.
- Banuett, F., and Herskowitz, I. (1989). Different alleles of *Ustilago maydis* are necessary for maintenance of filamentous growth but not for meiosis. *Proceedings of the National Academy of Sciences* 86, 5878-5882.
- Barraclough, D. (1995). ¹⁵N isotope dilution techniques to study soil nitrogen transformations and plant uptake. *Fertilizer research* 42, 185-192.
- Beijerinck, M. (1901). Über oligonitrophile mikroben. *Centbl Bakt[etc]*, Abt 2, 561-582.
- Beijerinck, M.W. (1908). Verslagen van de Gewone Vergaderingen der Wis- en Natuurkundige. Kon Akademie van Wetenschappen 11, 67-74.
- Beimforde, C., Feldberg, K., Nylinder, S., Rikkinen, J., Tuovila, H., Dorfelt, H., Gube, M., Jackson, D.J., Reitner, J., Seyfullah, L.J., *et al.* (2014). Estimating the Phanerozoic history of the Ascomycota lineages: Combining fossil and molecular data. *Mol Phylogenet Evol* 78, 386-398.

- Bender, S.F., and van der Heijden, M.G.A. (2015). Soil biota enhance agricultural sustainability by improving crop yield, nutrient uptake and reducing nitrogen leaching losses. *J Appl Ecol* 52, 228-239.
- Bentzon-Tilia, M., Farnelid, H., Jurgens, K., and Riemann, L. (2014). Cultivation and isolation of N₂-fixing bacteria from suboxic waters in the Baltic Sea. *Fems Microbiol Ecol* 88, 358-371.
- Biswas, K., and Morschhauser, J. (2005). The Mep2p ammonium permease controls nitrogen starvation-induced filamentous growth in *Candida albicans*. *Molecular Microbiology* 56, 649-669.
- Blackwell, M. (2011). The Fungi: 1, 2, 3 ... 5.1 million species? *American Journal of Botany* 98, 426-438.
- Boddey, R.M., de Oliveira, O.C., Alves, B.J., and Urquiaga, S. (1996). Field application of the 15N isotope dilution technique for the reliable quantification of plant-associated biological nitrogen fixation. In *Nitrogen Economy in Tropical Soils* (Springer), pp. 77-87.
- Boeckstaens, M., Andre, B., and Marini, A.M. (2007). The yeast ammonium transport protein Mep2 and its positive regulator, the Npr1 kinase, play an important role in normal and pseudohyphal growth on various nitrogen media through retrieval of excreted ammonium. *Molecular Microbiology* 64, 534-546.
- Bolker, M., Genin, S., Lehmler, C., and Kahmann, R. (1995). Genetic-Regulation of Mating and Dimorphism in *Ustilago-Maydis*. *Can J Bot* 73, S320-S325.
- Borneman, J., Skroch, P.W., O'Sullivan, K.M., Palus, J.A., Rumjanek, N.G., Jansen, J.L., Nienhuis, J., and Triplett, E.W. (1996a). Molecular microbial diversity of an agricultural soil in Wisconsin. *Applied and Environmental Microbiology* 62, 1935.
- Borneman, J., Skroch, P.W., O'Sullivan, K.M., Palus, J.A., Rumjanek, N.G., Jansen, J.L., Nienhuis, J., and Triplett, E.W. (1996b). Molecular microbial diversity of an agricultural soil in Wisconsin. *Applied and Environmental Microbiology* 62, 1935-1943.
- Bowman, D.H. (1946). Sporidial Fusion in *Ustilago maydis*. *Journal of Agricultural Research* 72, 223-244.
- Boyd, E., Anbar, A., Miller, S., Hamilton, T., Lavin, M., and Peters, J. (2011). A late methanogen origin for molybdenum-dependent nitrogenase. *Geobiology* 9, 221-232.
- Boyd, E.S., Costas, A.M.G., Hamilton, T.L., Mus, F., and Peters, J.W. (2015). Evolution of Molybdenum Nitrogenase during the Transition from Anaerobic to Aerobic Metabolism. *Journal of Bacteriology* 197, 1690-1699.
- Boyer, S.H. (1968). The genetic code: The molecular basis for genetic expression. *American Journal of Human Genetics* 20, 403-404.
- Brandes, J.A., Devol, A.H., and Deutsch, C. (2007). New developments in the marine nitrogen cycle. *Chem Rev* 107, 577-589.

- Brosius, J., Dull, T.J., Sleeter, D.D., and Noller, H.F. (1981). Gene organization and primary structure of a ribosomal RNA operon from *Escherichia coli*. *J Mol Biol* 148, 107-127.
- Burbano, C.S., Gronemeyer, J.L., Hurek, T., and Reinhold-Hurek, B. (2015). Microbial community structure and functional diversity of nitrogen-fixing bacteria associated with *Colophospermum mopane*. *Fems Microbiol Ecol* 91.
- Busse, M.D. (2000). Suitability and use of the ^{15}N -isotope dilution method to estimate nitrogen fixation by actinorhizal shrubs. *Forest Ecology and Management* 136, 85-95.
- Canfield, D.E., Glazer, A.N., and Falkowski, P.G. (2010). The evolution and future of Earth's nitrogen cycle. *science* 330, 192-196.
- Capone, D. (1993). Determination of nitrogenase activity in aquatic samples using the acetylene reduction procedure. *Handbook of methods in aquatic microbial ecology* 200, 621-631.
- Cavalier-Smith, T. (2002a). Chloroplast evolution: Secondary symbiogenesis and multiple losses. *Current Biology* 12, R62-R64.
- Cavalier-Smith, T. (2002b). The neomuran origin of archaeobacteria, the eubacterial root of the universal tree and bacterial megaclassification. *Int J Syst Evol Micr* 52, 7-76.
- Cavalier-Smith, T. (2006). Origin of mitochondria by intracellular enslavement of a photosynthetic purple bacterium. *P R Soc B* 273, 1943-1952.
- Cavalier-Smith, T. (2009). Megaphylogeny, Cell Body Plans, Adaptive Zones: Causes and Timing of Eukaryote Basal Radiations. *J Eukaryot Microbiol* 56, 26-33.
- Cavalier-Smith, T. (2013). Early evolution of eukaryote feeding modes, cell structural diversity, and classification of the protozoan phyla Loukozoa, Sulcozoa, and Choanozoa. *Eur J Protistol* 49, 115-178.
- Cavalier-Smith, T., Chao, E.E., Snell, E.A., Berney, C., Fiore-Donno, A.M., and Lewis, R. (2014). Multigene eukaryote phylogeny reveals the likely protozoan ancestors of opisthokonts (animals, fungi, choanozoans) and Amoebozoa. *Mol Phylogenet Evol* 81, 71-85.
- Chalk, P.M. (1985). Estimation of N_2 fixation by isotope dilution: An appraisal of techniques involving ^{15}N enrichment and their application. *Soil Biology and Biochemistry* 17, 389-410.
- Chou, J.H., Jiang, S.R., Cho, J.C., Song, J., Lin, M.C., and Chen, W.M. (2008). *Azonexus hydrophilus* sp nov., a nifH gene-harboring bacterium isolated from freshwater. *Int J Syst Evol Micr* 58, 946-951.
- Cooper, M. (2013). Molecular Evidence for Diazotrophic *Agrobacterium*. In *Biology* (Murray, KY: Murray State University).
- Cooper, M., and Perlin, M.H. (2013). Living on Air?: *Ustilago maydis* cells grow without being provided nitrogen in their growth media. Paper presented at: 27th Fungal Genetics Conference (Asilomar, Pacific Grove, CA).

- Crick, F.H.C. (1968). ORIGIN OF GENETIC CODE. *Journal of Molecular Biology* 38, 367-&.
- Cruz, A.F., and Ishii, T. (2011). Arbuscular mycorrhizal fungal spores host bacteria that affect nutrient biodynamics and biocontrol of soil-borne plant pathogens. *Biology open*, BIO2011014.
- Dabundo, R., Lehmann, M.F., Treibergs, L., Tobias, C.R., Altabet, M.A., Moisaner, P.H., and Granger, J. (2014). The contamination of commercial 15 N 2 gas stocks with 15 N-labeled nitrate and ammonium and consequences for nitrogen fixation measurements.
- Dalton, D.A., Kramer, S., Azios, N., Fusaro, S., Cahill, E., and Kennedy, C. (2004). Endophytic nitrogen fixation in dune grasses (*Ammophila arenaria* and *Elymus mollis*) from Oregon. *Fems Microbiol Ecol* 49, 469-479.
- Day, P.R., and Anagnost.SI (1971). Corn Smut Dikaryon in Culture. *Nature-New Biol* 231, 19-&.
- Dhakal, P., Matocha, C., Huggins, F., and Vandiviere, M. (2013). Nitrite reactivity with magnetite. *Environmental science & technology* 47, 6206-6213.
- Dilworth, M. (1966). Acetylene reduction by nitrogen-fixing preparations from *Clostridium pasteurianum*. *Biochimica et Biophysica Acta (BBA)-General Subjects* 127, 285-294.
- Doty, S.L., Oakley, B., Xin, G., Kang, J.W., Singleton, G., Khan, Z., Vajzovic, A., and Staley, J.T. (2009). Diazotrophic endophytes of native black cottonwood and willow. *Symbiosis* 47, 23-33.
- Edwards, H.G., and Vandenabeele, P. (2012). *Analytical archaeometry: selected topics* (Royal Society of Chemistry).
- Egholm, M., Buchardt, O., Nielsen, P.E., and Berg, R.H. (1992). PEPTIDE NUCLEIC-ACIDS (PNA) - OLIGONUCLEOTIDE ANALOGS WITH AN ACHIRAL PEPTIDE BACKBONE. *J Am Chem Soc* 114, 1895-1897.
- Etique, M., Jorand, F.P.A., Zegeye, A., Grégoire, B., Despas, C., and Ruby, C. (2014). Abiotic Process for Fe(II) Oxidation and Green Rust Mineralization Driven by a Heterotrophic Nitrate Reducing Bacteria (*Klebsiella mobilis*). *Environmental Science & Technology* 48, 3742-3751.
- Faeth, S.H., and Fagan, W.F. (2002). Fungal endophytes: Common host plant symbionts but uncommon mutualists. *Integr Comp Biol* 42, 360-368.
- Fedler, M., Kai-Stephen, L., Stelter, K., Nieto-Jacobo, F., and Basse, C.W. (2009). The a2 Mating-Type Locus Genes *lga2* and *rga2* Direct Uniparental Mitochondrial DNA (mtDNA) Inheritance and Constrain mtDNA Recombination During Sexual Development of *Ustilago maydis*. *Genetics* 181, 847-860.
- Fedorov, M., and Kalininskaya, T. (1959). Nitrogen-fixing activity of mixed cultures of oligonitrophile microorganisms. *Microbiologiya* 28, 323.
- Fowler, D., Coyle, M., Skiba, U., Sutton, M.A., Cape, J.N., Reis, S., Sheppard, L.J., Jenkins, A., Grizzetti, B., and Galloway, J.N. (2013). The global nitrogen cycle in the

twenty-first century. *Philosophical Transactions of the Royal Society of London B: Biological Sciences* 368, 20130164.

Franceschini, A., Szklarczyk, D., Frankild, S., Kuhn, M., Simonovic, M., Roth, A., Lin, J., Minguez, P., Bork, P., and von Mering, C. (2013). STRING v9. 1: protein-protein interaction networks, with increased coverage and integration. *Nucleic acids research* 41, D808-D815.

Gauthier, G.M., and Keller, N.P. (2013). Crossover fungal pathogens: The biology and pathogenesis of fungi capable of crossing kingdoms to infect plants and humans. *Fungal Genetics and Biology* 61, 146-157.

Gesteland, R., and Atkins, J. (1983). *The RNA world: the nature of modern RNA suggests a prebiotic RNA world* (Monograph/Cold Spring Harbor Laboratory, No 24).

Gilmore, M.R. (1919). *Use of plants by the Indians of the Missouri River region* (Washington, DC: Government Printing Office).

Gordon, A., Smirnov, A., Shumlas, S., Singireddy, S., DeCesare, M., Schoonen, M.A., and Strongin, D. (2013). Reduction of Nitrite and Nitrate on Nano-dimensioned FeS. *Orig Life Evol Biosph* 43, 305-322.

Hamelin, J., Fromin, N., Tarnawski, S., Teyssier-Cuvelle, S., and Aragno, M. (2002). *nifH* gene diversity in the bacterial community associated with the rhizosphere of *Molinia coerulea*, an oligonitrophilic perennial grass. *Environmental Microbiology* 4, 477-481.

Hibbett, D.S., Binder, M., Bischoff, J.F., Blackwell, M., Cannon, P.F., Eriksson, O.E., Huhndorf, S., James, T., Kirk, P.M., Lucking, R., *et al.* (2007). A higher-level phylogenetic classification of the Fungi. *Mycological Research* 111, 509-547.

Hill, S., and Postgate, J. (1969). Failure of putative nitrogen-fixing bacteria to fix nitrogen. *Journal of General Microbiology* 58, 277-285.

Hoefsloot, G., Termorshuizen, A.J., Watt, D.A., and Cramer, M.D. (2005). Biological nitrogen fixation is not a major contributor to the nitrogen demand of a commercially grown south african sugarcane cultivar. *Plant and Soil* 277, 85-96.

Holliday, R. (1964). A mechanism for gene conversion in fungi. *Genetics Research* 5, 282-304.

Holliday, R. (1974). Bacteria, bacteriophages, and fungi. In *Handbook of Genetics*, R. King, ed. (New York, NY: Plenum Press), p. 577.

Horbach, R., Navarro-Quesada, A.R., Knogge, W., and Deising, H.B. (2011). When and how to kill a plant cell: Infection strategies of plant pathogenic fungi. *Journal of Plant Physiology* 168, 51-62.

Horst, R.J., Zeh, C., Saur, A., Sonnewald, S., Sonnewald, U., and Voll, L.M. (2012). The *Ustilago maydis* Nit2 homolog regulates nitrogen utilization and is required for efficient induction of filamentous growth. *Eukaryotic cell* 11, 368-380.

Howarth, R.W. (2008). Coastal nitrogen pollution: a review of sources and trends globally and regionally. *Harmful Algae* 8, 14-20.

- Hwang, D.M., Dempsey, A., Tan, K.-T., and Liew, C.-C. (1996). A modular domain of NifU, a nitrogen fixation cluster protein, is highly conserved in evolution. *J Mol Evol* *43*, 536-540.
- Jin, H.J., Tu, R., Xu, F., and Chen, S.F. (2011). Identification of Nitrogen-Fixing *Paenibacillus* from Different Plant Rhizospheres and a Novel nifH Gene Detected in the *P. stellifer*. *Microbiology* *80*, 117-124.
- Kamagata, Y., and Tamaki, H. (2005). Cultivation of uncultured fastidious microbes. *Microbes Environ* *20*, 85-91.
- Kämper, J., Kahmann, R., Bölker, M., Ma, L.-J., Brefort, T., Saville, B.J., Banuett, F., Kronstad, J.W., Gold, S.E., Müller, O., *et al.* (2006). Insights from the genome of the biotrophic fungal plant pathogen *Ustilago maydis*. *Nature* *444*, 97-101.
- Kanvinde, L., and Sastry, G.R.K. (1990). *Agrobacterium tumefaciens* Is a Diazotrophic Bacterium. *Applied and Environmental Microbiology* *56*, 2087-2092.
- Kasting, J.F. (1993). Earth's early atmosphere. *Science* *259*, 920-926.
- Kellner, R.L. (2001). Suppression of pederin biosynthesis through antibiotic elimination of endosymbionts in *Paederus sabaeus*. *J Insect Physiol* *47*, 475-483.
- Khademi, S., and Stroud, R.M. (2006). The Amt/MEP/Rh family: structure of AmtB and the mechanism of ammonia gas conduction. *Physiology* *21*, 419-429.
- Klose, J., and Kronstad, J.W. (2006). The multifunctional β -oxidation enzyme is required for full symptom development by the biotrophic maize pathogen *Ustilago maydis*. *Eukaryotic cell* *5*, 2047-2061.
- Klosterman, S.J., Perlin, M.H., Garcia-Pedrajas, M., Covert, S.F., and Gold, S.E. (2007). Genetics of Morphogenesis and Pathogenic Development of *Ustilago maydis*. *Adv Genet* *57*, 1-47.
- Klotz, M., and Stein, L. (2008). Nitrifier genomics and evolution of the nitrogen cycle. *FEMS microbiology letters* *278*, 146-156.
- Knoll, A.H. (1992). The Early Evolution of Eukaryotes - a Geological Perspective. *Science* *256*, 622-627.
- Kriel, J., Haesendonckx, S., Rubio-Teixeira, M., Van Zeebroeck, G., and Thevelein, J.M. (2011). From transporter to transceptor: Signaling from transporters provokes re-evaluation of complex trafficking and regulatory controls Endocytic internalization and intracellular trafficking of nutrient transceptors may, at least in part, be governed by their signaling function. *Bioessays* *33*, 870-879.
- Kronstad, J., and Leong, S. (1989). Isolation of two alleles of the b locus of *Ustilago maydis*. *Proceedings of the National Academy of Sciences* *86*, 978-982.
- Kumar, V., Kayasth, M., Chaudhary, V., and Gera, R. (2014). Diversity of diazotrophs in arid and semi-arid regions of Haryana and evaluation of their plant growth promoting potential on Bt-cotton and pearl millet. *Ann Microbiol* *64*, 1301-1313.
- Kushnirov, V.V. (2000). Rapid and reliable protein extraction from yeast. *Yeast* *16*, 857-860.

- Kvasnikov, E., Zhuravel, A., and Kliushnikova, T. (1971). Thermophilic aerobic spore-forming hydrocarbon-utilizing oligonitrophilic bacteria and their physiology. *Mikrobiologiya* 40, 509.
- Laxman, S., Sutter, B.M., Shi, L., and Tu, B.P. (2014). Npr2 inhibits TORC1 to prevent inappropriate utilization of glutamine for biosynthesis of nitrogen-containing metabolites. *Sci Signal* 7.
- Lehman, R.M., Taheri, W.I., Osborne, S.L., Buyer, J.S., and Douds, D.D. (2012). Fall cover cropping can increase arbuscular mycorrhizae in soils supporting intensive agricultural production. *Applied Soil Ecology* 61, 300-304.
- Line, M., and Loutit, M.W. (1973). Nitrogen-fixation by mixed cultures of aerobic and anaerobic micro-organisms in an aerobic environment. *Journal of General Microbiology* 74, 179-180.
- Lorenz, M.C., and Heitman, J. (1998). The MEP2 ammonium permease regulates pseudohyphal differentiation in *Saccharomyces cerevisiae*. *Embo Journal* 17, 1236-1247.
- Lovely, C.B., Aulakh, K.B., and Perlin, M.H. (2011). Role of Hsl7 in Morphology and Pathogenicity and Its Interaction with Other Signaling Components in the Plant Pathogen *Ustilago maydis*. *Eukaryotic Cell* 10, 869-883.
- Lumini, E., Bianciotto, V., Jargeat, P., Novero, M., Salvioli, A., Faccio, A., Bécard, G., and Bonfante, P. (2007). Presymbiotic growth and sporal morphology are affected in the arbuscular mycorrhizal fungus *Gigaspora margarita* cured of its endobacteria. *Cell Microbiol* 9, 1716-1729.
- Mahlert, M., Vogler, C., Stelter, K., Hause, G., and Basse, C.W. (2009). The a2 mating-type-locus gene *Iga2* of *Ustilago maydis* interferes with mitochondrial dynamics and fusion, partially in dependence on a Dnm1-like fission component. *Journal of Cell Science* 122, 8-8.
- Mal'tseva, N., and Ivanitskaia, L. (1980). Capacity of oligonitrophilic bacteria to utilize exopolysaccharides as carbon nutrition sources. *Mikrobiologicheskii zhurnal* 42, 17.
- Maniatis, T., Fritsch, E.F., and Sambrook, J. (1982). *Molecular cloning: a laboratory manual*, Vol 545 (Cold Spring Harbor Laboratory Cold Spring Harbor, NY).
- Martin, W., and Russell, M.J. (2003). On the origins of cells: a hypothesis for the evolutionary transitions from abiotic geochemistry to chemoautotrophic prokaryotes, and from prokaryotes to nucleated cells. *Philosophical Transactions of the Royal Society of London B: Biological Sciences* 358, 59-85.
- Martinez-Argudo, I., Little, R., Shearer, N., Johnson, P., and Dixon, R. (2004). The NifL-NifA system: a multidomain transcriptional regulatory complex that integrates environmental signals. *Journal of bacteriology* 186, 601-610.
- Marzluf, G.A. (1997). Genetic regulation of nitrogen metabolism in the fungi. *Microbiology and Molecular Biology Reviews* 61, 17-32.
- Minerdi, D., Fani, R., Gallo, R., Boarino, A., and Bonfante, P. (2001). Nitrogen Fixation Genes in an Endosymbiotic Burkholderia Strain. *Applied and environmental microbiology* 67, 725-732.

- Mohr, W., Grosskopf, T., Wallace, D.W.R., and LaRoche, J. (2010). Methodological Underestimation of Oceanic Nitrogen Fixation Rates. *Plos One* 5.
- Montanez, A., Abreu, C., Gill, P.R., Hardarson, G., and Sicardi, M. (2009). Biological nitrogen fixation in maize (*Zea mays* L.) by N-15 isotope-dilution and identification of associated culturable diazotrophs. *Biol Fertil Soils* 45, 253-263.
- Montoya, J.P., Voss, M., Kahler, P., and Capone, D.G. (1996). A Simple, High-Precision, High-Sensitivity Tracer Assay for N₂ Fixation. *Applied and environmental microbiology* 62, 986-993.
- Mueller, D. (2013). Corn Disease Loss Estimates From the United States and Ontario, Canada - 2012 (Purdue Extension: Purdue University), pp. 5.
- Newton, W.E. (2007). Physiology, biochemistry, and molecular biology of nitrogen fixation. In *Biology of the Nitrogen Cycle*, H. Bothe, S.J. Ferguson, and W.E. Newton, eds. (Amsterdam; Boston: Elsevier), pp. 109-126.
- Olivier, J.G.J., Van Aardenne, J.A., Dentener, F., Ganzeveld, L., and Peters, J.A.H.W. (2005). Recent trends in global greenhouse gas emissions: regional trends and spatial distribution of key sources. In *Non-CO2 Greenhouse Gases (NCGG-4)*, A.v. Amstel, ed. (Rotterdam: Millpress), pp. 325-330.
- Orgel, L.E. (1968). EVOLUTION OF GENETIC APPARATUS. *Journal of Molecular Biology* 38, 381-&.
- Ott, L.E., Pickering, K.E., Stenchikov, G.L., Allen, D.J., DeCaria, A.J., Ridley, B., Lin, R.F., Lang, S., and Tao, W.K. (2010). Production of lightning NO_x and its vertical distribution calculated from three-dimensional cloud-scale chemical transport model simulations. *J Geophys Res-Atmos* 115, -.
- Ozawa, T., Ohwaki, A., and Okumura, K. (2003). < Original> Isolation and Characterization of Diazotrophic Bacteria from the Surface-Sterilized Roots of Some Legumes.
- Pataky, J.K., Snetselaar, M. A. (2006). Common smut of corn. *The Plant Health Instructor*.
- Paul, J.A., Barati, M.T., Cooper, M., and Perlin, M.H. (2014). Physical and Genetic Interaction between Ammonium Transporters and the Signaling Protein Rho1 in the Plant Pathogen *Ustilago maydis*. *Eukaryotic Cell* 13, 1328-1336.
- Pham, C.D., Yu, Z.Y., Sandrock, B., Bolker, M., Gold, S.E., and Perlin, M.H. (2009). *Ustilago maydis* Rho1 and 14-3-3 Homologues Participate in Pathways Controlling Cell Separation and Cell Polarity. *Eukaryotic Cell* 8, 977-989.
- Pike, N., and Kingcombe, R. (2009). Antibiotic treatment leads to the elimination of *Wolbachia* endosymbionts and sterility in the diplodiploid collembolan *Folsomia candida*. *Bmc Biol* 7, 1-6.
- Prechtel, J., Kneip, C., Lockhart, P., Wenderoth, K., and Maier, U.-G. (2004). Intracellular spheroid bodies of *Rhopalodia gibba* have nitrogen-fixing apparatus of cyanobacterial origin. *Mol Biol Evol* 21, 1477-1481.

- Ribbe, M., Gadkari, D., and Meyer, O. (1997). N₂ fixation by *Streptomyces thermoautotrophicus* involves a molybdenum-dinitrogenase and a manganese-superoxide oxidoreductase that couple N₂ reduction to the oxidation of superoxide produced from O₂ by a molybdenum-CO dehydrogenase. *J Biol Chem* 272, 26627-26633.
- Rodriguez, R., and Redman, R. (2008). More than 400 million years of evolution and some plants still can't make it on their own: plant stress tolerance via fungal symbiosis. *Journal of Experimental Botany* 59, 1109-1114.
- Rodriguez, R.J., White, J.F., Arnold, A.E., and Redman, R.S. (2009). Fungal endophytes: diversity and functional roles. *New Phytologist* 182, 314-330.
- Rousselet, G., Simon, M., Ripoche, P., and Buhler, J.-M. (1995). A second nitrogen permease regulator in *Saccharomyces cerevisiae*. *Febs Lett* 359, 215-219.
- Ruiz-Herrera, J., and Leon, C.G. (1995). Yeast-mycelial dimorphism of haploid and diploid strains of *Ustilago maydis*. *Microbiology (13500872)* 141, 695.
- Ruiz-Herrera, J., León, C.G., Guevara-Olvera, L., and Cárabez-Trejo, A. (1995). Yeast-mycelial dimorphism of haploid and diploid strains of *Ustilago maydis*. *Microbiology* 141, 695-703.
- Ruiz-Herrera, J., León-Ramírez, C., Vera-Nuñez, A., Sánchez-Arreguín, A., Ruiz-Medrano, R., Salgado-Lugo, H., Sánchez-Segura, L., and Peña-Cabriales, J.J. (2015). A novel intracellular nitrogen-fixing symbiosis made by *Ustilago maydis* and *Bacillus* spp. *New Phytologist*.
- Rutherford, J.C., Lin, X.R., Nielsen, K., and Heitman, J. (2008). Amt2 permease is required to induce ammonium-responsive invasive growth and mating in *Cryptococcus neoformans*. *Eukaryotic Cell* 7, 237-246.
- Samson, R., Legendre, J.B., Christen, R., Saux, M.F.-L., Achouak, W., and Gardan, L. (2005). Transfer of *Pectobacterium chrysanthemi* (Burkholder et al. 1953) Brenner et al. 1973 and *Brenneria paradisiaca* to the genus *Dickeya* gen. nov. as *Dickeya chrysanthemi* comb. nov. and *Dickeya paradisiaca* comb. nov. and delineation of four novel species, *Dickeya dadantii* sp. nov., *Dickeya dianthicola* sp. nov., *Dickeya dieffenbachiae* sp. nov. and *Dickeya zeae* sp. nov. *Int J Syst Evol Microbiol* 55, 1415-1427.
- Santos, J.D., Viana, T.D., de Jesus, C.M., Baldani, V.L.D., and Ferreira, J.S. (2015). Inoculation and Isolation of Plant Growth-Promoting Bacteria in Maize Grown in Vitória Da Conquista, Bahia, Brazil. *Rev Bras Cienc Solo* 39, 78-85.
- Santos, S.R., and Ochman, H. (2004). Identification and phylogenetic sorting of bacterial lineages with universally conserved genes and proteins. *Environmental Microbiology* 6, 754-759.
- Sarathambal, C., Ilamurugu, K., Balachandar, D., Chinnadurai, C., and Gharde, Y. (2015). Characterization and crop production efficiency of diazotrophic isolates from the rhizosphere of semi-arid tropical grasses of India. *Applied Soil Ecology* 87, 1-10.
- Sarić, Z. (1978). The influence of mineral fertilizers on the population of *Azotobacter* and *Oligonitrophilic* bacteria in chernozem. *Mikrobiologia* 15, 153-166.

- Sayavedra-Soto, L., Hommes, N., and Arp, D. (1994). Characterization of the gene encoding hydroxylamine oxidoreductase in *Nitrosomonas europaea*. *Journal of Bacteriology* *176*, 504.
- Schindelin, H., Kisker, C., Schlessman, J.L., Howard, J.B., and Rees, D.C. (1997). Structure of ADP·AIF₄-stabilized nitrogenase complex and its implications for signal transduction. *Nature* *387*, 370-376.
- Schmidt, I., Bock, E., and Jetten, M.S.M. (2001). Ammonia oxidation by *Nitrosomonas eutropha* with NO₂ as oxidant is not inhibited by acetylene. *Microbiology* *147*, 2247.
- Seefeldt, L.C., Hoffman, B.M., and Dean, D.R. (2009). Mechanism of Mo-dependent nitrogenase. *Annual review of biochemistry* *78*, 701.
- Shime-Hattori, A., Kobayashi, S., Ikeda, S., Asano, R., Shime, H., and Shinano, T. (2011). A rapid and simple PCR method for identifying isolates of the genus *Azospirillum* within populations of rhizosphere bacteria. *Journal of applied microbiology* *111*, 915-924.
- Shoushtari, A.N., Fuller, D., Kanvinde, L., and Sastry, G.R. (2010). *Agrobacterium Tumefaciens* Nitrogen Fixation System Expresses in *Sinorhizobium meliloti* (= *Rhizobium meliloti*). *Research Journal of Agriculture and Biological Sciences* *6*, 535-541.
- Simon, L., Bousquet, J., Levesque, R.C., and Lalonde, M. (1993). Origin and Diversification of Endomycorrhizal Fungi and Coincidence with Vascular Land Plants. *Nature* *363*, 67-69.
- Smith, B., Richards, R.L., and Newton, W.E. (2004). *Catalysts for nitrogen fixation : nitrogenases, relevant chemical models and commercial processes* (Dordrecht ; Boston: Kluwer Academic Publishers).
- Smith, D.G., Garcia-Pedrajas, M.D., Gold, S.E., and Perlin, M.H. (2003). Isolation and characterization from pathogenic fungi of genes encoding ammonium permeases and their roles in dimorphism. *Molecular Microbiology* *50*, 259-275.
- Steinberg, G. (2014). Endocytosis and early endosome motility in filamentous fungi. *Current opinion in microbiology* *20*, 10-18.
- Steinberg, G., and Perez-Martin, J. (2008). *Ustilago maydis*, a new fungal model system for cell biology. *Trends in Cell Biology* *18*, 61-67.
- Steinberg, G., Schliwa, M., Lehmler, C., Bolker, M., Kahmann, R., and McIntosh, J.R. (1998). Kinesin from the plant pathogenic fungus *Ustilago maydis* is involved in vacuole formation and cytoplasmic migration. *Journal of cell science* *111*, 2235-2246.
- Stirling, A., Rozgonyi, T., Krack, M., and Bernasconi, M. (2015). Pyrite in contact with supercritical water: the desolation of steam. *Physical Chemistry Chemical Physics* *17*, 17375-17379.
- Summers, D.P., Basa, R.C., Khare, B., and Rodoni, D. (2012). Abiotic nitrogen fixation on terrestrial planets: Reduction of NO to ammonia by FeS. *Astrobiology* *12*, 107-114.

- Swain, H., and Abhijita, S. (2013). Nitrogen fixation and its improvement through genetic engineering. *J Global Biosci* 2, 98-112.
- Szklarczyk, D., Franceschini, A., Kuhn, M., Simonovic, M., Roth, A., Minguéz, P., Doerks, T., Stark, M., Müller, J., and Bork, P. (2011). The STRING database in 2011: functional interaction networks of proteins, globally integrated and scored. *Nucleic acids research* 39, D561-D568.
- Taylor, J.W., and Berbee, M.L. (2006). Dating divergences in the Fungal Tree of Life: review and new analyses. *Mycologia* 98, 838-849.
- Terfrüchte, M., Jöhnk, B., Fajardo-Somera, R., Braus, G.H., Riquelme, M., Schipper, K., and Feldbrügge, M. (2013). Establishing a versatile Golden Gate cloning system for genetic engineering in fungi. *Fungal Genetics and Biology*.
- Tracy, W., Vargas, C., Zepeda, L., Pataky, J., Chandler, M., Janick, J., and Whipkey, A. (2007). Production and marketing of huitlacoche. *Issues in new crops and new uses*, 233-236.
- Valdez-Morales, M., Barry, K., Fahey, G.C., Domínguez, J., de Mejia, E.G., Valverde, M.E., and Paredes-López, O. (2010). Effect of maize genotype, developmental stage, and cooking process on the nutraceutical potential of huitlacoche (*Ustilago maydis*). *Food Chemistry* 119, 689-697.
- Vitousek, P., Aber, J.D., Howarth, R.W., Likens, G.E., Matson, P.A., Schindler, D.W., Schlesinger, W.H., and Tilman, D.G. (1997). HUMAN ALTERATION OF THE GLOBAL NITROGEN CYCLE: SOURCES AND CONSEQUENCES. *Ecol Appl* 7, 13.
- Wächtershäuser, G. (1988). Before enzymes and templates: theory of surface metabolism. *Microbiological Reviews* 52, 452-484.
- Wächtershäuser, G. (2007). On the Chemistry and Evolution of the Pioneer Organism. *Chemistry & Biodiversity* 4, 584-602.
- Wacker, T., Garcia-Celma, J.J., Lewe, P., and Andrade, S.L.A. (2014). Direct observation of electrogenic NH₄⁺ transport in ammonium transport (Amt) proteins. *Proceedings of the National Academy of Sciences of the United States of America* 111, 9995-10000.
- Wibberg, D., Blom, J., Jaenicke, S., Kollin, F., Rupp, O., Scharf, B., Schneiker-Bekel, S., Sczcepanowski, R., Goesmann, A., and Setubal, J.C. (2011). Complete Genome Sequencing of *Agrobacterium* sp H13-3, the former *Rhizobium lupini* H13-3, Reveals a Tripartite Genome Consisting of a Circular and a Linear Chromosome and an Accessory Plasmid but Lacking a Tumor-Inducing Ti-Plasmid. *Journal of Biotechnology*.
- Wuchter, C., Abbas, B., Coolen, M.J.L., Herfort, L., Van Bleijswijk, J., Timmers, P., Strous, M., Teira, E., Herndl, G.J., and Middelburg, J.J. (2006). Archaeal nitrification in the ocean. *Proceedings of the National Academy of Sciences* 103, 12317.
- Zarnack, K., Eichhorn, H., Kahmann, R., and Feldbrugge, M. (2008). Pheromone-regulated target genes respond differentially to MAPK phosphorylation of transcription factor Prf1. *Molecular Microbiology* 69, 1041-1053.

Zehr, J.P., Crumbliss, L.L., Church, M.J., Omoregie, E.O., and Jenkins, B.D. (2003a). Nitrogenase genes in PCR and RT-PCR reagents: implications for studies of diversity of functional genes. *Biotechniques* 35, 996-+.

Zehr, J.P., Jenkins, B.D., Short, S.M., and Steward, G.F. (2003b). Nitrogenase gene diversity and microbial community structure: a cross-system comparison. *Environ Microbiol* 5, 539-554.

Zehr, J.P., and McReynolds, L.A. (1989). Use of degenerate oligonucleotides for amplification of the *nifH* gene from the marine cyanobacterium *Trichodesmium thiebautii*. *Appl Environ Microbiol* 55, 2522-2526.

APPENDICES

Primers

These primers were designed for use in qPCR experiments but were not used.

Table 9. Unused Primers for qPCR

using primer3plus set for qpcr (verified no similar targets by BLAST)

Pair/Size	Name	Size	Tm	GC%	sequence (5' to 3')
um01714	um01714F	20	60.3	50	GTATGATCCGATTGCCAAGG
amp: 113 bp	um01714R	20	59.7	50	TGCGGAAGATGTGGTATGAG
um02414	um02414F	20	60	50	GCGAAAGAATTCAGCAGGAC
amp: 74 bp	um02414R	20	59.6	50	TACGTCCCACGCTCATATTG
um02908	um02908F	20	59.5	50	CGTCTTGCTGTTCAACTTGG
amp: 73 bp	um02908R	20	60.4	50	AAGGATCAACTGAGCGATGC
um03264	um03264F	20	59.9	50	TGCTTGACCCTACCCAATTC
amp: 91 bp	um03264R	20	60	50	TCTTGCGAGTCAAACGTGTC
um03351	um03351F	20	59.9	50	TTGTCAACTCGGACAAGTGC
amp: 125 bp	um03351R	20	59.9	50	CGAGATAAAGGCGATCTTGC
um03557	um03557F	20	60.1	50	CATCATCATCACCGAGCAAC
amp: 125 bp	um03557R	20	60.1	50	AGGACGAGCATATGGATTCC
um04962	um04962F	20	60.1	50	ACCGTCAAAGGACGAATCAG
amp: 123 bp	um04962R	20	59.8	50	TTCTCTTCGCTTGCCTCTTC
um05632	um05632F	20	60	50	TGTCTTTGGTGCTGCTGTTT
amp: 88 bp	um05632R	20	60.5	50	GAGGAACGATCCAACATTGC
um05947	um05947F	20	61.3	50	TCCAAGATTCAGCCGAGATG
amp: 145 bp	um05947R	20	60.1	50	AGAATGCCAACCAGAGGATG
um10086	um10086F	20	60.1	50	TACCCGAATGCAAGCTATCC
amp: 115 bp	um10086R	20	59.9	50	TCACGTCGATACCTTTGCTG
um11448	um11448F	20	58.9	50	ATTGTCGAGACGCAGAACAC
amp: 121 bp	um11448R	20	59.3	50	CGTAGATGTTGGCTGCAATC
um11098	um11098F	20	61.2	50	TTGTCCTTGCCGAATGCTAC
amp: 83 bp	um11098R	20	59.1	50	CTGGGTCATGATCTTGTTGC

Sequence Data

CRR-15 16S

Size (bp) **Sequencing Primer**

1009 68F

Significant Match	Score	Expected	Identities	Gaps
HM016083.1	1467	0.0	991/1020	23/1020

Erwinia chrysanthemi strain CRR-15 16S ribosomal RNA gene, partial sequence

Sequence (FASTA)

>CRR-15 16S

```
GGCGCTGAGTGCATTCTGATCTACGATTACTAGCGATTCCGACTTCATGGAGT
CGAGTTGCAGACTCCAATTGGACCTGACGTACTTTATGAGGTCCGCTTGCTCT
CGCGAGGTCGCTTCTCTTTGTATACGCCATTGTAGCACGTGTGTAGCCCTACT
CGTAAGGGCCATGATGACTTGACGTCATCCCCACCTTCTCCAGTTTATCACT
GGCAGTCTCCTTTGAGTTCCCGACCGAATCGCTGGCAACAAAGGATAAGGGT
TGCGCTCGTTGCGGGACTTAACCCAACATTTACAACACGAGCTGACGACAG
CCATGCAGCACCTGTCTCAGAGTTCCCGAAGGCACCAAGGCATCTCTGCCAA
GTTCTCTGGATGTCAAGAGTAGGTAAGGTTCTTCGCGTTGCATCGAATTAAAC
CACATGCTCCACCGCTTGTGCGGGCCCCGTCAATTCATTTGAGTTTTAACCT
TGCGGCCGTACTCCCCAGGCGGTTCGATTTAACGCGTTAGCTCCGGAAGCCAC
GCCTCAAGGGCACAACCTCCAAATCGACATCGTTTACAGCGTGGACTACCAG
GGTATCTAATCCTGTTTGCTCCCCACGCTTTCGCACCTGAGCGTCAGTCTTCGT
CCAGGGGGCCGCCTTCGCCACCGGTATTCCTCCAGATCTCTACGCATTTACCC
GCTACACCTGGAATTCTACCCCCCTCTACGAGACTCTAGCTTGCCAGTTTTGA
ATGCAGTTCCCAGGTTAAGCCCCGGGGATTTACATCCAACCTAACAAACCGC
CTGCGTGCCTTTACGCCAGTCATTCCGATTAACGCTTGCACCCTCCGTATT
ACCGCGGCTGCTGGCACGGAGTTAGCCCCGGTGTCTTCTTCTGCGAGTAACGTC
ATCAACAAGGTTATACTACTGCTTCTCTCGCTGAAGTGCTTACACCGAGCTTC
CTCACACACGCGCATGGCTGCATCAGCTGCCCATTTGTGCAATATTCCCCACT
GCCTGCCT
```

CRR-15 nifH

Size **Sequencing**
(bp) **Primer**

360 nifHF

Significant Match	Score	Expected	Identities	Gaps
CP002038.1	82.4	5e-12	123/172	2/172

Dickeya dadantii 3937, complete genome

Sequence (FASTA)

>CRR-15 16S

```
GCGAAATCTCGGATCGCACACACATTATGGAATGATCGATCACGTCGGTTCA
GTTGAAGACCGCGAAATGGGAGACGGTTTGCCTGACGGCTATGGCAACGGGC
GCTGTGCCGAATTC AATGGCCCCGAGCCGGGTGTGGGCTGTGACCTACGCTC
AATGACCACCGCCGTCCACTTCCTGTAAGAAGTTTTTGCCGGGAGGAAGATC
```

TTGATATTTGCGCTGATCACCGCTTGCCGTGCTATCGCCAATACACTATCGGC
 GTTATGATTACCAATGGAAGTGC GAAGAGATTAACCTTGGGCGCTCCGCGGA
 GATGATGATGGTAGTCCGGTGCGGCTGTGGCGGGAAGATAGAGCTAA

FB1 wild-type 16S-sized fragment

Size **Sequencing**
(bp) **Primer**

1025 68F

Significant Match	Score	Expected	Identities	Gaps
GQ900609.1	1555	0.1	970/1022	26/172

Pseudomonas synxantha strain A1 16S ribosomal RNA gene, partial sequence

Sequence (FASTA)

>CRR-15 16S

```
GGGGCGGTCGCGATTCTGATTCGCGATTACTAGCGATTCCGACTTCACGCAGT
CGAGTTGCAGACTGCGATAGGAAACAATCGGTTTTATGGGATTAGCTCCACC
TCGCGGCTTGAAACCCTCTGTACCGACCATTGTAGCACGTGTGTAGCCCAG
GCCGTAAGGGCCATGATGACTTGACGTCATCCCCACCTTCCCTCCGGTTTGCA
CCGGCAGTCTCCTTAGAGTGCCCAACATAACGTGCTGGTAACTAAGGACAAG
GGTTGCGCTCGTTACGGGACTTAACCCAACATCTCACGACACGAGCTGACGA
CAGCCATGCAGCACCTGTCTCAATGTTCCCGAAGGCACCAATCTATCTCTAGA
AAGTTCATTGGATGTCAAGGCCTGGTAAGGTTCTTCGCGTTGCTTCGAATTAA
ACCACATGCTCTTCCGCTTGTGCGGGCCCCCGTCAATTCATTTGAGTTTTAAC
CTTGCGGCCGTACTCCCCAGGCGGTCAACTTAATGCGTTAGCTGCGCCACTAA
AAGCTCAAGGCTTCCAACGGCTAGTTGACATCGTTTACGGCGTGGACTACCA
GGGTATCTAATCCTGTTTGCTCCCCACGTTTCGCACCTCAGTGTCAGTATTA
GTCCAGGTGGTGCCTTCGCCACTGGTGTTCCTTCCCTATATCTACGCATTTAC
CGCTACACAGGAAATTCCACCACCCTCTACCATACTCTAGTCAGTCAGTTTTG
AATGCAGTTCCCAGGTTGAGCCCGGGGATTCACATCCA ACTTAAACAAACC
ACCTACGCGCGCTTTACGCCAGTAATCCGGATTAACGGCTTGCACCCCTCT
GTATTACCGGCGGCTGCTGGCACAGAAGTTTAGCCGGTGCTTATTTCTGTCGG
TAACGTCAAAATTGCACAAATATAGACGTTGACCCCTTCCCTCCCCACATAA
GGTCTTACAATTCGAAGACTTCTACACGCGGCATGCTGATTCAGCTTTCGCC
AATGTGGTCCAAATATTTCCCA
```

Δ ump1, Δ ump2 16S

Size **Sequencing**
(bp) **Primer**

901 M13(-21)F

Significant Match	Score	Expected	Identities	Gaps
XM_011390636.1	1510	0.0	860/869	7/1020

Ustilago maydis 521 hypothetical protein partial mRNA, locus UMAG_02524

Sequence (FASTA)

>DUMP1216SFRAGMENT

GTGTGCCTCGACTTGCGCGATCTGCCATGGCGGCTCTTGCATCTGGAGTTGCA
TCGATCGCCCCCAAGAGGGCAGTGAGGACGTAGATGGTCATCTCATCGTACG
TTTCTGCCGAGACGGCAGCCAGCCAACGGAGGATGGCCAAAATGTTGGAGGT
TGTTAGAAGAGACGAGATGGACAGCAAGTAAAGCAGGTGACCAAGTTCGCG
TCGTTCTTCGCGCAGCCATCCAAGACGGTCAAGTTGGATCTCATCGCTGAGTC
TGCCACCGCTGGCAGTGGATGTGGATGATGGCTGTTTTGCGGTTTGGCTACTA
CCAAGACCGAAGAAGTTGGACGTTTGTGTCTGGATGCCTTGATTTGCGATGTT
GGAGCCAGGCGATTTCGAGAGATGCCTTGACATGTGCAGTGGACTGTTTGACG
TTGTCAATTTAGCGAGGATCCTTTCGGCAAGCGTGAGCTTGCGTGTGGATGT
GGAAGTGGAGCCGACCGAAGCCTCGATGCTGACGAGCGATTTCGACGAGTTGT
TCCATCTTGAGACCCATGCGTTGGGCTTCTAGGTCTTCGTCAAAGGCATGGT
GAGTGCATTACGGAGTAGCTCCTTGAGGCACGCAAGCAATGCAAGTCGTTTCG
CGGTGATAGAGGATGCAAGCGACCTCGACGGCGGGACGGCCCCATTTTGCAC
GACCAGCAAGACCTTGCTGGAGCAAAGAAGCAGCAAAGTGCTCCGAGACGA
CCAATTCGCGAGCCAGCAAGAGCGACTGCTGCGCAAAGTCAGGGTTGAGGCT
TTGCGTGTGCGCTGATTGTGATCTTGCCGGACTCGATCTCTTTGGCGCCTC
GACATCGGAATGGGTGGGACGGAACCCTTGCCCGGAGGGTTCTCGGCCAAAA
GTTCCAAGAAAG

Δump1,Δump2 nifH-1 fragment

Size **Sequencing**
(bp) **Primer**

556 M13(-21)F

Significant Match	Score	Expected	Identities	Gaps
XM_011388406.1	205	1e-48	113/113	0/113
	161	1e-35	92/94	0/94

Ustilago maydis 521 hypothetical protein partial mRNA, locus UMAG_10959

Sequence (FASTA)

>DUMP12NIFH1FRAGMENT

TACTCGTATAGGGCGATTGGGACCTCTAGATGCATGCTCGAGCGGCCGCCAG
TGTGATGGATATCTGCAGAACCGCCCTTTGCGACCCGAAGGCCGATCGTCGT
GCTCAGAGAAGTATTCGATATGCAGCTGGGGTGAGATACTCTGCATGACGAT
GGAGCGCAGTAGTGTGTCCGCGTGCTGTAAGTGGTGTGTTTGCGGTCCAGGA
CGTCTTGGGCGAAGGGAACAACAGATTAGCGTGTTCTGCAAGCGACGACGCC
AGAAGTGCACAGAGCCTGAGCTGGGATCAAGGACATGATCGGCATTCCACCT
TAAGTGATCGTACAGGATTGGCAGAGTATTGAGCAGGTGACGGTTGAGGGCG
AAAGGCTCCATGACTTGGCTTCTCGACCAACAAGGGGGCGAGTGATCTCAAC
AAGGGTGGTGGGACGAAGGGTTCGCCGTAGGTGTCTCCTCGCAATGGACAGGA
CAATGTGTGAGTCTAGGCGGGATGATGGCATTAAAGGGCGAATTCCAGCACAC
TGCGCGCCGTTACTAGTGGATCCGAGCTCGGTACCA

Δump1,Δump2 nifH-2 fragment

Size
(bp)

Sequencing
Primer

477 M13(-21)F

Significant Match	Score	Expected	Identities	Gaps
XM_011393498.1	619	1e-173	348/351	0/351

Ustilago maydis 521 putative Splicing factor 3b, partial mRNA, locus UMAG_05454

Sequence (FASTA)

```
>DUMP12NIFH2FRAGMENT
GAATCCTTTTGGGGGAACAATGGGGCCCTCCACATGCATGTGCGAGCGGTTCG
CCAGTGTGATGGATATAAGAGAACACCCCTGTCCCCTGGGGCCTACTGGGCA
AAAGCGGCTGCTCCAAAACAAACGAGGCATCGAAAAGCCTGCTTACCAACTA
CCCTCGTACATCGCCGAAACCCGCATAGCCACCATCAAGGACGCGCTCAACG
AAAAGGAAGCCGACTACTCACTCAAACAAAAAACGCGCGATCGCGTGCAGC
CCAAGATGGGCAAGATCGAAATCGACTACCAGAAGCTCTACGATGCGTTTTT
CAAGTTTCAGAGCAAACCATCGCTCAGCATGTACGGCGACGTTTACTACGAA
GGCAAGGATTTTCGAGACAAAGTACAAGGATAAGCGACCGGGCCAGTTGAGC
TCCGAGCTGATCGAGGCGCTCTCCATCCTACCACTCGCACCTCCGCCTTGGGG
TCGCAAAGGG
```

U. maydis strain ½ 16S-like fragment

Size (bp) **Sequencing Primers**

1484 M13(-21)F M13R

Significant Match	Score	Expected	Identities	Gaps
BX571856.1	2358	0.0	1313/1317	0/1317

Staphylococcus aureus subsp. *aureus* strain MRSA252, complete genome, 16S rRNA, bases 2337212-2335896

Sequence (FASTA)

```
>ONEHALF16S
AACCATATAAGGCGAGTGGGCCAACAGATGCAAGCGCGAGCTTGCGCCGTGT
GAGGATTCTTAAACGTGAATCGAAATGGAGTGAGGAATCAGAAAAGCTTGCT
TCTCTGATGTTAGCGGCGGACGGGTGAGTAACACGTGGATAACCTACCTATA
AGACTGGGATAACTTCGGGAAACCGGAGCTAATACCGGATAATATTTTGAAC
CGCATGGTTCAAAGTGAAAGACGGTCTTGCTGTCCTTATAGATGGATCCG
CGCTGCATTAGCTAGTTGGTAAGGTAACGGCTTACCAAGGCAACGATGCATA
GCCGACCTGAGAGGGTGATCGGCCACACTGGAAGTGAAGACACGGTCCAGACT
CCTACGGGAGGCAGCAGTAGGGAATCTTCCGCAATGGGCGAAAGCCTGACG
GAGCAACGCCGCGTGAGTGATGAAGGTCTTCGGATCGTAAAACCTCTGTTATT
AGGGAAGAACATATGTGTAAGTAACTGTGCACATCTTGACGGTACCTAATCA
GAAAGCCACGGCTAACTACGTGCCAGCAGCCGCGGTAATACGTAGGTGGCA
AGCGTTATCCGGAATTATTGGGCGTAAAGCGCGCGTAGGCGGTTTTTTAAGTC
TGATGTGAAAGCCCACGGCTCAACCGTGGAGGGTCATTGGAAACTGGAAAAC
TTGAGTGCAGAAGAGGAAAGTGAATTCATGTGTAGCGGTGAAATGCGCAG
AGATATGGAGGAACACCAGTGGCGAAGGCGACTTTCTGGTCTGTAACCTGACG
```

CTGATGTGCGAAAGCGTGGGGATCAAACAGGATTAGATACCCTGGTAGTCCA
CGCCGTAAACGATGAGTGCTAAGTGTTAGGGGGTTTCCGCCCTTAGTGCTGC
AGCTAACGCATTAAGCACTCCGCCTGGGGAGTACGACCGCAAGGTTGAAACT
CAAAGGAATTGACGGGGACCCGCACAAGCGGTGGAGCATGTGGTTTAATTTCG
AAGCAACGCGAAGAACCTTACCAAATCTTGACATCCTTTGACAACCTCTAGAG
ATAGAGCCTTCCCCTTCGGGGGACAAAGTGACAGGTGGTGCATGGTTGTCGT
CAGCTCGTGTGCTGAGATGTTGGGTTAAGTCCCGCAACGAGCGCAACCCTTA
AGCTTAGTTGCCATCATTAAAGTTGGGCACTCTAAGTTGACTGCCGGTGACAAA
CCGGAGGAAGGTGGGGATGACGTCAAATCATCATGCCCTTATGATTTGGGC
TACACACGTGCTACAATGGACAATACAAAGGGCAGCGAAACCGCGAGGTCA
AGCAAATCCCATAAAGTTGTTCTCAGTTCGGATTGTAGTCTGCAACTCGACTA
CATGAAGCTGGAATCGCTAGTATTCTTAGGTCAGCATGCTACGGTGAATGCG
TTCCCGCTAATCCTTTAACCCGTAAGGGCGAATTCAGCACACTGGCGGCCGT
GCTAGTGGTCCGAGCTCGAGGCAGAG

U. maydis strain FB2 16S-like fragment

Size (bp) Sequencing Primers

1506 M13(-21)F M13R

Significant Match	Score	Expected	Identities	Gaps
CP007447.1	1891	0.0	1216/1301	25/1301

Staphylococcus aureus strain XN108, complete genome, 16S rRNA, bases 1993271 to 1994549

Sequence (FASTA)

>FB216S

CTTGGGTTGGGGGCCCTTTTCCTGATCAGGCCCGAGAGCCCCAACAACAAA
AAGCGCCCGGAAAGACCGGAGGAATTGATTGTTTTATCTGGATCGTTGAAAG
TTCTATAAAAACCCTATGTGATTACGAGACAGCGATTGCGGCTTCATGGAGC
CAGTTGGGGACTACAATCCGAAGTATAACAACCTTTATGGGATTTGCTTGACC
TCGCGGTTTCGCTGCCCTTTGTATTGTCCATTGTAGCACGTGTGTAGCCAAA
TCATAAGGGGCATGATGATTTGACGTCATCCCCACCTTCCCGGTTTGTAC
CGGCAGTCAACTTAGAGTGCCCAACTTAATGATGGCAACTAAGCTTAAGGGT
TGCGCTCGTTGCGGGACTTAACCCAACATCTCACGACACGAGCTGACGACAA
CCATGCATCACCTGTCACCTTTGTCCCCGAAGGGGAAGGCTCTATCTCTAGAG
TTGTCAAAGGATGTCAAGATTTGGTAAGGTTCTTCGCGTTGCTTCGAATTA
CCACATGCTCCACCGCTTGTGCGGGTCCCCCGTCAATCCCCTTTGAGTTTCAA
CCTTGCGGTCGTACTCTCCAGGCGGAGTGCTTAATGCGTTAGCTGCAGCACT
AAGGGGGCGGAAACCCCTAACACTTTAGCACTCATCGTTTACGGCGTGGAC
TACCCAGGGGTATCTAATCCCTGTGGATTCCCCACGCTTTTGTACATCAGC
GGTCAGTGTAACACCAGAAGAATGGTCTTCGCCACCGGGGTTCTTCCTAAA
TATCGCGCATATCTCCCCGACACACAGAAAACCCCTCTCCTTCTTTTGCACA
CAAATGTTCCCCAGTTCCCAAAGCCCCCCCCAGGTTGAGACCCGGAGGTTT
TTCATCTCAGACTTAAAAACACCGCCTACGCGCGCTTTACGCCCAATAATTC
GGGATAACGCTTGCCACCTACGTATTACCGCGGCTGCTGGCACGTAGTTACC
CGTGGCTTTCTGATTAGGTACCGTCAAGATGTGCACAGTTACTTACACATATG
TTCTTCCCTAATAACAGAGTTTTACGATCCGAAGACCTTCATCACTCACGCGG

CGTTGCTCCGTCAGGCTTTCGCCATTGCGGAAGATTCCCTACTGCTGCCTCC
 CGTAGGAGTCTGGACCGTGTCTCAGTTCCAGTGTGGCCGATCACCCCTCTCAGG
 TCGGCTATGCATCGTTGCCTTGGTAAGCCGTTACCTTACCAACTAGCTAATGC
 AGCGCGGATCCATCTATAAGTGACAGCAAGACCGTCTTTCACCTTTTGAACCAT
 GCGGTTCAAAATATTATCCGGTATTAGCTCCGGTTTCCCGAAGTTATCCCAGT
 CTTATAGGTAGGTTATCCACGTGTTACTCACCCGTCCCCCCCCAACGTCAGAGA
 ACCAGCTTCTATAATTCCCACACCTTAATCAGGCGAATCCAGCACACTGGCG
 GCCGTCCTAGTGGTCCGAGCGCGACCTGGAC

U. maydis strain FB1nifH-like fragment

Size (bp) Sequencing Primers

372 M13(-21)F

Significant Match	Score	Expected	Identities	Gaps
XM_011393498	643	0.0	376/385	3/385

Ustilago maydis putative splicing factor, UMAG_05454

Sequence (FASTA)

>FB1NIFH-LIKE

CCAAGGGGAGGGCGAGTGGAGGGAGGGGCGCGCCTCGATCAGCTCGGAGCT
 CAACTGGCCCGGTCGCTTATCCTTGTACTTTGTCTCGAAATCCTCGCCTTCGTA
 GTAAACGTCGCCGTGCATGCTGAGCGATGGTTTGTCTGAAACTTGAAAAAC
 GCATCGTAGAGCTTCTGGTAGTCGATTTTCGATCTTGCCCATCTTGGGCTGCAC
 GCGATCGCGCGTTTTTTGTTTTGAGTGTGTAGTCGGCTTCCTTTTCGTTGAGCGC
 GTCCTTGATGGTGGCTATGCCGGTTTCGGCGATGTACGAGGGTAGTTGGTAA
 GCAGGCTTTTCGATGCCTCGTTTTGTTTTGGAGGTAGTCGCGCTTGTTGGCCCA
 GTGACCAGCTTCTATAATTCCCACACCTTAATCAGGCGAATCCAGCACACTG
 GCGGCCGTCCTAGTGGTCCGAGCGCGACCTGGAC

Golden Gate Cloning

This method (Terfrüchte et al., 2013) was attempted numerous times in the course of this work. I devised a modification to the method which appears to make construct production reliable; however not enough time remained to fully take advantage of this alteration. This modification was to pre-digest the vectors pDest and pStor with SSP1, then gel-purify the digest prior to using the vectors in the one-pot reaction. With a confirmed construct several transformations of *U. maydis* strains FB1 and FB2 were attempted but none yielded transformants. Table 11 identifies the loci that were selected as targets for knock-outs while Table 12 lists the primers used for the construct flanks.

As there was no similarity found between any *U. maydis* DNA and either the canonical *nif* structural genes or the sequences from the putative nitrogenase-like proteins derived from *Streptomyces thermophiles* other efforts were made to identify putative genes that might be involved in atmospheric nitrogen assimilation. Target genes, Table 10, were selected based on predicted interactions in the STRING network with genes predicted to be involved in nitrogen metabolism (Franceschini et al., 2013; Szklarczyk et al., 2011), predicted iron-sulfur domains, predicted involvement in nitrogen metabolism, changes in gene expression under nitrogen starvation as in Horst, et al., 2012 (Horst et al., 2012), possessed of transcription factor (TF) domains either within the gene or TF binding regions upstream of the predicted start codon or, particularly, if those are GAL4-like DNA binding domains that are known to be involved in nitrogen metabolic regulation in *Saccharomyces cerevisiae* (Marzluf, 1997).

Table 10. Top 11 Loci Selected for Use in Golden Gate Reactions.

Locus: UMAG_00037 (um00037)

Predicted Domains (UniProt):

Gene3D	2.102.10.10 . 1 hit. 3.30.390.30 . 1 hit. 3.50.50.60 . 2 hits.
InterPro	IPR023753 . FAD/NAD-binding_dom. IPR016156 . FAD/NAD-linked_Rdtase_dimer. IPR004099 . Pyr_nucl-diS_OxRdtase_dimer. IPR017941 . Rieske_2Fe-2S. [Graphical view]
Pfam	PF07992 . Pyr_redox_2. 1 hit. PF00355 . Rieske. 1 hit. [Graphical view]
SUPFAM	SSF50022 . SSF50022. 1 hit. SSF51905 . SSF51905. 1 hit. SSF55424 . SSF55424. 1 hit.
PROSITE	PS51296 . RIESKE. 1 hit.

Significant predicted interactions by STRING 9.05:

Nir1, nitrite reductase

Comment: UMAG_00037 was selected because of the iron-sulfur cluster as well as its expression being differentially upregulated under no-nitrogen conditions in a mutant U. maydis in which expression of Nit2, a transcription factor identified as being involved in nitrogen catabolite repression, was obviated (Horst et al., 2012).

Locus: UMAG_02462 (um02462)

Predicted Domains (UniProt):

Gene3D	4.10.240.10 . 1 hit.
InterPro	IPR007219 . Transcription_factor_dom_fun. IPR001138 . Zn2-C6_fun-type_DNA-bd. [Graphical view]
Pfam	PF04082 . Fungal_trans. 1 hit. PF00172 . Zn_clus. 1 hit. [Graphical view]
SMART	SM00906 . Fungal_trans. 1 hit. SM00066 . GAL4. 1 hit. [Graphical view]
SUPFAM	SSF57701 . SSF57701. 1 hit.
PROSITE	PS00463 . ZN2_CY6_FUNGAL_1. 1 hit. PS50048 . ZN2_CY6_FUNGAL_2. 1 hit. [Graphical view]

Significant predicted interactions by STRING 9.05:

None

Comment: UMAG_02462 is predicted to be a GAL4-like transcription factor having two predicted TF-like zinc finger binding domains. This could indicate involvement in nitrogen catabolite repression, possibly influencing atmospheric nitrogen assimilation.

Locus: UMAG_03264 (UM03264)

Predicted Domains (UniProt):

Gene3D	1.10.150.120 . 1 hit. 3.10.20.30 . 1 hit. 3.30.365.10 . 6 hits. 3.30.43.10 . 1 hit. 3.30.465.10 . 1 hit. 3.90.1170.50 . 1 hit.
InterPro	IPR002888 . 2Fe-2S-bd. IPR001041 . 2Fe-2S_ferredoxin-type. IPR006058 . 2Fe2S_fd_BS. IPR000674 . Ald_Oxase/Xan_DH_a/b. IPR016208 . Ald_Oxase/xanthine_DH. IPR008274 . AldOxase/xan_DH_Mopterin-bd. IPR012675 . Beta-grasp_dom. IPR005107 . CO_DH_flav_C. IPR016169 . CO_DH_flavot_FAD-bd_sub2. IPR016166 . FAD-bd_2. IPR016167 . FAD-bd_2_sub1. IPR002346 . Mopterin_DH_FAD-bd. [Graphical view]
Pfam	PF01315 . Ald_Xan_dh_C. 1 hit. PF02738 . Ald_Xan_dh_C2. 1 hit. PF03450 . CO_deh_flav_C. 1 hit. PF00941 . FAD_binding_5. 1 hit. PF00111 . Fer2. 1 hit. PF01799 . Fer2_2. 1 hit. [Graphical view]
PIRSF	PIRSF000127 . Xanthine_DH. 1 hit.
SMART	SM01008 . Ald_Xan_dh_C. 1 hit. SM01092 . CO_deh_flav_C. 1 hit. [Graphical view]

SUPFAM	SSF47741 . SSF47741. 1 hit. SSF54292 . SSF54292. 1 hit. SSF54665 . SSF54665. 1 hit. SSF55447 . SSF55447. 1 hit. SSF56003 . SSF56003. 1 hit. SSF56176 . SSF56176. 1 hit.
--------	--

PROSITE	PS00197 . 2FE2S_FER_1. 1 hit. PS51085 . 2FE2S_FER_2. 1 hit. PS51387 . FAD_PCMH. 1 hit. [Graphical view]
---------	--

Significant predicted interactions by STRING 9.05:

UM02943.1 hypothetical protein
UM00672.1 Uricase

Comment: UMAG_03264 is a putative xanthine dehydrogenase containing predicted protein domains for electron carrier activity, a 2 Fe, 2 S cluster as well as FAD binding, Fe-Fe binding and oxidoreductase activity. Predicted to have involvement in nitrogen metabolism.

Locus: UMAG_03351
Predicted Domains (UniProt):

Gene3D	3.40.50.300 . 2 hits.
--------	---------------------------------------

InterPro	IPR017896 . 4Fe4S_Fe-S-bd. IPR003593 . AAA+_ATPase. IPR003439 . ABC_transporter-like. IPR017871 . ABC_transporter_CS. IPR013283 . ABCE. IPR027417 . P-loop_NTPase. IPR007209 . RNaseL-inhib_metal-bd_dom. [Graphical view]
----------	---

PANTHER	PTHR19248 . PTHR19248. 1 hit.
Pfam	PF00005 . ABC_tran. 2 hits. PF00037 . Fer4. 1 hit. PF04068 . RLI. 1 hit. [Graphical view]
PRINTS	PR01868 . ABCEFAMILY.
SMART	SM00382 . AAA. 2 hits. [Graphical view]
SUPFAM	SSF52540 . SSF52540. 3 hits.
PROSITE	PS51379 . 4FE4S_FER_2. 2 hits. PS00211 . ABC_TRANSPORTER_1. 1 hit. PS50893 . ABC_TRANSPORTER_2. 2 hits. [Graphical view]

Significant predicted interactions by STRING 9.05:

UM06108.1 hypothetical protein

UM06323.1 Eukaryotic translation initiation factor 3 subunit C

Comment: Probably RLI1, similar to RNaseL in *Candida* which, in humans, degrades all RNA as part of the interferon-mediated antiviral response. Possible 4Fe-4S metal binding domain for RNaseL inhibitor, RLI and having 2 ABC transporter domains. Homologs present in *Debarvomyces hansenii*, *Neorospira crassa*, *Yarrowia lipolytica*. If this actually is the preinitiation complex assembly-promoting protein in *U. maydis* its loss could likely be fatal as, in *Saccharomyces*, it is required for the processing and nuclear

export of the 60S and 40S ribosomal subunits. Also possibly related to ATM1.

Locus: UMAG_03612

Predicted Domains (UniProt):

InterPro:	IPR011701 . MFS. IPR020846 . MFS_dom. [Graphical view]
Pfam:	PF07690 . MFS_1. 1 hit. [Graphical view]
SUPFAM:	SSF103473 . SSF103473. 1 hit.
PROSITE:	PS50850 . MFS. 1 hit. [Graphical view]

Significant predicted interactions by STRING 10:

UM03501.1 DNA topoisomerase 2
UM05642.1 putative uncharacterized protein

Comment: Has a GAL4-like potential binding site upstream, related to GIT1, glycerophosphoinositol transporter, potentially involved in mycelium development.

Locus: UMAG_03689

Predicted Domains (UniProt):

InterPro	IPR016192 . APOBEC/CMP_deaminase_Zn-bd. IPR002125 . CMP_dCMP_Zn-bd. IPR016193 . Cytidine_deaminase-like. [Graphical view]
Pfam	PF00383 . dCMP_cyt_deam_1. 1 hit. [Graphical view]

SUPFAM	SSF53927 . SSF53927. 1 hit.
PROSITE	PS00903 . CYT_DCMP_DEAMINASES_1. 1 hit. PS51747 . CYT_DCMP_DEAMINASES_2. 1 hit. [Graphical view]

Significant predicted interactions by STRING 10:

UM02015.1 Uridine kinase
UM03873.1 hypothetical protein

Comment: Differentially regulated in Horst et al., 2012 (Horst et al., 2012), 36.65-fold downregulated. Predicted to be related to TAD2, subunit of tRNA-specific adenosine-34 deaminase. Also predicted to be secreted (by SignalP v. 4.0) by the 1-18 positions.

Locus: UMAG_11104, UM03848 (*nirI*)

Predicted Domains (UniProt):

Gene3D	2.102.10.10 . 1 hit.
InterPro	IPR007419 . BFD-like_2Fe2S-bd_dom. IPR005117 . NiRdtase/SiRdtase_haem-b_fer. IPR012748 . Nitri_red_NirD. IPR006067 . NO2/SO3_Rdtase_4Fe4S_dom. IPR006066 . NO2/SO3_Rdtase_FeS/sirohaem_BS. IPR017941 . Rieske_2Fe-2S. [Graphical view]
Pfam	PF04324 . Fer2_BFD. 1 hit. PF01077 . NIR_SIR. 1 hit. PF03460 . NIR_SIR_ferr. 1 hit. [Graphical view]
PRINTS	PR00397 . SIROHAEM.

SUPFAM	SSF50022 . SSF50022. 1 hit. SSF55124 . SSF55124. 1 hit.
TIGRFAMs	TIGR02378 . nirD_assim_sml. 1 hit.
PROSITE	PS00365 . NIR_SIR. 1 hit. PS51296 . RIESKE. 1 hit. [Graphical view]

Significant predicted interactions by STRING 10:

UM03849.1 hypothetical protein
UM03847.1 Nitrite reductase
UM00037.1 hypothetical protein

Comment: Putative nitrite reductase, reducing nitrite to ammonia. A knock-out of this gene resulting a mutant still able to incorporate atmospheric nitrogen would indicate that nitrite is not a likely intermediate in this assimilation pathway.

Locus: UMAG_05063

Predicted Domains (UniProt):

Gene3D	1.10.840.10 . 2 hits.
InterPro	IPR000651 . Ras-like_Gua-exchang_fac_N. IPR023578 . Ras_GEF_dom. IPR001895 . RASGEF_cat_dom. [Graphical view]
Pfam	PF00617 . RasGEF. 1 hit. PF00618 . RasGEF_N. 1 hit. [Graphical view]
SMART	SM00147 . RasGEF. 1 hit. SM00229 . RasGEF_N. 1 hit

	[Graphical view]
SUPFAM	SSF48366 . SSF48366. 5 hits.
PROSITE	PS50009 . RASGEF_CAT. 1 hit. PS50212 . RASGEF_NTER. 1 hit. [Graphical view]

Significant predicted interactions by STRING 10:

None

Comment: Predicted guanine nucleotide exchange factor (GEF), RAS-like GTPase, perhaps involved in nitrogen catabolite repression. This has a possible GAL4-like binding site upstream.

Locus: UMAG_05632 (Iron-sulfur cluster assembly protein)

Predicted Domains (UniProt):

InterPro	IPR011339 . ISC_FeS_clus_asmbI_IscU. IPR002871 . NIF_FeS_clus_asmbI_NifU_N. [Graphical view]
Pfam	PF01592 . NifU_N. 1 hit. [Graphical view]
TIGRFAMs	TIGR01999 . iscU. 1 hit.

Significant predicted interactions by STRING 10:

UM05524.1 hypothetical protein
UM05776.1 putative uncharacterized protein
UM04428.1 hypothetical protein

Comment: Homology with NifU-like N terminal domain. This domain is not directly

involved in nitrogen fixation and the N-terminal region specifically has similarity amongst many non-nitrogen fixing organisms including humans (Hwang et al., 1996).

This domain is an iron-sulphur cluster assembly domain.

Locus: UMAG_05820

Predicted Domains (UniProt):

Gene3D	4.10.240.10 . 1 hit.
InterPro	IPR001138 . Zn2-C6_fun-type_DNA-bd. [Graphical view]
Pfam	PF00172 . Zn_clus. 1 hit. [Graphical view]
SMART	SM00066 . GAL4. 1 hit. [Graphical view]
SUPFAM	SSF57701 . SSF57701. 1 hit.
PROSITE	PS00463 . ZN2_CY6_FUNGAL_1. 1 hit. PS50048 . ZN2_CY6_FUNGAL_2. 1 hit. [Graphical view]

Significant predicted interactions by STRING 10:

None

Comment: Another potential Gal4-like transcription factor involved in nitrogen metabolism.

Locus: UMAG_10086 (UM00279)

Predicted Domains (UniProt):

InterPro	IPR009348 . NPR2. [Graphical view]
PANTHER	PTHR12991 . PTHR12991. 3 hits.
Pfam	PF06218 . NPR2. 4 hits. [Graphical view]

Significant predicted interactions by STRING 10:

UM02998.1 hypothetical protein
 UM05022.1 hypothetical protein
 UM06340.1 hypothetical protein
 UM01612.1 Vacuolar membrane-associated protein IML1

Comment: Predicted to be related to NPR2, nitrogen permease regulator. This is a more recent indication in the new pedant3 database. It was initially selected simply for its predicted involvement in nitrogen metabolism. Two NPR2 domains are predicted. In *Saccharomyces cerevisiae* a defect in that gene resulted in a strongly increased transcription of *dur3* which is involved in urea active transport (Rousselet et al., 1995) as well as conditionally inhibiting TORC1(Laxman et al., 2014).

Locus: UMAG_11379 (UM01975)

Predicted Domains (UniProt):

Gene3D	4.10.240.10 . 1 hit.
InterPro	IPR001138 . Zn2-C6_fun-type_DNA-bd. [Graphical view]
Pfam	PF00172 . Zn_clus. 1 hit. [Graphical view]

SMART	SM00066 . GAL4. 1 hit. [Graphical view]
SUPFAM	SSF57701 . SSF57701. 1 hit.
PROSITE	PS00463 . ZN2_CY6_FUNGAL_1. 1 hit. PS50048 . ZN2_CY6_FUNGAL_2. 1 hit. [Graphical view]

Significant predicted interactions by STRING 10:

None

Comment: Another fungal Zn2-CY6 zinc finger-coding putative protein suggested to be involved in nitrogen metabolism.

Locus: UMAG_06128

Predicted Domains:

Predicted signal peptide (SignalP v4.0, position 1-27)

Transmembrane region, positions 7-29

Significant predicted interactions by STRING 9.05:

None

Comment: Possible nitrate transporter. If confirmed to be a nitrate transporter it could be useful to knock-out and test N₂ accumulation with a nitrate source.

UMAG_01456 (UM01456 on chr 03)

Predicted to be related to PPR1, transcription factor regulating pyrimidine pathway, as well as UMAG_00113, transcriptional activator acu-15.

UMAG_02462 (UM02462, on chr 05)

Predicted to possess GAL4-like DNA binding domains; also possibly related to PPR1.

UMAG_03386 (UM03386, on chr 08)

Transcription of this gene was also differentially regulated in Horst et al., 2012 (Horst et al., 2012), downregulated 653.65 fold in the knock-out relative to SG200. Perhaps a knock-out of this gene could result in a failure to grow in N-free media. Predicted to be related to JLP-1, iron(2)-dependent sulfonate.

UMAG_03613 (UM03613, on chr 09)

Predicted zinc-finger-based TF, related to PPR1.

UMAG_04294 (UM04294)

Has a GAL4-like binding site upstream, predicted to be related to peroxin-11, related to peroxisome organization and fission.

UMAG_06257 (UM06257, on chr 22)

Has two predicted zinc-finger domains.

Table 11. Primers for Golden Gate Cloning.

Pair/Size	Name	Size (bp)	T _m (°C)	GC%	Sequence (5' to 3')
0037D	0037D1	31	73.5	61.3	GGTCTCCGGCCTTTTTGTGCGATGCGGTGAG
	0037D2	37	72.8	51.4	GGTCTCGCTGCAATATTCCGAGTGGTGAACGAGT GAA
870 bp	0037U2	38	73.8	52.6	GGTCTCGCCTGCAATATTACGGGAGATGTACGGT GAGA
0037U	0037U3	31	73.5	61.3	GGTCTCCAGGCAGACTTGTTGGTCAGCCTCG
875 bp	2462D1	31	73.5	61.3	GGTCTCCGGCCTGATACGTTCCGGCATCTGCA
2462D	2462D2	35	73.0	54.3	GGTCTCGCTGCAATATTCATGTAGTACCAGCGCCC GGTCTCGCCTGCAATATTCTTGGAGCAGTTCGTGG CTA
2462U	2462U2	38	73.8	52.6	GGTCTCCAGGCCAGCGCGAAATCAACGAGAG
973 bp	2462U3	31	73.5	61.3	GGTCTCCAGGCCAGCGCGAAATCAACGAGAG
3264D	3264D1	31	76.1	67.7	GGTCTCCGGCCGGTCGAGCTGAGTATGGTTCG GGTCTCGCTGCAATATTACCTACCGTCTGAGGTTC GA
1006 bp	3264D2	37	72.8	51.4	GGTCTCGCCTGCAATATTCTGCGATACGTTGTTGC TGG
3264U	3264U2	38	73.8	52.6	GGTCTCCAGGCTGCGATGGTCAGGAGAATCG
1086 bp	3264U3	31	73.5	61.3	GGTCTCCAGGCTGCGATGGTCAGGAGAATCG
3351D	3351D1	31	73.5	61.3	GGTCTCCGGCCTCATGTGTCCCATGAGCTT GGTCTCGCTGCAATATTAAGGCGTACCCGTGTA GAC
507 bp	3351D2	37	72.8	51.4	GGTCTCGCCTGCAATATTGATCACGTGCAGTC GACA
3351U	3351U2	36	72.9	52.8	GGTCTCCAGGCGTGGCGATGAGGACAGTTGA
1378 bp	3351U3	31	73.5	61.3	GGTCTCCAGGCGTGGCGATGAGGACAGTTGA
3612D	3612D1	31	74.8	64.5	GGTCTCCGGCCATCGTGAGTCGTGAGTCGTG GGTCTCGCTGCAATATTCCAGAAGGGAATATCGG GGC
815 bp	3612D2	37	73.9	54.1	GGTCTCGCCTGCAATATTCCACAAACAGTCGAC TCGA
3612U	3612U2	38	73.8	52.6	GGTCTCCAGGCCGAAGTCAAAGGGGAACGGA
1109 bp	3612U3	31	73.5	61.3	GGTCTCCAGGCCGAAGTCAAAGGGGAACGGA
3689D	3689D1	31	73.5	61.3	GGTCTCCGGCCTCCTTGTTGTTTCGCGCTTC GGTCTCGCTGCAATATTAGACCAGGGCAGAGAG TGAA
932 bp	3689D2	37	72.8	51.4	GGTCTCGCCTGCAATATTGGTGTGCTTGGCTTTG AGTG
3689U	3689U2	38	73.8	52.6	GGTCTCCAGGCAAGAACCCTTGTGAGCGCA
544 bp	3689U3	31	72.1	58.1	GGTCTCCAGGCAAGAACCCTTGTGAGCGCA
3848D	3848D1	31	74.8	64.5	GGTCTCCGGCCTAGGCCAAGGAGTCTGTGA GGTCTCGCTGCAATATTGTGAGAGAGCGATGGGG ATG
1016 bp	3848D2	37	73.9	54.1	GGTCTCGCCTGCAATATTAGACAGCGTGCTTACC CTC
3848U	3848U2	38	73.8	52.6	GGTCTCCAGGCTTGCCGTACATGAGCATGC
1338 bp	3848U3	31	73.5	61.3	GGTCTCCAGGCTTGCCGTACATGAGCATGC
5063D	5063D1	31	74.8	64.5	GGTCTCGGGCCGCTTCCTTTGACCTGCTCCT GGTCTCGCTGCAATATTGTTGCAGTAGCCGT TGAT
674 bp	5063D2	36	71.7	50.0	GGTCTCGGGCCGCTTCCTTTGACCTGCTCCT GGTCTCGCTGCAATATTGTTGCAGTAGCCGT TGAT

5063U	5063U2	38	73.8	52.6	GGTCTCGCCTGCAATATTCACGATTCAAGCATGC GAGG
1176 bp	5063U3	31	72.1	58.1	GGTCTCCAGGCATGCGATGGAAGTCAGCCAA
5632D	5632D1	31	74.8	64.5	GGTCTCCGGCCTGGTTTCGTCCGTGGGTTAG GGTCTCGCTGCAATATTGTTCTGGAGTGTAC
940 bp	5632D2	36	72.9	52.8	CGTG GGTCTCGCCTGCAATATTGCCGTGTCTCAGAGAA CACA
5632U	5632U2	38	73.8	52.6	GGTCTCCAGGCGAGTCACGAGCCACGATCAT
1094 bp	5632U3	31	73.5	61.3	GGTCTCCGGCCAGCGTCCTCTGTTTTAAATACGT GGTCTCGCTGCAATATTCGAGAGCGTGTAATA
803 bp	5820D1	35	73.0	54.3	TACCCTGT GGTCTCGCCTGCAATATTTTGTACTGTGCGCG TTGG
5820U	5820U2	36	72.9	52.8	GGTCTCCAGGCATCGTAGCCTTTTGCCGTCA
1029 bp	5820U3	31	72.1	58.1	GGTCTCCGGCCCCTTGTACATTGGGCTTGC GGTCTCGCTGCAATATTGTTTGTGTACCACGC ACCG
6138D	6138D1	31	74.8	64.5	GGTCTCGCCTGCAATATTCGTCGCTGCATGTTACA GTG
457 bp	6138D2	37	72.8	51.4	GGTCTCCAGGCGAGGCGGAGAGAGAAGCAAG
6138U	6138U2	38	73.8	52.6	GGTCTCCGGCCCTGTCAACAAGCGTTCGTTGA GGTCTCGCTGCAATATTATGGCGTGTGCACAG ACA
709 bp	6138U3	31	74.8	64.5	GGTCTCGCCTGCAATATTGCCTCTCTGATGTG TCCG
6257D	6257D1	32	73.3	59.4	GGTCTCCAGGCGCCAGTTAGAGGGGCAGAG
311 bp	6257D2	35	71.8	51.4	GGTCTCCGGCCCACGTTCCGTTGCGAAACTC
6257U	6257U2	36	74.0	55.6	
1004 bp	6257U3	30	75.0	66.7	
4294D	4294D1	31	74.8	64.5	
Pair/Size	Name	Size (bp)	Tm (°C)	GC%	Sequence (5' to 3')
344 bp	4294D2	37	72.8	51.4	GGTCTCGCTGCAATATTGGGGCTCAATCGTGATC GTT GGTCTCGCCTGCAATATTGTGTCATTGGTGCCT GTAC
4294U	4294U2	38	73.8	52.6	GGTCTCCAGGCGATGATGGAGGCGGAAGAG
1130 bp	4294U3	31	74.8	64.5	GGTCTCCGGCCTCGCTCATCCTGATTAGCCC
3513D	3513D1	31	74.8	64.5	GGTCTCGCTGCGTGGCTCACGGTGACAGATC GGTCTCGCCTGCAATATTTTCCGATTGCCTC CCGA
160 bp	3513D2	31	74.8	64.5	GGTCTCCAGGCCGTACTGGCCGACGTTGATA
3513U	3513U2	36	72.9	52.8	GGTCTCCGGCCGTAGGATTTGGCTCGCCTGT GGTCTCGCTGCAATATTCTCCTTACCGGTGC ACTAGC
606 bp	3513U3	31	73.5	61.3	GGTCTCGCCTGCAATATTACACGGGTTCGAA ATTGGGA
3386D	3386D1	31	74.8	64.5	GGTCTCCAGGCTCGAATCGCAAGCTCAGACC
385 bp	3386D2	37	73.9	54.1	GGTCTCCGGCCCGGTACCAACACAAACTGCG
3386U	3386U2	38	72.7	50.0	GGTCTCGCTGCAATATTGACGACTTGCCCACT
542 bp	3386U3	31	73.5	61.3	
2808D	2808D1	31	74.8	64.5	
729 bp	2808D2	37	72.8	51.4	

Pair/Size	Name	Size (bp)	T _m (°C)	GC%	Sequence (5' to 3')
					GTGTA
2808U	2808U2	38	73.8	52.6	GGTCTCGCCTGCAATATTGCCAAAGACATAGC
214 bp	2808U3	31	73.5	61.3	TTCGCG
1975D	1975D1	31	74.8	64.5	GGTCTCCAGGCAAACGATGGAGACCGTGACC
575 bp	1975D2	37	72.8	51.4	GGTCTCCGGCCGGCAACGGTACACAGCAAAG
1975U	1975U2	38	73.8	52.6	GGTCTCGCTGCAATATTCACAAACCAAGCCAG
373 bp	1975U3	31	73.5	61.3	GAACG
1456D	1456D1	31	74.8	64.5	GGTCTCGCCTGCAATATTAAACTCCTATCGCTC
322 bp	1456D2	37	72.8	51.4	CGCTC
1456U	1456U2	38	73.8	52.6	GGTCTCCAGGCACCTGATTGAGCGAAGACGG
409 bp	1456U3	31	72.1	58.1	GGTCTCCAGGCTGGTTGGCATGCATTGTTGG
0279D	0279D1	31	74.8	64.5	GGTCTCCGGCCCGGCATCGATCCAGAT
360 bp	0279D2	37	72.8	51.4	GGTCTCGCTGCAATATTACCATCTCGCCAACC
0279U	0279U2	38	73.8	52.6	ATGAG
385 bp	0279U3	31	73.5	61.3	GGTCTCGCCTGCAATATTCGATCGTAAGGCTT
0195D	0195D1	31	74.8	64.5	GGTGGT
400 bp	0195D2	37	72.8	51.4	GGTCTCCAGGCTTCGTCGTACCACAACAGGG
0195U	0195U2	38	73.8	52.6	GGTCTCCGGCCCGTGC GTGTATCTCGGTGAT
496 bp	0195U3	31	73.5	61.3	GGTCTCGCTGCAATATTACTTTACACCTCACAG
					GCCCCG
					GGTCTCGCCTGCAATATTCTGTTCTCAAACAC
					ACGCGG
					GGTCTCCAGGCCAAGTTGAGCGTGAACGTGG
0097D	0097D1	31	73.5	61.3	GGTCTCCGGCCCGCTGAACGTTGCGCAAGTTA
325 bp	0097D2	36	72.9	52.8	GGTCTCGCTGCAATATTGTCTTTCTGCTTCGC
0097U	0097U2	38	72.7	50.0	CCTC
800 bp	0097U3	31	73.5	61.3	GGTCTCGCCTGCAATATTAGTGATGATACGCG
0023D	0023D1	31	74.8	64.5	CCACAT
501 bp	0023D2	36	72.9	52.8	GGTCTCCAGGCTAGGTGGAGTTCTTGCCGTG
0023U	0023U2	38	73.8	52.6	GGTCTCCGGCCTTCTGGCTCCATCCCCTTTG
1000 bp	0023U3	31	73.5	61.3	GGTCTCGCTGCAATATTACAAAACCTCGACCT
					CGCC
					GGTCTCGCCTGCAATATTCGTGAATGGAAGAC
					GTGAGG
					GGTCTCCAGGCTGGACATCCCCGATACGAGT

Table 12. Transformant Screening Primers.

Pair/Size	Name	Size (bp)	Tm (°C)	GC%	Sequence (5' to 3')
internal 00037	i37F	20	59.4	55.0	ATGCCGACAAGGTTACCTGG
607 bp	i37R	20	59.4	55.0	TTGGTAGCGGGAGAAACACC
internal 03848	i48F	20	59.4	55.0	ACCAACGATCGATACCTCGC
1340 bp	i48R	20	61.4	60.0	GCATCCGACTCCTCAGTAGC
internal 03689	i89F	20	59.4	55.0	AGAATCGTACCTCACACGCC
914 bp	i89R	20	59.4	55.0	AGTCGAGACAAGCACGAAGG
internal 03351	i3351F	20	59.4	55.0	AAGTTCCAGGGCAGTACG
533 bp	i3351R	20	59.4	55.0	AAGAAGTACTGACCAGCGGC
internal 06138	i6138F	20	59.4	55.0	TCACCAACAACCTCGTCTCG
752 bp	i6138R	20	59.4	55.0	CTTGATTTGCGCGGTTAGG
hygromycin	gghygF	20	59.4	55.0	CTGCTTTGCTCCGCGAATAC
730 bp	gghygR	20	57.3	50.0	ATTGACCGATTCTTGCGGT
external 00037	o37F	20	57.3	50.0	TTTTTGCTTGTCTCTGCGC
external 03848	o48F	20	59.4	55.0	GTTACATAGCGTTGCAGCGG
external 03689	o89F	20	59.4	55.0	AGCAGACAAAGAGGTGGTCCG
external 03351	o3351R	20	57.3	50.0	AAGCTTGCATGTTGGCTGTG
external 06138	o6138R	20	59.4	55.0	CCGACGATTGCATGCTCTTG

Growth of *Zea mays* under nitrogen starvation

Summary

One tangential experiment that was conducted but is not being formally reported here was a brief investigation of Golden Bantam corn grown in sand supplemented with Hoagland's Solution with and without a nitrogen source. This experiment was to see if there might be a symbiotic interaction under nitrogen starvation in infected plants as measured by dry plant biomass. The net effect measured indicated that nitrogen-starved, infected seedlings had a statistically significant higher mean dry mass as compared to nitrogen-starved uninfected seedlings while both were significantly lower in average dry mass as compared to seedlings provided with a nitrogen source.

Introduction

The obligate biotrophic nature of *Ustilago maydis* can perhaps suggest a potential and previously undiscovered symbiotic interaction when its *Zea mays* host is stressed. As previously indicated it is known that some endophytes and many ectomycorrhiza contribute to host survival by conferring at least some resistance to stressors including herbivory, by virtue of toxins noxious to predators, drought and nutrient limitation. Considering that *U. maydis* is autoecious and has ability to adapt and survive under nitrogen starvation by a method that includes converting atmospheric dinitrogen into cellular biomass perhaps it also has a capacity, however limited, to support its host under conditions of extreme nitrogen starvation.

A common metric for growth success in plant work is direct measurement of dry biomass. Other morphometric traits measuring height or leaf length are also employed in general. Considering the nutrient restriction imposed in testing this hypothesis dry mass

appeared both the easiest to measure and more potentially representative of any change induced by the infection. Subsequent experiments could employ other traits, including stable isotope either by devising a way to use dinitrogen tracer to look for accumulation from atmospheric dinitrogen or very low levels of heavy, stable nitrogen introduced as ammonium, nitrite or nitrate and analyzing the resulting biomass for less tracer than uninfected treatments. The former would be more definite but more impractical to set-up while the latter could have its own limitations in discriminatory power but would be much easier to conduct.

What this pilot experiment cannot determine is what the source is of the change in biomass. Contributions to mass by developing fungal mycelium could only be guessed-at by the proliferation of any galls formed. Significant change, though, could indicate merit for conducting further work.

Methods

An overnight culture of *U. maydis* SG200 was inoculated into YPD (1% yeast, 2% peptone, 2% dextrose) broth and incubated at 27°C until an OD A_{600} of at least 0.5 was achieved. Those cells were centrifuged and washed in sterile water then diluted to either 10^2 or 10^4 cells/mL. Seedlings were inoculated with approximately 100 μ L of either 10^2 or 10^4 cells/mL, sterile water-washed SG200 cells approximately 7 days post-germination. Golden Bantam corn [W. Altee Burpee & Co., Warminster, PA] were planted in 6" terracotta pots containing medium grit sand and coffee filters. These were placed in plastic trays in the incubator and bottom-watered using either a 1/10 dilution of Hoagland's No. 2 Basal Salt Solution (606.6 mg/L potassium nitrate, 656.4 mg/L calcium nitrate, 240.76 mg/L magnesium sulfate, 115.03 mg/L monobasic ammonium phosphate,

1.81 mg/L manganese chloride*4H₂O, 2.86 mg/L boric acid, 0.016 mg/L molybdenum trioxide, 0.22 mg/L zinc sulphate*7H₂O, 0.08 mg/L copper sulfate*5H₂O, 5 mg/L ferric tartrate) [HOP01-50LT, Caisson Labs, North Logan, UT] or a 1/10 dilution of Hoagland's Modified Nitrogen Free No. 2 Basal Salt Mixture (2.86 mg/L boric acid, 554.9 mg/L calcium chloride, 0.045 mg/L copper II chloride, 33.0 mg/L EDTA, iron sodium salt, 240.325 mg/L magnesium sulfate, 1.81 mg/L manganese chloride*4H₂O, 0.025 mg/L molybdic acid sodium salt*2H₂O, 372.7 mg/L potassium chloride, 136.025 mg/L monobasic potassium phosphate, 0.11 mg/L zinc chloride) [HOP03-50LT, Caisson Labs, North Logan, UT]. Watering occurred as needed to maintain water levels in the tray at about 1/4" from the bottom of each pot for 28 days at which time the plants were collected in envelopes, dried for 48 hours then weighed.

Results

There were some indications of small galls on a fraction of the infected plants; there was no significant evidence of disease based on infection by this solopathogenic strain at these inoculation levels. Plant masses were distributed as indicated in Figure 26. There were 30 plants in the uninfected with ammonium group (A), 85 plants in the uninfected without ammonium (B), 54 plants in the low-level infection (C) and 52 plants in the higher-level infection groups (D). A series of student T-tests on these groups indicated that there was a significant difference between A and B, as expected. Further a significant difference was found between A and C as well as A and B with C being closer of higher overall biomass than B. D was not significantly different from either B or C but was significantly different from A.

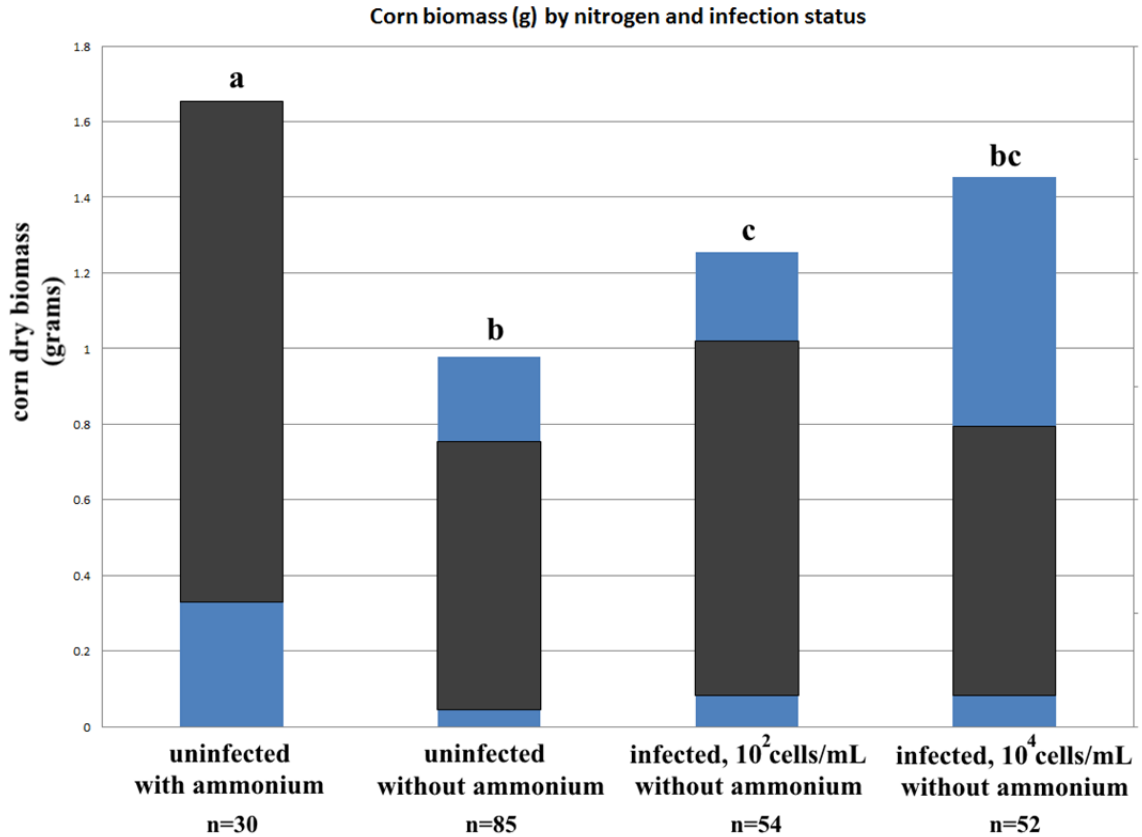


Figure 26. Corn biomass by nitrogen availability and infection status.

Discussion

This first experiment indicated that further work to support or refute this hypothesis could be warranted as it did appear that corn infected with *U. maydis* solopathogenic strain SG200 achieved more average biomass than uninfected corn under the same nitrogen-deprived condition while not reaching the same average biomass as uninfected, nitrogen supplemented corn plants. A disease index was not performed because of the intentionally low infection levels and very few, small galls were observed on some infected plants; none of those were larger than a millimeter. This experiment could warrant repetition upon which, if these results are confirmed, additional questions could be investigated; primarily whether or not the observed differences are based simply

on growing mycelium and independent of corn growth. Adding measurements of height and leaf length could contribute to that analysis.

CURRICULUM VITAE

NAME: Michael Reginald Larson Cooper
ADDRESS: 507 W St Catherine St.
Louisville, KY 40203
DOB: Murray, Kentucky – November 9, 1970

Education

2015 Ph.D. in Molecular, Cellular and Developmental Biology
University of Louisville, Louisville, KY

2013 M.S. in Biology, concentration in Molecular Biology
Murray State University, Murray, KY

2008 B.S. in Biochemistry and Molecular Biology
Murray State University, Murray, KY

2001 Associate's Degree in Arts and Sciences
Olympic College, Bremerton, WA

1991 Naval Nuclear Propulsion Plant Operator
Nuclear Power Training Unit, S5G
INEL, Idaho Falls, ID
Nuclear Power School, Orlando, FL

1990 Electrician's Mate
Nuclear Field "A" School
NFAS, Orlando, FL

Awards

2015 Graduate Dean's Citation, University of Louisville

2015 Dissertation Completion Grant, University of Louisville

2014 Graduate Teaching Assistantship, University of Louisville
2012

- 2013 Graduate Research Fellowship, University of Louisville
2011
- 2008 Graduate Student Teaching Assistantship, Murray State University
- 2006 Biology and Mathematics in Population Studies Fellowship,
Murray State University
- 2005 Outstanding Senior in Biology, Murray State University
Outstanding Undergraduate Teaching Assistant, Murray State
University

Presentations

Poster 2013, Cooper, M. "Living on Air?: *Ustilago maydis* cells grow without being provided nitrogen in their growth media." 27th Fungal Genetics Conference, Asilomar, Pacific Grove, CA.

Presentation 2013, "Living on Air?: *Ustilago maydis* cells grow without being provided nitrogen in their growth media." 27th Fungal Genetics Conference, Asilomar, Pacific Grove, CA.

Poster 2011, "Physical and genetic interactions among *Ustilago Maydis* ammonium transporters and a central signaling protein." Graduate Research Symposium, University of Louisville

Presentation 2010, "Molecular evidence for diazotrophic *Agrobacterium tumefaciens*." Master's Thesis, Murray State University, Murray, KY.

Publications

Paul, J. A., M. T. Barati, M. Cooper and M. H. Perlin (2014). "Physical and Genetic Interaction between Ammonium Transporters and the Signaling Protein Rho1 in the Plant Pathogen *Ustilago maydis*." *Eukaryotic Cell* 13(10): 1328-1336.

Agarwal, C., K. B. Aulakh, K. Edelen, M. Cooper, R. M. Wallen, S. Adams, D. J. Schultz and M. H. Perlin (2013). "Ustilago maydis phosphodiesterases play a role in the dimorphic switch and in pathogenicity." *Microbiology-Sgm* **159**: 857-868.

Pham, C. D., Z. Yu, C. Ben Lovely, C. Agarwal, D. A. Myers, J. A. Paul, M. Cooper, M. Barati and M. H. Perlin (2012). "Haplo-insufficiency for different genes differentially reduces pathogenicity and virulence in a fungal phytopathogen." *Fungal Genetics & Biology* 49(1): 21-29.

Teaching Experience

2015	GTA for Microbiology and Genetics, UL
2012, 2014	GTA for Microbiology, UL
2010	GTA for General Biology, MSU
2008-2010	GTA for Microbiology, MSU
2007	UTA for Microbiology and Genetics, MSU
2006	UTA for Microbiology, MSU
2005	UTA for Microbiology and Zoology, MSU

Work History

2002-2004	Assistant Director <i>C&C Tractor Trailer Training Center, LLC</i> Boaz, KY
2001 -2002	Service Administrator <i>Johnson Controls, Inc.</i> Milwaukee, WI
2000-2001	Electrician <i>AMSEC, LLC.</i> Bremerton, WA
1999 -2000	Technical Director <i>Community Theatre, Inc.</i> Bremerton, WA
1998 -1999	Technician <i>Predict/DLI Engineering, Inc.</i> Bainbridge Island, WA
1990 - 1996	Electrician's Mate (E-5/EM2), Nuclear <i>US Navy</i> Various Locations